A MASS-SPECTROMETRIC TECHNIQUE FOR THE STUDY OF FAST GASEOUS ATOMIC REACTIONS.

NOVEMBER 1964.

Being a Thesis presented by William David Woolley to the University of St. Andrews, in application for the Degree of Doctor of Philosophy.

DECLARATION.

I hereby declare that this Thesis is a record of my own experimental work, that the Thesis is my own composition, and that it has not previously been presented for a Higher Degree.

The investigations were carried out in the Chemical Research Laboratories of St. Salvator's College in the University of St. Andrews, under the supervision of Dr. Charles Horrex.

William D. Woolley.

CERTIFICATE.

I hereby certify that William David Woolley has spent twelve terms at Research Work under my supervision, that he has fulfilled the conditions of Ordinance No. 16 (St. Andrews), and that he is qualified to submit the accompanying Thesis in application for the Degree of Doctor of Philosophy.

C. Horrex, M.Sc., Ph.D.,
Director of Research.

UNIVERSITY CAREER.

I first matriculated in the University of St. Andrews in October 1957, and graduated B.Sc., with Second Class Honours in Chemistry in July, 1961.

The work described in this Thesis was carried out during the period from October, 1961 to November, 1964.

ACKNOWLEDGEMENTS.

I wish to record my thanks and appreciation to Dr. C. Horrex for all the encouragement and help he has given me throughout my University career and in particular throughout the period of this research.

I should like to thank the Department of Scientific and Industrial Research for a Research Grant and also the Late Professor J. Read, and Professor J.I.G. Cadogan for the laboratory facilities.

I also wish to thank Dr. D. Calvert, Mr. G.R. Woolley, and Mr. R.B. Moyes for many helpful discussions, Mr. T. Norris for his assistance in the workshop, Mr. Z.M. Zochowski for certain miscellaneous help, and Mr. R. Morris for his help with the photographs.

Finally I thank my wife Maureen for her help especially with the typing of this Thesis.

TABLE OF CONTENTS.

1. INTRODUCTION.

The great reactivity of atoms and radicals plays an important role in modern reaction kinetic studies, but a knowledge of the rates of reaction has more often been derived from a study of a complex sequence of reactions rather than a direct observation of the bimolecular processes which they undergo. This is essentially due to the very high reaction rates involved since only a few collisions are necessary to achieve reaction but there is also the difficulty of measuring the exact concentration of these species.

More than thirty years ago, Polanyi [1] produced a method of creating dilute steady state reaction zones a few centimetres in diameter by allowing sodium atoms to diffuse into a range of other reactants. In this Diffusion Flame technique as it has often been called the concentration of sodium atoms at different points in the reaction zone was shown by the fluorescence produced when illuminated by a sodium resonance lamp. Unfortunately, this technique is not easily modified to free atom and radical reactions in general because they cannot all be made to show their presence optically in this way.

In 1952 Kistiakowsky [23] using the same low pressure inter-diffusion system extended the method to other fast reactions. In this case the amount of chemical reaction in a volume element of the reaction zone was monitored by recording the temperature reached by a sensitive thermocouple probe. Providing that the reactions are exothermic, which is usually the case in fast reactions, the method is one of wide

applicability but unfortunately the detection system is completely without chemical specificity.

It has been shown that suitably constructed mass-spectrometers are capable of detecting certain free radicals and atoms. Generally such studies have been limited to pyrolytic furnaces or discharge tubes situated immediately above a small pin hole leak leading to the ion chamber and much quantitative data has not been obtained.

It was the aim of the research described in this thesis to adapt the diffusion flame method to the study of atomic reactions using mass-spectrometric estimation of the reaction species. In general it was felt that if the mass-spectrometer could be made to follow the concentration of the so called nozzle (atomic) reagent then it would be an easy matter to monitor the concentrations of the other reactants and products which are often stable molecules.

In order to achieve the above aims the following problems had to be considered and overcome.

(i) A methcd was required for producing a steady supply of free atoms for the nozzle reagent. There is an extensive literature on the methods used for this purpose and a summary of these is given in the initial pages of this thesis. Some form of electrical discharge seemed to be the obvious choice but various problems of electrical interference with the highly sensitive and stable mass-spectrometer electronic circuits would have to be faced. This trouble would be particularly noticeable for the following reasons.

(a) Atoms cannot traverse distances of many centimetres in gases at pressures of a few millimetres of mercury and the end of the discharge tube would have to be fixed immediately above the pin hole leak into the mass-spectrometer.

(b) The power supplies of the mass-spectrometer required stability of about 1 in 10,000 for the ion accelerating voltage and 1 in 20,000 for the magnet current.

(c) The reactants under investigation would be present at pressures of about 10^{-3} mm. Hg. and produce ion currents of about 10^{-13} amp.

(ii) The ordinary mass-spectrometer has a tortuous path into the ion source and would clearly not be suitable for free atom work since collisions with metal surfaces generally results in the recombination of the atoms. Consequently, specially constructed ion chambers with direct line of sight transit paths from the pin hole are necessary.

When beginning this research the author did not have any experimental experience of suitable systems for producing free atoms, nor was any available in the department. A mass-spectrometer of a conventional Nier type pattern was available with associated electronic equipment and it was considered that this should be modified for this work.

In order to make progress on separate fronts, different gaseous discharge systems were tried using simple hot wire detection to assess their efficiency. At the same time their operation in the same room as the mass-spectrometer, even several feet from it, gave preliminary indications of the electrical troubles. In the subsequent pages the

details of these evaluating trials are given. The initial modifications to the mass-spectrometer involved only the ion gun but when the discharge tube was mounted close to the ionization chamber various other difficulties were encountered connected with the inadequacy of the differential pumping in the ion source region and also with the sensitivity of the collector system for use at low atomic concentrations.

The final system has been tested using nitrogen atoms which have the advantage of relatively long life. The velocity constants of their reaction with NO and C_2H_4 have been evaluated to confirm the method. Some mass-spectrometric work on the reactions of free nitrogen atoms has been done by Kistiakowsky (99)(100)(101) and certain other authors but the reaction with NO was rated by Kistiakowsky as being too fast to measure and he could only estimate a lower limit for the velocity constant. In general the rate constants calculated later in this thesis show good agreement with existing data.

Before dealing with the experimental work the relevant literature will be discussed. The general methods for the study of fast gaseous reactions will be given with particular reference to diffusion flame techniques. The production, detection and estimation of free gaseous atoms are discussed but only detailed attention has been given to those aspects of direct relevance to this research. Finally some general nitrogen atom chemistry and particularly the reactions with NO and C_2H_4 are discussed.

2. SOME METHODS OF INVESTIGATING FAST GASEOUS REACTIONS.

a) Introduction.

For a reaction between two gases where the energy of activation is zero the velocity constant will be about 10^{11} litre. $mole^{-1}$. sec^{-1}. If the reactants are at pressures of one atmosphere (i.e. about 1/20 mole. $litre^{-1}$.) the half life period will be $1/(10^{11} \times 1/20) = 2 \times 10^{-10}$ sec.

The duration of the reaction can be increased by lowering the concentrations of the reactants and if 10^{-6} atmospheres (10^{-3} mm. Hg.) is used the half life period would become 2×10^{-4} sec.

From the point of view of the experimentalist who is trying to follow the rate of the process both cases are very difficult. The lengthening of the time scale produced by energies of activation of a few kilo-calories is clearly of assistance to the investigator but, in general, reactions are referred to as fast if more than 1 in 100,000 collisions are effective and special methods of observation have been devised for their study. A discussion of the general methods for studying these simple non-chain fast gaseous reactions is given below.

b) Static Systems.

(i) General Techniques.

There are many experimental difficulties in the study of fast reactions in static systems. The reagents have to be brought together, mixed and possibly heated in a very short interval of time and then the reaction monitored at similar very small time intervals. A general apparatus and the experimental difficulties involved in such a reaction system has recently been discussed by Johnston [2]. An apparatus is

outlined using a Hartridge and Roughton [3] type mixing chamber followed by isolation of the mixture in a static system for the study of a variety of reactions involving oxides of nitrogen, oxygen and fluorine. After initiation the reactions were followed by absorption spectroscopy by photographing a C.R.O. trace from a phototube in a similar way to that described later under flash photolysis techniques. Johnston was able to measure reaction rates with half lives no shorter than 10^{-1} sec. but more usually around 0.5 sec.

Generally for reactions with half lives less than 10^{-1} sec. the conventional methods of mixing and heating are quite inadequate but special heating techniques such as shock wave treatment [4] has brought some success into this field. Unfortunately the temperature profiles introduced into the reaction system by a shock wave and the subsequent involved mathematical treatment impose severe restriction and limitation to the method.

A type of static reaction system which has had much success in fast reaction studies uses the photochemical technique of flash photolysis and this is discussed in detail below.

(ii) Flash Photolysis Techniques.

In flash photolysis the active species (atoms or radicals) is generated homogeneously within the reaction system by molecular absorption of photo-energy from the flash giving dissociation products via excited molecular states. In certain cases where the starting material will not readily absorb in the required wave length-region, as in the case of the lower saturated hydrocarbons, the photon energy may

be relayed by mercury photosensitization. The production time of the active species depends solely on the flash duration and the method has the advantage that in the flash photolysis of gaseous mixtures the reactants may be thoroughly mixed and if necessary preheated before initiation. Reaction studies with half lives of the order of milliseconds are quite common and the fastest reaction studied to date in this way had a half life of about 5 μsec.

Considerable progress has been made during the last few years in the design and construction of high output short duration flash equipment. Flash tubes capable of producing over 7,000 joules at 5 to 25 μsec. duration times are quite common and lower energy flashes of 900 joules at 2 μsec. and 4 μjoules at 10 mμsec. have been reported.(5) Generally after flash initiation two important methods of following the reaction have been developed.

In the first method a second and much lower intensity flash tube is fired at a short but known time interval (10^{-5} to 1 sec.) after the main flash and this is used to photograph the absorption spectrum of the system (6). The second flash is usually triggered by an electronic timer actuated by the photolytic flash. A study of the spectrum at different time intervals gives useful data on the reaction kinetics.

Alternatively a light beam of the appropriate wave length (car headlamp bulb and filter system) is passed through the reaction cell and focused on a phototube or photomultiplier connected to an oscilloscope (7). The oscilloscope time base is triggered by the flash and the resulting trace may be photographed.

It is interesting to compare the merits of these two monitoring techniques. In the first method each flash run records a complete spectrum at one specific time of reaction whereas in the second method the absorption intensity for one wave-length only is recorded over the complete time of reaction. For a particular system the choice of monitoring technique must depend upon the particular experimental difficulties and requirements.

c) Flow Systems.

Consider a reagent flowing down a straight tube at a high linear velocity and a second reagent introduced at a point in this line. Providing that mixing has been achieved, reaction takes place and an examination of the concentrations of reagents or products at known distances down the tube can give valuable kinetic data on the reaction velocity. With modern gas handling systems linear flow rates of 10 metres/sec. and more are quite common, such that a distance of 10 centimetres from the injection point would correspond to a reaction time of 10^{-2}sec. Generally the main difficulties with this type of system are the mixing of the reagents and the measurement of the extent of reaction. Methods of analysis by sampling and immediate quenching are not common and spectral observations are usually preferred. In certain cases, methods specific to the reaction can be used. For example Clyne and Thrush have recently measured the rate of $N + NO_2$ in a fast flow system by monitoring the nitrogen atoms at different points down the tube by nitric oxide titration. (8)

FIGURES 1 and 2.

THE METHOD OF HIGHLY DILUTE FLAMES.

Fig. 1.

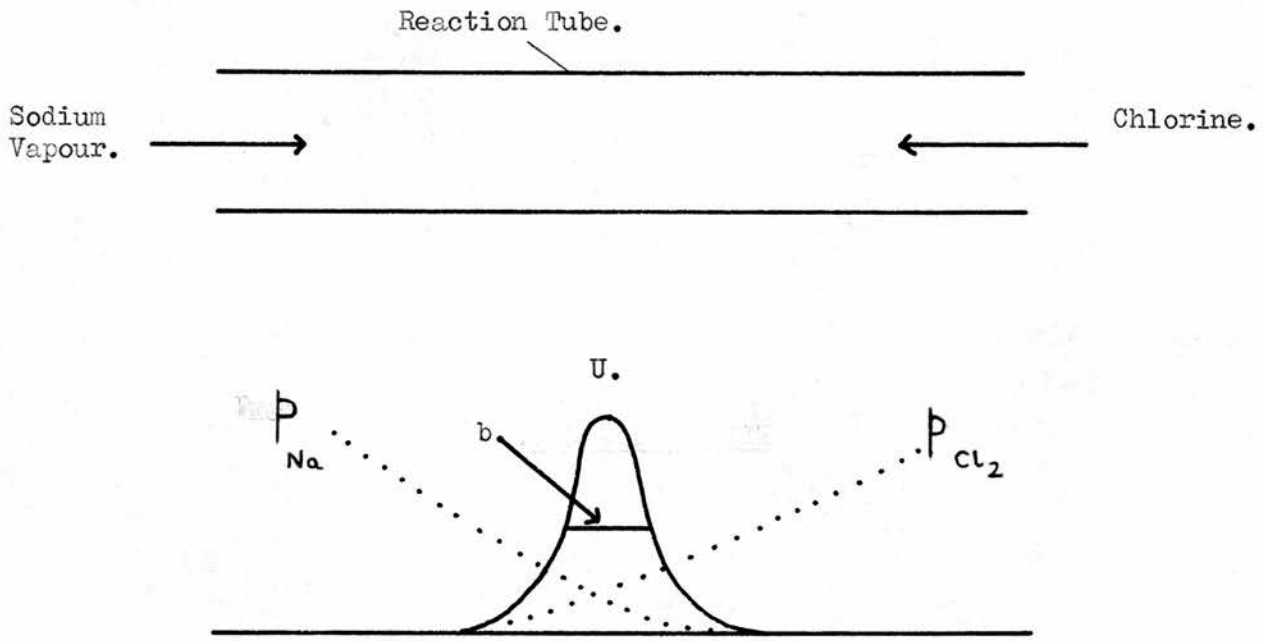

THE NOZZLE FLAMES METHOD.

Fig. 2.

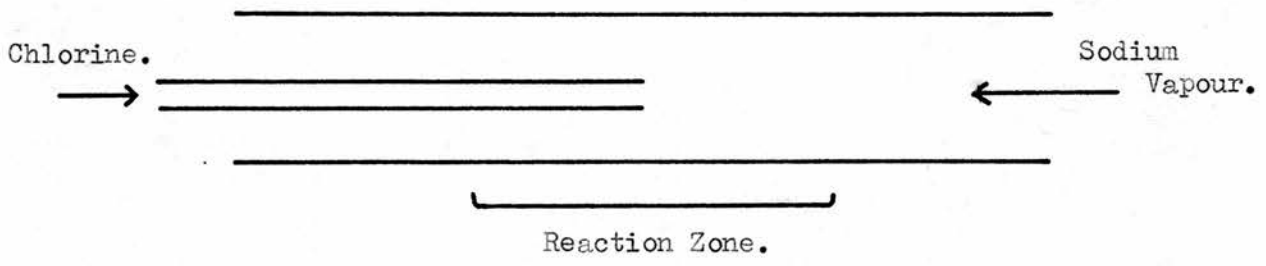

d) The Polanyi Diffusion Flame Methods.

In 1922 Haber and Zisch [9] studied the burning of sodium vapour in Cl_2, Br_2, I_2 and O_2 at atmospheric pressure. In these experiments sodium vapour in a stream of nitrogen was introduced into the reactant and produced a small cone shaped flame which emitted a chemiluminescence later identified as the Na_D line. Polanyi realised that this technique could be used to study chemical reactivity and in 1925 introduced the method of Highly Dilute Flames [10].

(i) The Method of Highly Dilute Flames.

The method is essentially a modification of the ordinary flow method and is suitable for very fast reactions which proceed at virtually every collision and has been applied to the reaction of Na atoms with the halogens and various halides.

The two reactants (e.g. Na and Cl_2) are introduced from the opposite ends of a reaction tube (100 cm. x 3 cm.) maintained at 300-350°C. The pressures are so low (10^{-3}mm.Hg.) that the mean free paths of the reactants are greater than the diameter of the tube so that the gases mix solely by diffusion. As the sodium penetrates into the chlorine it is consumed and its pressure decreases to zero. Similarly with chlorine penetrating into sodium giving the type of graph shown in Fig.1. The reaction tube emitted a chemiluminescence over about 10 cm. near the centre with NaCl deposited on the walls. The chemiluminescence and the highly dilute nature of the system gave rise to the term "Highly Dilute Flames Method". The curve U represents the product $p_{Na} \cdot p_{Cl_2}$ and is plotted either by collecting and weighing the NaCl deposit or by

optical density measurements of the deposit on the tube walls.

The essential feature of the method is the calculation of the rate constant from the breadth of the curve [1]. It is evident that a relationship of this type should exist since the slower the reaction the further the reactants will penetrate into one another before being consumed by reaction. The exact relationship is:-

$$K = \frac{27.}{b^3. 2q. U. k_{Na}. k_{Cl_2}.}$$

where K is the rate constant, k_{Na} and k_{Cl_2} are the diffusion coefficients, q is the cross-section of the tube, U is the amount of reaction and b is the half-breadth of the curve U.

The method is suitable for reactions which proceed at not less than 1 in 100 collisions and which are insensitive to wall phenomena.

From determinations of the rate constants and an examination of the chemiluminescence, Polanyi and his co-workers have obtained considerable data about the reactions of Na and K with the halogens and many volatile halides.

A year later in 1926 the experimental method was modified [11] and it was found that the light emission was greatly increased by using a method known as The Nozzle Flames Method. In this technique the chlorine was introduced into the sodium vapour down a 3 mm. tube as shown in Fig. 2. (p.9). The experiments with this so-called jet arrangement supplied the main data for the explanation of the luminescence phenomena and the associated chemical reactions, namely:-

$$Na + Cl_2 \longrightarrow NaCl + Cl + 40.7 \text{ Kcal.} \qquad (i)$$

$$Cl + Na_2 \longrightarrow NaCl + Na + 80 \text{ Kcal.} \qquad \text{(ii)}$$

$$Na + Cl \xrightarrow{Wall} NaCl + 97.5 \text{ Kcal.} \qquad \text{(iii)}$$

where the heats of reaction are calculated from more recent values of bond dissociation energies and differ from the values in the original paper by a few Kilo-calories. The excitation of the Na_D line requires about 48.3 Kcal. and the chemiluminescence must therefore be associated with reaction (ii) since reaction (i) cannot supply the sufficient energy.

The study of highly dilute flames was continued without much alteration by Polanyi and his co-workers with a study of Na and K reactions with a wide range of organic and hydrogen halides and the halides of certain inorganic elements such as Hg, Sn, Zn and Cd. Further information and many references about these reactions can be found in an excellent review by Bawn[12].

In 1930, however, a major advance was made by Hartel and Polanyi [13] with the introduction of the well-known diffusion flame method.

(ii) The Diffusion Flame Method.

The diffusion flame method is similar to the dilute flames method in the sense that the reaction velocity is derived from measurements of the distance which one component will penetrate into the other before being consumed. In order to make this distance fairly short a foreign gas (usually H_2 or N_2) is added at pressures up to 10 mm. Hg. This slows down diffusion and also acts as a carrier gas for the reactants. The essentials of the apparatus are shown in Fig. 3. (p. 13). The carrier gas flows through a container holding sodium at about 250°C and picks up sodium vapour to a partial pressure of about 2×10^{-3} mm. Hg. The gas

FIGURES 3 & 4.

DIFFUSION FLAME APPARATUS.

Fig. 3.

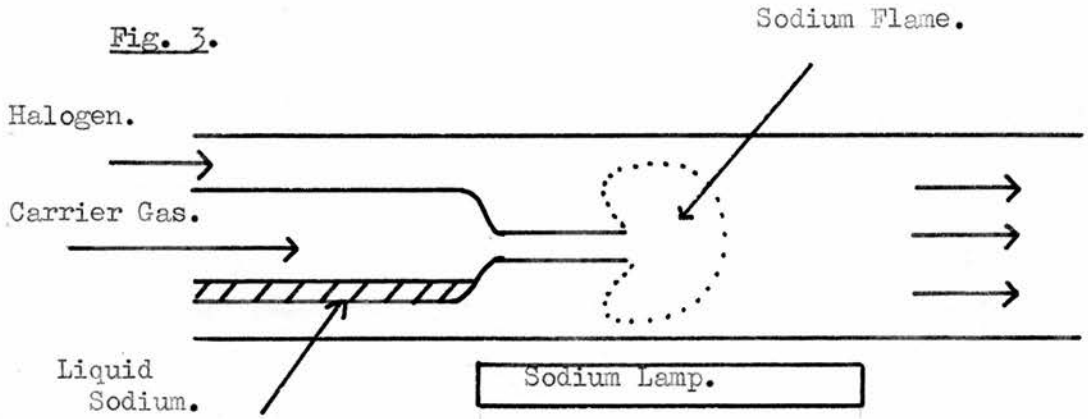

DIFFUSION FLAME STUDIES BY MASS-SPECTROMETRY.

Fig. 4.

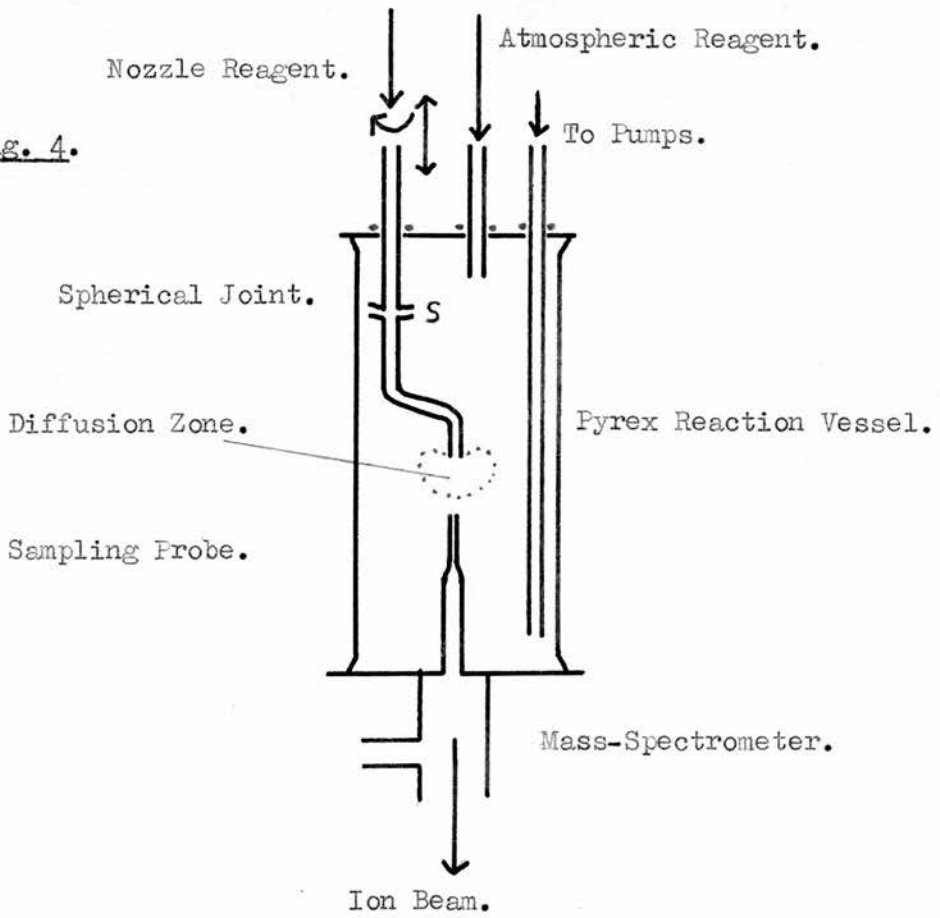

stream carries the sodium vapour through a nozzle (2.5 mm. internal diameter) into the reaction volume (3 cm. diameter tube) where it reacts with the halogen also at a low pressure (10^{-2} to 10^{-1} mm. Hg.). If necessary the sodium vapour fluorescence is excited by an external Na_D resonance lamp giving a visual indication of how far the sodium vapour penetrates into the halogen before its partial pressure has reached the limit of detection.

By considering steady state spherical flame conditions and integrating the following simple formula for the rate constant K may be derived (1):-

$$K = \frac{(\log_e p_T/p_0)^2}{R^2} \cdot \frac{D_{Na}}{p_{X_2}} \qquad \text{(iv)}$$

where p_T is the partial pressure of sodium at the nozzle, P_0 is the limiting pressure of sodium at the edge of the flame, P_{X_2} is the partial pressure of halogen, R the flame radius and D_{Na} the diffusion coefficient of sodium under the temperature and pressure conditions of the experiment.

By slight variation of P_{X_2} the flame radius R may be adjusted and a series of values for K obtained and averaged to give a more accurate rate constant. In practice in the production of a convenient sized flame (about 3 cm. diameter) the pressure of the atmospheric reagent is gradually increased from zero and the flame shrinks back to the nozzle. The pressure required to give a certain flame size immediately gives some data about the reaction rate. For example with CH_3I where reaction occurs at almost every collision a partial pressure of 10^{-3} mm. is sufficient to produce a good flame but on the other hand CH_3F even at

10 mm. Hg. produces such a slow reaction that the whole reaction tube remains full of sodium vapour (i.e. less than 1 in 10^6 collisions are effective). In general, the range of reaction rates which may be studied lie between 1 in 10 and 1 in 10^5 effective collisions.

The derivation of equation (iv) depends on the validity of several important assumptions which in this early work may not have been strictly fulfilled. Heller [14] in 1937 made a thorough and elaborate investigation of the method and determined mathematically the conditions necessary to give good rate constant data. The following conditions are derived from a summary in his original paper.

(i) For uniform distribution of the atmospheric reagent in the flame the value v/D must be less than 12 cm^{-1}, where v is the nozzle velocity and D the diffusion coefficient of the nozzle reagent.

(ii) The atmospheric reagent presure must be as low as possible to eliminate back diffusion into the nozzle. This is fulfilled for $v/D > 5$ cm^{-1}.

(iii) Flames must be greater than 3 cm. and less than 5.5 cm. diameter for uniform pressure of the atmospheric reagent and negligible back diffusion. Smaller flames fail even though v/D lies within the correct range.

(iv) The atmospheric reagent pressure must be sufficiently low such that it has little effect on the diffusion coefficient of the nozzle reagent.

Using the original method Hartel and Polanyi [13] and Hartel, Meer and Polanyi [15] systematically examined the reactivity of a wide range of organic halides with atomic sodium. The data showed reactivity which

increased with:-

(a) Variation of halogen from F to I in the Me,Et, and Ph halides.

(b) Lengthening of the hydrocarbon chain.

(c) Passage from primary, secondary to tertiary carbon.

(d) Introduction of double bonds or carbonyl groups adjacent to the halogen.

(e) Multiple substitution by halogen.

The laws were simple but precise and yielded much of the early information and data in the study of chemical reactivity. In the next few years Polanyi and his co-workers successfully extended the method to the reactions of several inorganic halides with various metallic atoms. A discussion of these reactions together with the relevant references can be found in reviews by Bawn [12] in 1942 and Warhurst [16] in 1951 and these will not be discussed in this report.

In the calculation of the rate constant, the diffusion flame method relied on rather approximate and vague assumptions about the stationary reaction state. A modified method for determining the rate constant was developed by Frommer and Polanyi [17] in 1934. The method was based upon the general experimental features of the diffusion flame method but utilised a different set of measurements for the determination of K. The new method, known as the Life Period Method and applicable to a wider range of reaction velocities and reactants than the diffusion flame method is outlined below.

(iii) The Life Period Method.

Sodium vapour together with an inert carrier gas is introduced via a nozzle into an excess of halide forming a stationary reaction zone as in the diffusion flame method. Instead of measuring the size of the flame, the number of Na atoms introduced in unit time (n) and the number present in the steady state flame (N) are measured and the ratio $n/N = T$ represents the average lifetime (T) of Na atoms in the reaction vessel. By considering a steady state volume element and integrating for total reaction the equations $n = K.c.N.$ or $K = n/c.N. = 1/c.T.$ may be readily derived, where c is the concentration of halogen and K the rate constant. Both n and c can be determined from flow rate data and the temperature of the sodium oven. N is more difficult but can be derived by measuring the absorption of Na_D resonance radiation when passed through the system. In the initial investigations this latter was determined by photographic measurements but was soon replaced by a sensitive photometer which measured the light intensity directly (18).

(iv) Some Relevant Comments and Recent Work on the Diffusion Flame Method.

The Polanyi diffusion flame method presents a convenient way of measuring the rate constants of a wide range of fast chemical reactions. The flame is usually small in relation to the reaction vessel such that reaction takes place entirely in the gas phase and the method is therefore suitable for reactions sensitive to wall effects. Since fast reactions, especially those involving free atoms or radicals are often particularly sensitive to surface effects it is rather surprising that the method has not been more widely used in modern reaction kinetic studies.

Since Polanyi's pioneering work a series of papers on the diffusion flame method have been published in Canada and America by Cvetanovic and Le Roy [19][20], Smith [21], and Reed and Rabinovitch [22] but these have mainly dealt with the theoretical aspects of the method.

In 1952 however, Garvin and Kistiakowsky [23][24] realised the potential of the method and used a modified flame method to study the rate of reaction of boron trifluoride with ammonia and various amines according to the general equation:-

$$BF_3 + NR_3 \longrightarrow F_3B : NR_3$$

The method used a reaction system similar to the one used by Polanyi. The reaction vessel was a pyrex cylinder 40 cm. long and 10 cm. in diameter. The nozzle reagent in a carrier gas was introduced into the system by a fine jet (.09 to .05 cm. internal diameter) at a velocity of 10^3 to 10^4 cm./sec. and reacted with the atmospheric reagent in the usual way. The diffusion flame, or rather diffusion zone had a diameter of a few centimetres and was scanned by a thermocouple probe fitted through a sliding seal assembly. The reaction, as is generally the case in very fast reactions is highly exothermic such that the heat developed at any point in the flame is a measure of the extent of reaction. In this way Kistiakowsky obtained rate constants reproducible to within a factor of 2 for the association of BF_3 with mono, di and tri-methylamines. The original papers should be consulted for further details.

This work placed the diffusion flame technique on a more general level. However, the analysis of a flame by a fine thermocouple probe left much to be desired. Ideally, the detection system should be as

general as possible and if the concentrations of reactants, intermediates and products could be determined specifically within the flame, the accuracy, applicability and general handling of the flame system would be greatly assisted.

This has been the basic aim of some recent work in St. Andrews in 1961 [25]. An apparatus was constructed based on the Polanyi flame technique and used to study the fast gaseous reactions between H_2O and SO_3 and also between Hg and I_2. A unique feature of the system was the analysis of the diffusion zone by a fine mass-spectrometer probe. A diagram of the general apparatus is shown in Fig. 4. (p.13). For practical reasons the flame was scanned by moving the nozzle rather than the mass-spectrometer leak. The nozzle was fitted to a spherical joint S and with a system of sliding seals the flame could be moved relative to the leak such that horizontal and vertical scanning facilities were available. The reaction vessel was fitted directly over the mass-spectrometer so that the product H_2SO_4 in the case of the H_2O and SO_3 reaction might be detected. In fact H_2SO_4 was not detected and the majority of the work was done with the reaction between Hg and I_2. Concentration contours of the nozzle reagent were plotted throughout the flame clearly demonstrating the spherical nature of the reaction zone and an analysis of specific reactant gradients yielded the kinetic data of the reaction.

The work described in this thesis originates from the above idea. If a discharge system is introduced into the nozzle line a diffusion flame of atomic species (e.g. atomic hydrogen or nitrogen) could be

produced and the diffusion flame monitored with the mass-spectrometer probe system. The mass-spectrometer could most probably be modified to detect these free atoms (providing that the probe-ion box distance is short) such that the majority of the reaction species (reactants, intermediates and products) could be monitored in the flame. The reaction would take place purely in the gas phase without the complications of wall interactions and the method should be applicable to the study of a very wide range of atomic reactions.

Before proceeding to the actual experimental data, further relevant literature will be discussed. In each case this will be discussed in relation to the final problem. For example, it seemed evident that a discharge system would be the most suitable means of producing a steady supply of atoms for a flame analysis and although a complete survey of the methods of producing atoms will be given emphasis will be placed on discharge methods. Similarly in an outline of the methods of detecting and analysing free atoms the emphasis will be placed on mass-spectrometric techniques.

3. THE PRODUCTION OF FREE ATOMS.

a) Introduction.

For the production of a Polanyi-type diffusion flame with atomic nitrogen or hydrogen as the nozzle reagent it is necessary to provide a continuous and steady supply of free atoms. Ideally, the atoms should be present in a single electronic state (preferably the ground state) but this is not always easy to achieve.

Atoms are produced from stable molecules by supplying sufficient energy for dissociation. This energy can be supplied in a number of ways but the electrical discharge is now universally recognised as the most effective and convenient way of producing atoms in high concentration in flow systems.

The Wood's tube, [26] introduced in 1922 is probably the best known method of producing atoms by a low frequency electrical discharge and was originally devised as a tube for investigating the Balmer series of hydrogen. It has since been used extensively without much alteration in numerous investigations of atomic hydrogen, nitrogen and oxygen but is now generally replaced by the electrodeless discharge. This is much more simple in construction, has higher stability, is more efficient and gives atomic products of greater purity since there is no electrode contamination of the gases.

Discharge techniques are not the only methods used in atom production and it is relevant at this stage to discuss the merits and disadvantages of the methods available for producing free atoms. The methods will be discussed generally but an emphasis placed on techniques

suitable for atomic hydrogen and nitrogen.

b) Thermal Methods.

Thermal methods have been used to produce low concentrations of atoms in both static and flow systems. The method of supplying this energy depends largely on the bond dissociation energy involved. For example, the atoms of weakly bonded molecules such as Na_2 vapour may be formed to a certain extent simply by flowing the gas through a hot oven. The method is successful for sodium atoms but has not been widely applied to other species since even with the weakest halogen, iodine, the equilibrium concentration of atoms at moderate temperatures is very low and photochemical methods of generating these atoms are preferred.

For molecules of high dissociation energy (D_{H_2} = 103, D_{O_2} = 117 Kcal. per mole.)much higher temperatures (about 2000°K) are required to give any appreciable dissociation. This temperature is impossible to obtain by normal oven techniques and it is necessary to incorporate a heated filament in the gas stream. This rather limits the applicability of the method since there must be no chemical interaction of the gas with the hot filament.

Langmuir in 1912 [27] produced atomic hydrogen by dissociating molecular hydrogen on a hot tungsten filament in an ordinary lamp bulb. The atoms diffused to the walls of the vessel where the reducing action on various metallic oxides was shown. The method was used again in 1932 by Storch [28] and in 1934 by Belchetz and Rideal [29] in work on free radicals.

In 1949 Le Roy [30] developed the method of producing atomic

FIGURES 5 and 6.

REACTION SYSTEM BY LE ROY.

Fig. 5.

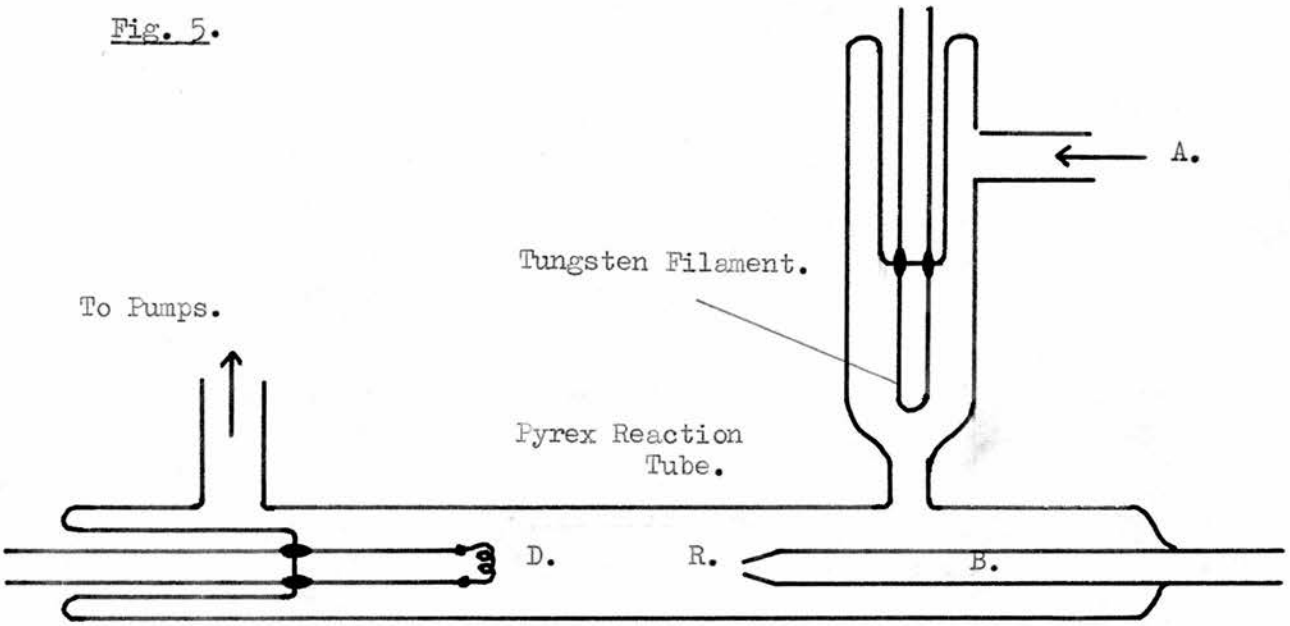

WOOD-BONHOEFFER DISCHARGE TUBE.

Fig. 6.

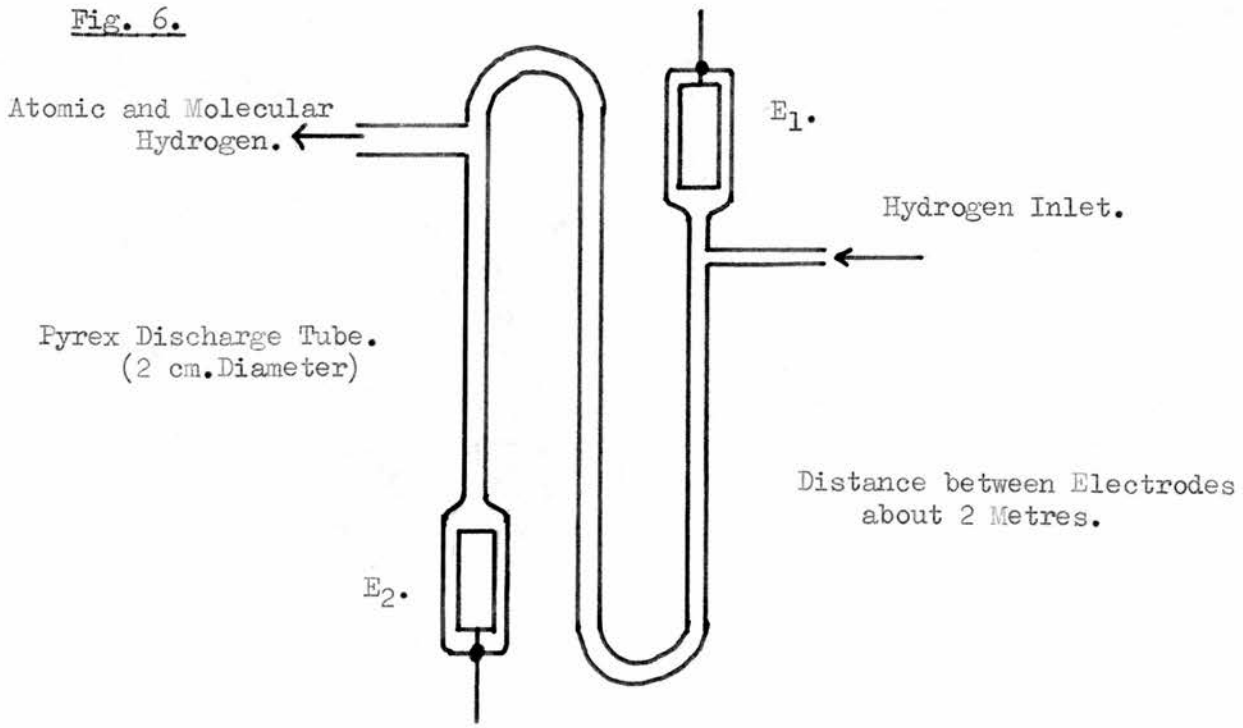

hydrogen in order to study its chemical reactivity. The essential features of the apparatus are shown in Fig. 5. Hydrogen (0.1 mm. Hg.) enters at A and flows at high speed past a hot tungsten filament maintained at about 1700°K. Dissociation occurs and the resulting atom-molecule mixture enters the reaction vessel R. The second reagent enters the system via the inlet B and the interaction takes place in the reaction vessel. The concentration of hydrogen atoms with and without the reagent is estimated by the temperature of the platinum detector D. The platinum acts as a good catalytic surface for atom recombination and the heat generated by this process is measured by the resistance change of the platinum. In order to inhibit the loss of atoms on the reaction vessel walls the system was thoroughly coated with meta-phosphoric acid. Further details about this detection method are discussed in a later section.

Recently Klein and Scheer [31] have used the method to produce atomic hydrogen (0.1% H) in low pressure static systems and there is even a report in the literature of a supply containing 8 to 23% H at 10 to 30 mm. Hg. from a filament maintained at 2600°K [32].

c) Photochemical Methods.

In recent years photochemical techniques have been widely used for producing free atoms in static or flow systems over a wide range of pressures. Dissociation occurs as a result of the absorption of photon energy in excess of the bond dissociation energy. The amount of energy absorbed per molecule can be controlled by the incident light wave-length and the rate of absorption controlled by the light intensity.

Generally, since even high power lamps have low photon emission the concentration of atoms produced in this way is usually low.

Unfortunately, in certain cases molecules do not absorb in accessible regions of the spectrum even though these energies would be quite adequate for dissociation. N_2, H_2 and O_2 for example absorb only in the extreme vacuum ultra-violet region which produces serious experimental difficulties. The halogens on the other hand readily absorb and are dissociated by 4,800 Å radiation.

Since the direct photolysis of N_2, H_2 and O_2 is not easy two other photochemical techniques have been developed. In the first method the atomic species is generated indirectly by photolysis of molecules which will readily absorb. For example, nitrogen atoms are formed in the primary step in the photolysis of N_2O and this technique has been used in certain kinetic studies.

In the second method the energy for dissociation is relayed by a photo-sensitiser. Hydrogen has a dissociation energy of 103 Kcal/mole. corresponding to a quantum of wave-length 2,776 Å but absorption does not begin until 850 Å. If a substance is added which will absorb readily at 2,776 Å and transfer its energy to hydrogen a photo-sensitised decomposition can be produced. Generally the sensitisers are metallic atoms (particularly mercury) since they are readily excited by similar resonance lamps.

Photochemical techniques for atom production are described with many references in several excellent texts (33)(34)(35) and it is not proposed to discuss them further in this report.

d) Radiolysis.

This technique has found little application to the production of free atoms. γ-radiation has been used to a certain extent in atomic nitrogen studies but the radiation is inefficient and is also thought to yield a series of ionised species formed both from direct γ-ray collisions and from electron impact with high energy electrons liberated in the primary collisions or derived from the reaction vessel walls. The true atom reactions are usually difficult to isolate from the total results.

e) Discharge Systems.

The discharge tube has been widely used for a number of years to produce high concentrations of free atoms in flow systems and has recently been reviewed and discussed by Shaw (36) and Jennings (35). The original techniques of the low frequency discharge, as in the well-known Wood's tube, have now been superseded by the electrodeless radio-frequency and micro-wave discharges and it is convenient to classify the methods in this way for this discussion. In each case the atoms are generated mainly from collisions of high energy electrons with gaseous molecules, where the electron accelerating influence is provided by the applied electric field (37)(38). As would be expected the atoms are generated together with a complex series of ionised and activated species. Surprisingly however, the atoms are produced almost entirely in the ground state and the percentage of higher electronic atomic states is extremely small.

(i) Low Frequency Discharges.

The low frequency electrical discharge was first described by Wood in 1922 (26) in a study of the atomic spectra of hydrogen. The method

was quickly modified by Taylor and Marshall (39) and Bonhoeffer (40) to produce atomic hydrogen for reaction studies. The tube has since remained virtually unchanged and is generally known as the Wood-Bonhoeffer tube. A typical design of the tube is shown in Fig. 6. (p.23). The electrodes E_1 and E_2 are usually sheet aluminium sealed into the tube as shown. The exit dissociated gas is extracted from the centre of the discharge tube since this is the region of highest atomic concentration due to the catalytic effect of the metal electrodes. The discharge is activated by several kilo-volts (A.C.) at 250 to 500 milliamps. This input power produces considerable heat and it is usually necessary to cool the tube with an air blast or water circulation. Hydrogen pressures vary between 0.2 and 1 mm. Hg. since this is the easiest range in which to get the discharge to strike and for a good atomic yield the discharge should be a fiery purple. A high concentration of molecules is indicated by a blue colour (see p. 182 ref. 5.). The output of atoms depends upon the hydrogen flow rate and linear velocities of several metres per second are quite common.

As mentioned earlier the discharge tube has remained unchanged since 1922. Although originally developed for atomic hydrogen studies it has been widely applied to the production of atomic oxygen and nitrogen and to a lesser extent to the halogens (33).

In nitrogen where the bond dissociation energy is relatively large it is often better to use a pulsed or condensed discharge (41). The discharge system is essentially the same as the Wood-Bonhoeffer tube but the discharge power is provided by a high voltage source pulsing at 5 to 30 cycles/sec. A satisfactory explanation as to why this is

better than a conventional A.C. supply is not available but the pulses are much more powerful than could be maintained steadily and this may provide the answer. The pulsed discharge has been widely used in active nitrogen studies [36] and recently Winkler has reported 100% dissociation in a condensed nitrogen discharge [42][43].

(ii) The Radio-Frequency Discharge (Low Frequency).

In this case the electrons in the discharge tube are accelerated by the radio-frequency field applied to the tube. It is found that the power required for breakdown of the gas and to maintain a powerful discharge is very much less that the equivalent operating power of a Wood's tube [36][37][38]. Also, since the effect of the radio-frequency field is not appreciably diminished by the glass discharge tube and the electrodes can be fitted outside the tube, this has led to the term electrodeless discharge. This has the advantage that there is now no metallic surfaces in the discharge tube and this greatly assists the atom concentration.

Generally radio-frequency discharge tubes are quite simple in construction and dur to their higher efficiency less input power, usually 200 to 300 watts, is required. This power can be provided by radio transmitters, industrial radio-frequency heating units cr diathermy units and can be coupled to the discharge tube either by electrostatic or electromagnetic coupling as shown in Fig. 16. (p. 79). In the electromagnetic case the radio-frequency power passes through a coil wound round the discharge tube. In electrostatic coupling the power is transferred to the discharge by sleeve aluminium electrodes

wrapped round the tube. The coil size and electrode dimensions will depend largely on the experimental conditions and the diagrams serve only as a general guide. At 300 watts the radio-frequency discharge tube can supply an equivalent concentration of atoms to a Wood's tube operating at around 1,000 watts. However, a 300 watt radio-frequency discharge produces sufficient heat to melt pyrex glass and the discharge tubes are generally air-cooled pyrex, or made from quartz. Some attempts have been made to cool the discharge tubes by water circulation(44) but this has generally been avoided due to loss of power into the water.

With radio-frequency discharges there has been some concern over the spread of the glow region, as it is not easy to confine the glow to the electrode regions. This spread is most apparent at about 0.1 mm. and can spread several metres down the exit line. Earthed metal screens around the tube sometimes reduced this spread but generally not significantly (45).

(iii) The Micro-Wave Discharge.

Micro-wave discharges have become popular over the last twenty years following the development of powerful micro-wave generators. The method is analogous to the low frequency discharge system and is again electrodeless. The generators usually supply a few hundred watts at 2,500 to 3,000 Mc/sec. and because of this very high frequency special coupling methods are necessary. An excellent survey into the general experimental wave-guide systems can be found in the review by Shaw (36). Generally the discharge tube is a quartz tube passing through a tuned

resonance cavity fed by a standard 3" x 1" wave-guide from the generator. It is usually necessary to initiate the discharge with a tesla coil spark and an attenuator must be fitted to absorb the energy before the discharge strikes. The electric field is limited to the cavity and produces extremely intense and localised discharges with little tendency to spread. The technique can be applied to a wide range of pressures, the upper limit being a few centimetres of mercury and has been used extensively in the production of atoms from nitrogen, oxygen, hydrogen and certain halogens.

4. SURFACE EFFECTS AND WALL INHIBITION.

It has been known for a long time that the condition and nature of the discharge tube walls can critically govern the output of atoms. A series of materials have been suggested and used, with varying degrees of success, to inhibit the recombination processes on the walls and hence increase the atomic yield. Generally, this work has been purely empirical with little or no attempts to correlate and understand the nature of this wall phenomenon.

In early discharge tube experiments, Wood [26] noticed that traces of water vapour in the hydrogen stream greatly assisted the production of atoms. He explained this by the formation of a thin adsorbed water layer on the glass which reduced surface recombination of the atoms. A few years later, presumably in a search for a material with a strong affinity for water and which could be easily deposited on the discharge tube walls, Von Wartenberg and Schulze [46] tried phosphoric acid with immediate success. Since then, phosphoric acid, particularly meta-phosphoric acid and a wide range of salts have been used in wall inhibition but in all cases the coating had to be moist for maximum effect.

Smith in 1943 [47] examined the poisoning effect of these materials in hydrogen atom recombination. Hydrogen was dissociated in a Wood's tube and the atoms diffused down a side arm coated with the material under investigation. The atoms which were not lost by wall recombination were detected at the end of the side arm with a platinum-thermocouple probe. A high probe temperature thus indicated

good inhibition. In this way Smith investigated the inhibition properties of meta-phosphoric acid, quartz, pyrex, K_2SiO_3, KCl, KOH, K_2CO_3, Na_3PO_4 and certain metallic oxides under moist and dry conditions and was also able to estimate the recombination coefficients for these surfaces. Further details may be obtained by consulting the original paper but of the compounds tested meta-phosphoric acid was the most efficient inhibitor and in all cases the results clearly demonstrated the greatly reduced inhibition with the dry coatings.

More recently a variety of other materials have been suggested as inhibitors. These include teflon, paraffin wax, polyethylene [48][49] and certain non-wetting agents [50][51]. In general these coatings are not as good as meta-phosphoric acid, often give irreproducible results and in certain cases require traces of water vapour for effective poisoning.

In the case of active nitrogen where the atoms are relatively stable to wall collisions, surface deactivation is less important. A wide range of inhibitors have been tested in atomic nitrogen systems with the same general results as obtained for hydrogen but with less distinct results. Of the materials tested meta-phosphoric acid always gave the most efficient deactivation. It is not proposed to discuss these materials in detail since there is a recent comprehensive review on active nitrogen by Mannella [52].

5. THE DETECTION AND ESTIMATION OF FREE ATOMS.

A variety of methods have been used to detect and estimate free gaseous atoms. Many of these methods date back to the 1920's and were introduced only a few years after the Wood-Bonhoeffer discharge tube became available. Generally the methods were inaccurate and irreproducible. Relative atom concentrations were fairly successful but attempts to measure the same atom concentration in absolute terms with different detectors gave results differing by as much as 25%.(53)

Ideally, in a reaction study the detector should be capable of monitoring the atoms at a specific point without interfering with the reaction system to any appreciable extent. Usually, since atoms are present at a fraction of a millimetre pressure this ideal state is not easy to achieve.

The general methods for the detection and estimation of free atoms are outlined below and have recently been reviewed by Jennings (35) and Steacie (33). The methods are discussed generally but the mass-spectrometric techniques being relevant to this report are discussed in detail.

a) Calorimetry.

In the calorimetric techniques the concentration of free atoms is determined from the heat developed when the atoms recombine on a catalytic surface. The heat may be measured by the temperature rise of a probe or by isothermal calorimetry. In the latter case, the catalyst is maintained electrically at a certain temperature and the decrease in electrical input required to maintain this temperature

when atoms are present is a measure of the atom concentration.

The methods have been used on hydrogen, nitrogen and oxygen atoms and to a lesser extent on halogen atoms. The amount of heat liberated by recombination is essentially the bond dissociation energy and the detection sensitivity should increase with increasing bond strength. This is only partly true however since the catalytic activity of the surface differs for each atomic species. Hydrogen atoms recombine very readily on metal surfaces and on clean platinum the recombination coefficient is virtually unity. Nitrogen atoms on the other hand are known to survive many wall collisions even with metals and it is not surprising that much of the work with catalytic probes has been limited to atomic hydrogen studies.

In an early paper, Wood [26] reported that certain metals when placed in atomic hydrogen streams became incandescent and suggested that this could be used as a visual indication of the presence of the atomic species. Shortly afterwards in 1924 Bonhoeffer [40] displayed the method of the catalytic probe by placing coated thermometers in the atom stream and noting the temperature rise. The method was rather crude and was soon modified by a number of workers by replacing the thermometer with a fine thermocouple junction.

Relative atom concentrations have been measured reasonably well in this way but absolute measurements were difficult. Cooling corrections, depending upon the probe temperature and the flow rate over the probe were difficult to apply and the catalytic surface was readily prone to poisoning. Probe cleaning by the usual flash or thermal heating methods

were difficult to arrange and this factor coupled with the other uncertainties has rather restricted the use of the method.

The isothermal calorimeter was introduced in an attempt to overcome these difficult cooling corrections. Also, where the catalytic probe is designed to remove only a few atoms from the system, the isothermal calorimeter removes them all and thus yields absolute atom concentrations. Tollefson and Le Roy [30] have developed the method as an accurate quantitative detector for hydrogen atoms using the well-known hot wire method. The calorimeter consisted of a fine platinum filament forming part of a Wheatstone's bridge circuit so that its resistance could be accurately measured. The bridge current was adjusted so that the filament resistance corresponded to a temperature of about 400°C. When hydrogen atoms were present less bridge current was required to maintain the filment at 400°C and the total energy of recombination could be accurately determined. Cooling corrections were not necessary since the filament temperature was identical for each measurement and the poisoning uncertainties eliminated by operating the filament at 400°C.

A variation of the hot wire technique has been used by Schwab [54] and his co-workers in chlorine atom studies. The calorimeter consisted of a thermocouple fixed to a small metal plate. The plate could be heated electrically and was maintained at a certain temperature by monitoring the thermocouple output. Again, the decrease in electrical input with atoms present indicated the concentration of free atoms.

b) The Wrede Gauge

The pressure difference set up by the diffusion and subsequent recombination through a small orifice in the atom stream has been used to measure the concentration of atoms. The method was introduced by Wrede [55] and Harteck [56] in 1928 and the apparatus is known as the Wrede-Harteck or quite often simply the Wrede gauge. For a variety of reasons the method has been limited to atomic hydrogen studies but some work has been done on atomic nitrogen and oxygen estimations. The method is fairly accurate and gives absolute concentrations but can only be used in simple systems containing a relatively large atom concentration normally associated with discharge techniques.

The gas stream containing the atomic and molecular species flows down a tube and passes a small capillary or slit in the tube wall leading to a small closed volume containing a catalytic material. A sensitive differential pressure gauge records the pressure developed between the gas stream and the catalytic volume. Providing that the mean free path of the gas is less than the orifice diameter the flow through the hole is purely by diffusion and the recombination of atoms in the catalytic volume produces the pressure differential.

The mathematical treatment of the steady state diffusion system has recently been reviewed in detail by Greaves and Linnett [58]. Essentially hydrogen atoms diffuse $\sqrt{2}$ times faster than the parent molecule but a molecule transports twice as much mass as an atom. Thus if p_1 is the total pressure in the gas stream and p_2 the pressure in the catalytic volume then for 100% atoms:-

$$p_1/p_2 = 2/\sqrt{2} = 1.41$$

and for a fraction α, of atoms:-

$$\alpha = \frac{p_1 - p_2}{p_1 (1 - \frac{1}{2}\sqrt{2})} = \frac{3.41 \ (\Delta p)}{p_1}$$

where Δp is the pressure difference across the orifice.

The time taken to reach the steady state equilibrium is directly dependent on the catalytic volume and the differential pressure is usually measured with a Pirani (thermal conductivity) gauge. McLeod gauges are avoided because of their large volumes but simple oil filled U-tube manometers have been used in high atom concentration measurements.

Generally the Wrede gauge is limited to simple systems since foreign gases must be absent from the gas stream but it has been shown that relatively large molecules present at 10 to 15% do not appreciably alter the gauge reading.(59).

c) Spectroscopic Methods.

(i) General Spectroscopy.

A very wide range of literature is available on the study of gaseous free radical reactions by absorption spectroscopy. Much of this work is related to the detection and estimation of unstable radicals in kinetic spectroscopic studies in flash photolysis. A study of this literature is beyond the scope of this report and there is an excellent review together with many references compiled by Norrish and Thrush (7). The techniques have not been extended to any appreciable degree to the analysis of non-metallic atoms for a variety of reasons.

Emission spectra has been little used, since it requires the atom to be present in an excited state. Such excited atoms are readily

detected in discharges but the method has found little application to kinetic studies and other techniques are generally preferred. However, certain specific emission spectroscopic methods are extremely useful. For example, the nitrogen afterglow is now known to be an emission spectrum from activated nitrogen molecules formed in the 3rd body recombination of N (^4S) nitrogen atoms [110]. The intensity of this emission is readily related to the concentration of atoms and this has been used on certain occasions for monitoring nitrogen atoms [61].

As mentioned earlier absorption spectroscopy has found little application to kinetic studies involving free atoms. In general, ground state atoms apart from metallic atoms do not absorb in readily accessible parts of the spectrum. In spite of this, Tanaka, Jursa and Leblanc [62] have examined the absorption spectrum of the nitrogen afterglow in the 1000 to 1500 Å region using a 2 metre vacuum ultra-violet spectrograph. They were able to identify the absorption spectrum of ground state N (^4S) atoms (0.1% N) together with traces of N (^2P) and N (^2D) metastable atomic species. These latter excited states were present at about 1/500th of the N (^4S) atom concentration.

(ii) Micro-wave Spectroscopy.

It seems likely that with the major advances in micro-wave technology in the last few years the micro-wave method of detecting atoms and free radicals will soon become an important analytical method. Essentially, micro-wave techniques can be divided into two main groups. In the first case the method is analogous to the normal absorption spectra techniques except that the minute energies at micro-wave

frequencies give pure simple rotational spectra. The experimental equipment and the analysis of the data is more complex than studies in the normal regions for a variety of reasons. The method is applicable to the studies of free atoms and radicals but so far has been mainly limited to radical detection. A detailed discussion of the method will not be given here and further experimental information and some spectral data on OH and OD radicals may be found in a text by Ingram (63).

The second and more important micro-wave technique is the Electron Spin Resonance (E.S.R.) method. In this case a powerful magnetic field is used to alter the normally inaccessible electron spin transitions to the micro-wave region. For analysis by E.S.R. the entity must possess a magnetic moment associated with an unpaired electron which makes it ideally suited to atom and radical studies. In the strong magnetic field the free electron will align its spin and magnetic moment either parallel or anti-parallel to the applied field. The micro-wave generator frequency can then be adjusted until the absorption frequencies are located. The absorption is specific to the atom or radical and the intensity of absorption is dependent upon the concentration of atoms or radicals. The method is extremely sensitive and partial atom pressures of 10^{-3}mm. Hg. and less can be readily detected. The method has been used to a limited exetent in atomic nitrogen, oxygen and hydrogen studies and further relevant information can be found in references (35)(63).

d) Chemical Methods.

A variety of chemical methods have been devised to demonstrate the presence of free atoms. Among the earliest of these was the reduction of metallic oxides by atomic hydrogen in 1922 by Cario and Franck [64]. In recent years Melville and Robb [65] have developed the use of MO_3 as a quantitative test for atomic hydrogen. The oxide turns blue in the presence of the atoms and with care the rate of change of colour may be calibrated.

Chemical methods have mainly been used with atomic oxygen and nitrogen using the well-known titration techniques. Hydrogen atoms are best analysed by physical methods although tracer methods have been used in certain cases [66]. Farkas and Sachsse [67] for example have used the para-ortho conversion of hydrogen, catalysed by atomic hydrogen to measure the atom concentration in the mercury photosensitised decomposition of hydrogen using the para-ortho kinetic data compiled by Geib and Harteck [68], and Farkas [69].

In a directly analogous manner the exchange reactions

$$H + D_2 \longrightarrow HD + D$$

$$D + H_2 \longrightarrow HD + H$$

can be used to measure the concentration of atomic hydrogen. The kinetics of this exchange has been investigated by Farkas and Farkas [70] and the data enabled Trenner, Morikava and Taylor [71] to study the action of atomic hydrogen with certain paraffins. More recently, Schiff [53] and his co-workers have used the very fast reaction of D with C_2H_4 to monitor deuterium atom concentrations. The reaction

yields a variety of deuterated products and the total deuterium yield in these products indicates the atom input rate.

In oxygen atom detection the very fast reaction

$$O + NO_2 \longrightarrow O_2 + NO \qquad (v).$$

followed by the relatively slow

$$O + NO \longrightarrow NO_2 + h\nu. \qquad (vi).$$

has been used to estimate atomic oxygen concentrations [72]. A small bleed of NO_2 is fed into the atom stream and the NO from reaction (v) reacts with oxygen atoms as in (vi) producing the well-known white-green air afterglow. As the NO_2 injection rate is increased more NO is formed but there are now less oxygen atoms present to produce the glow. Finally, a point is reached when the afterglow is just extinguished and then the input rate of NO_2 and O are equivalent. The method gives surprisingly accurate and reproducible results and has been used widely in investigations of atomic oxygen reactions [35].

In nitrogen, two different titration techniques have been used. The first method utilises the very fast reaction

$$N + NO \longrightarrow N_2 + O \qquad (vii).$$

in a directly analogous way to that used in atomic oxygen analysis. If a small quantity of NO is added to the nitrogen atom stream reaction (vii) converts the nitrogen atoms to oxygen atoms almost instantaneously. The system then contains oxygen and nitrogen atoms and a blue emission

$$N + O + M \longrightarrow NO^{*} + M$$

$$NO^{*} \longrightarrow NO + h\nu. \quad (\text{blue})$$

is observed. If the nitric oxide input rate is increased such that all

the nitrogen atoms are consumed the oxygen atoms then react:-

$$O + NO \longrightarrow NO_2 + h\nu. \text{ (white-green)}$$

thus, with increasing nitric oxide injection rate the familiar yellow nitrogen afterglow turns blue then white-green. At the onset of the white-green the NO and N flow rates are equal.

In the second titration technique nitrogen atoms are analysed by the HCN formed by:-

$$N + C_2H_4 \longrightarrow HCN + CH_3$$

This reaction is known to be very rapid and is thought to give a quantitative yield of HCN. The HCN is trapped out of the gas stream over a period of time and enables the nitrogen atom flow rate to be calculated.

The two titration techniques have been widely used in nitrogen atom studies and on the whole give good reproducible results [52]. Unfortunately, attempts to measure the same nitrogen atom concentration by the two methods gives rather conflicting results with the NO method yielding N flow rates as much as 1.5 times higher than expected from the HCN formation [73]. An investigation of these two reactions forms the major part of the work described in this thesis and they are discussed in more detail in a later section.

6. MASS-SPECTROMETRY

a) Introduction.

The mass-spectrometer offers an excellent technique for the investigation of reactions involving free atoms and radicals.[74][75][76][77] The method is extremely specific and essentially identifies the radical by its molecular weight. The mass-spectrometer ion-gun operates at pressures around 10^{-5} mm. Hg. such that reactions may be studied without sampling to any appreciable extent from the system. The method is applicable to mixed systems recording both the stable and free radical species and with fast scanning devices can record rapid changes in the concentration of several species at once.

In the work described in this thesis the interest lies intrinsically in the mass-spectrometer as a method of analysing for nitrogen and hydrogen atoms in diffusion flame experiments. Generally however, the development of atomic and radical mass-spectrometers has been slow, being hindered by a variety of difficult experimental problems. In spite of these difficulties about 75 different radicals have so far been successfully detected from reaction systems [74]. In free atom work, which is basically an extension of free radical mass-spectrometry only the very stable nitrogen atoms which are known to survive many wall collisions have been analysed to any appreciable extent.

As explained later in this thesis it was found extremely difficult to detect atomic hydrogen. Atomic nitrogen was simple to produce, required less surface inhibition and was readily detected by the mass-spectrometer with sufficient sensitivity for a diffusion flame analysis

FIGURES 7 and 9.

ESSENTIAL FEATURES OF A FREE RADICAL MASS-SPECTROMETER.

Fig. 7.

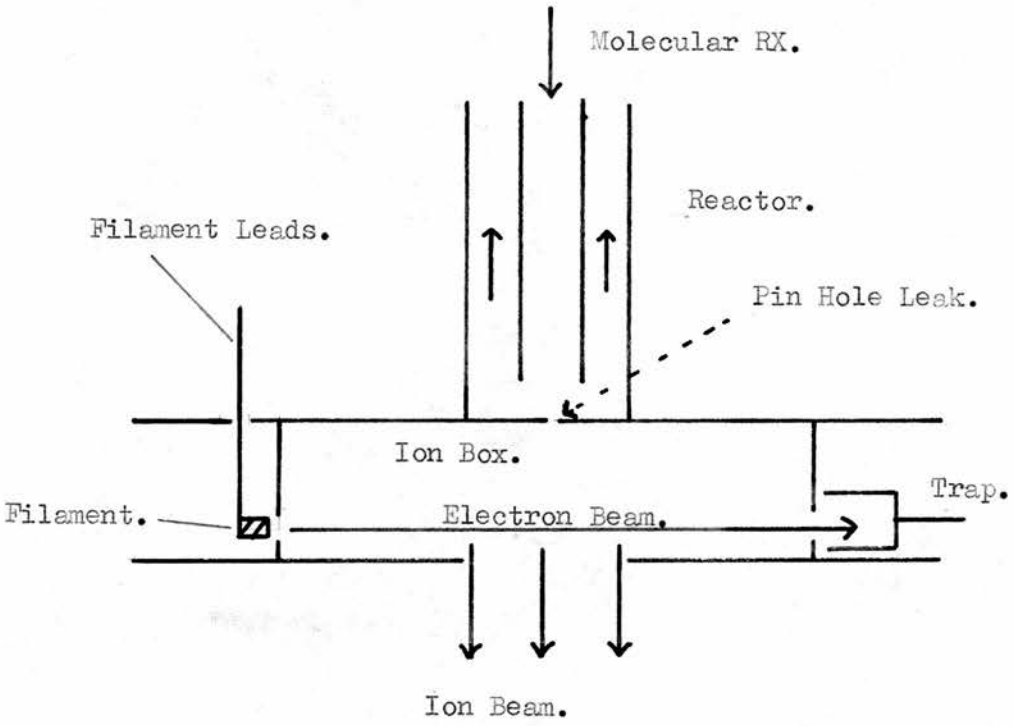

MOLECULAR BEAM SAMPLING SYSTEM BY FONER AND HUDSON.

Fig.9.

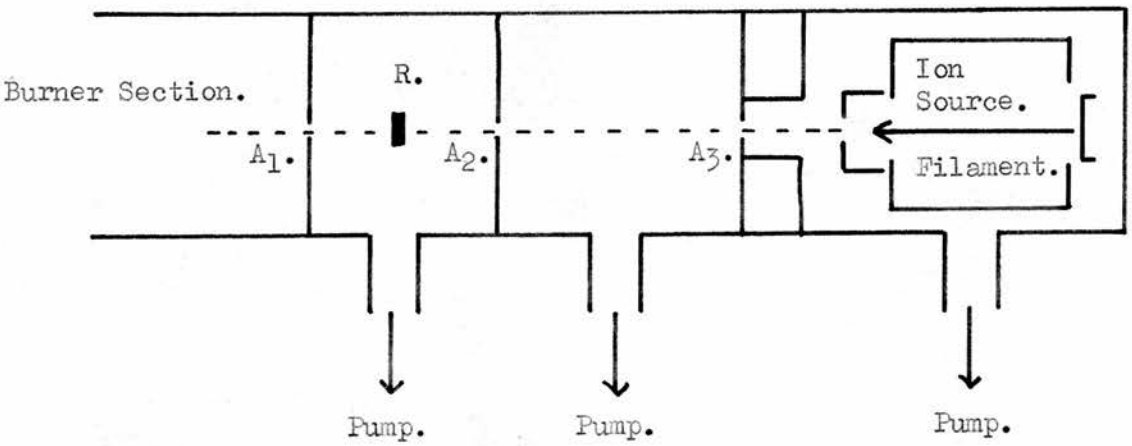

and consequently the reaction studies were limited to atomic nitrogen reactions. It is relevant therefore at this stage to discuss the existing literature on free radical mass-spectrometry and in particular the methods dealing with free nitrogen atom detection.

b) General Principles of Free Radical Detection.

Fig. 7. shows a general schematic diagram of the essential features of a free radical mass-spectrometer. Radicals R are generated from RX molecules in the reactor and pass at low pressure into the ion chamber where they are ionised by an electron beam and analysed in the usual way. The reactor can be any system which generates free radicals from the parent molecules (e.g. pyrolysis, hot wire, discharge tube etc.).

In the first case when the reactor is off the ions formed will be the same as those occurring in a normal mass-spectrometer and the processes and appearance potentials (A.P.) are listed below:-

$$(1) \quad RX \xrightarrow{e} RX^+ + e \qquad A.P_1.$$

$$(2) \quad RX \xrightarrow{e} R^+ + X + e \qquad A.P_2.$$

$$(3) \quad RX \xrightarrow{e} R + X^+ + e \qquad A.P_3.$$

If the reactor is now activated such that radicals R and X are generated two new processes occur:-

$$(4) \quad R \xrightarrow{e} R^+ + e \qquad A.P_4.$$

$$(5) \quad X \xrightarrow{e} X^+ + e \qquad A.P_5.$$

Thus if the radical of interest is R the mass-spectrometer observes a peak R^+ due to processes (2) and (4) and it is necessary to discriminate between these processes in order to evaluate the radical concentration from the reactor. In general, two techniques based on the use of high

and low energy ionising electrons have been used for this discrimination and are discussed below.

(i) Low Energy Electrons.

Process (2) involves the breaking of the R-X bond and the ionisation of one of the dissociation products, in this case R. Process (4) involves only the ionisation potential of the free radical R. Thus the appearance potential of R^+ from RX ($A.P_2.$) is less than the appearance potential of R^+ from R ($A.P_4.$) such that $A.P_2. = A.P_4. + D_{R-X}$ where D_{R-X} is the R-X bond dissociation energy. This energy is usually around 2 to 3 eV. for most compounds but can be as high as 9 eV. for strongly bonded molecules as in nitrogen. It is therefore possible to use electrons with insufficient energy to promote process (2) but with sufficient energy to detect the free radical.

(ii) High Energy Electrons.

This is not as direct a method as the low energy technique but has been particularly favoured in radical sensitivity determinations. In this case electrons having 50 eV. and more are used. The mass-spectrometer is first calibrated with the reactor off and the absolute sensitivities of R^+ from RX and RX^+ from RX determined. The reactor is activated and the new R^+, RX^+ peak heights determined. The contribution of the R^+ peak from RX is known so that the actual R^+ radical peak height may be determined by subtraction. Assuming a 100% material balance between the stoichiometric loss of RX and the again in R the absolute radical sensitivity may be determined.

The method is applicable to a wide range of radical studies but is

unfortunately limited in sensitivity. Generally, the decrease of RX^+ and the gain in R^+ when the reactor is activated are very small compared with the basic peak heights such that delicate backing-off equipment is necessary. In spite of this difficulty Lossing [78] and his co-workers have successfully determined the sensitivity of CH_3 as 0.47 of the CH_4 sensitivity. One further disadvantage which applies to both methods of analysis is the formation of radicals by the pyrolysis of RX on the hot filament (1500 to 2000°C). This can give an appreciable radical background in the mass-spectrometer and complicates the reactor radical determinations.

c) Mass-Spectrometry of Free Radicals.

In the simplest case of free radical mass-spectrometry the radicals are produced in a reactor connected directly to the ion-chamber. In this way Hipple and Stevenson [79] in 1943 pyrolysed lead tetramethyl and lead tetraethyl in a heated tube immediately above a mass-spectrometer ion-box and obtained the mass-spectra and appearance potentials of methyl and ethyl radicals. In a similar way Robertson [80] in 1949 detected free radicals by the pyrolysis of methane, ethane and butane on a hot platinum filament.

Other workers have extended the study to other radicals but the method is very limited in application. The main disadvantage is that the reactor pressure must be maintained at the normal ion-box pressure of about 10^{-5} mm. Hg.

Eltenton [81][82][83] was the first to successfully detect free radicals by sampling from a high pressure system. He began the work in

the laboratories of Semenov and Krondiev before 1939 in Leningrad but did not publish the work until later. Eltenton realised that the normal methods of sampling from reaction systems by porous plugs or fine capillaries would be of little use in free radical work since a practically collision free path from the reactor to the ion-chamber would be required. This was achieved by separating the reactor from the ion-box with a thin sheet of gold foil containing a small circular orifice, situated as near to the box as possible. The reactor gases were sampled through the orifice and immediately entered the ion-box. The ion-chamber and filament section were pumped separately to reduce the background radical peak from the filament products. The reactor, essentially a heated tube was fitted close to the gold foil and the reagent gases circulated down the reactor and over the orifice. In this way Eltenton using low energy electrons was able to detect certain free radicals from the pyrolysis of simple hydrocarbons at pressures up to 10 centimetres of mercury in the reactor. The mass-spectrometer was a 180° Dempster type in which the whole of the ion source is contained in a magnetic field and which is consequently less accessible than other types.

Shortly after Eltenton's pioneering work, Lossing in Canada published a series of papers on the mass-spectrometry of free radicals. The apparatus was similar to that used by Eltenton but was based on a 90° Nier type instrument. A typical form of the apparatus by Lossing and Tickner [84] is shown in Fig. 8. Radicals were produced in the reactor by thermal decomposition and sampled by a quartz cone containing

FIGURE 8.

Fig. 8.

THERMAL REACTOR AND ION SOURCE BY LOSSING.

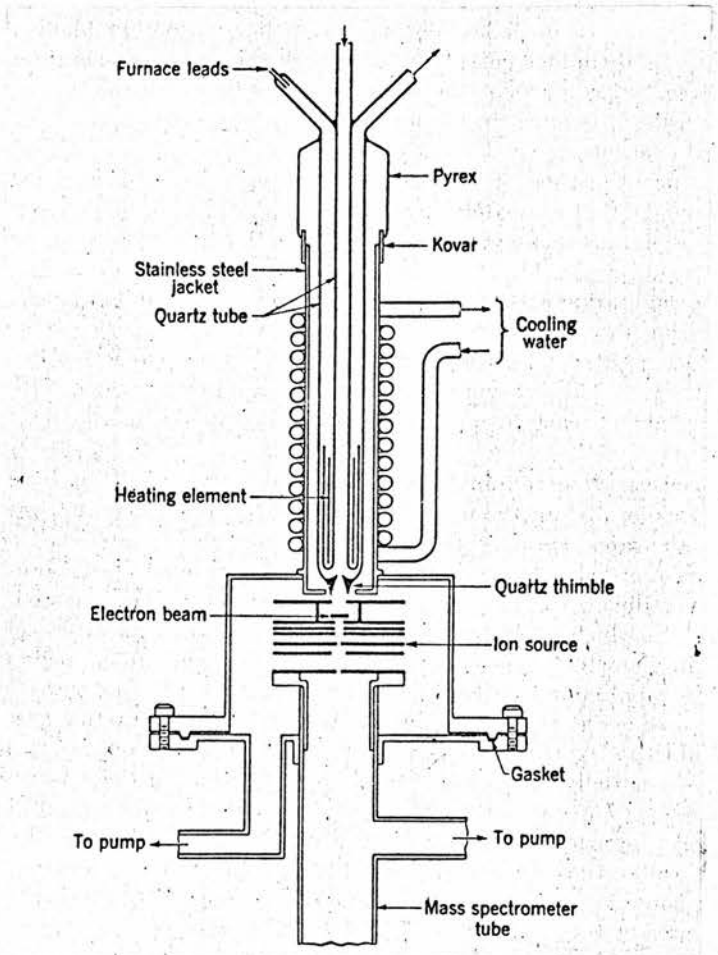

a small orifice punctured by a sharp tesla spark. The radicals had a direct line of sight access into the electron beam and were ionised and detected in the usual Nier type manner. To reduce the radical background the filament area was closed off and pumped separately down the main ion-tube via a series of holes drilled in the ion source plates. The majority of the gas sampled by the leak was removed by the main head pump. The ion-gun plates were insulated from one another by circular glass spacers which also served to isolate the filament and ion-tube from the main head region. The only access between these regions was therefore via the electron beam entry slit in the ion-box or the slit in the box bottom. This ensured that the filament region operated at a much lower pressure than the ion-box and hence any back diffusion of the filament products was reduced to a minimum.

In this way Lossing and his co-workers were able to examine the mass-spectra of simple radicals from a wide range of hydrocarbons and simple organic compounds (see references (74)(75)). Also, using mercury dimethyl as a source of methyl radicals and assuming a 100% carbon balance between the loss of reactants and gain of products Lossing was able to determine the methyl radical sensitivity as 0.47 ± 0.07 of the methane sensitivity at 50 eV. (78)(84).

A variety of other workers have examined a range of reactions involving free radicals in this way. Linnett (85) for example has studied the reaction of CH_3 with oxygen using a converted MS.2. The apparatus used a differential filament pumping system and for maximum sensitivity an electron lens system was used to collimate as much of

the electron emission from the filament as possible. In recent years Lossing has extended his original mass-spectrometer to the analysis of free radicals in the mercury photosensitised decomposition of ethylene [86] and certain other simple unsaturated hydrocarbons (see references (74)(75)).

In general there are two main disadvantages of the Eltenton-Lossing instrument which later workers have attempted to overcome in order to gain improved radical sensitivity. In the first place the simple pin hole sampling leaks are only partially satisfactory in that they yield a molecular beam spread through a wide angle. As a result a large proportion of the molecules and radicals in the beam have suffered a series of surface collisions before entering the ion-box. Secondly, it has been shown that the chance of ionisation of a species during its first passage through the electron beam is extremely small [87][88]. Robertson [89] has calculated that the probability of ionisation for a propyl radical in a single electron beam passage is about 1 in 10^6. Le Goff [90] has further analysed the problem and has calculated that in a conventional Nier type source a molecule makes some 50 to 100 wall collisions before being pumped out.

It is not surprising therefore that in free radical studies where the radical is particularly susceptible to wall recombination that the detection sensitivity is extremely low or even nil.

Foner and Hudson [91] attempted to overcome these difficulties using a selective molecular beam sampling system for radical studies in flames. The essential details of the apparatus are shown in Fig.9. (see p.44.). A series of small coaxial apertures between the burner

section and the ion-box selected a narrow beam of the reaction species which had passed directly through all three apertures. The enclosures between the apertures were pumped separately so that any molecules which did not pass directly through the apertures were removed. The collimated beam then entered the ion source along the same axis as the electron beam. This gave a much improved chance of ionisation. The basic sensitivity of the instrument was increased further by a vibrating reed unit R driven electrically at about 200 cycles/sec. producing a pulsed molecular beam. This simplified the amplification of the output signal since more sensitive and stable A.C. amplifiers could be used.

In this way Foner and Hudson were able to examine a hydrogen-oxygen flame and showed the presence of H, O, and OH radicals. In a similar experiment with a methane-oxygen flame the mass-spectrum of the products was rather complex and only CH_3 could be unambiguously detected.

Ouellet and a number of co-workers (92)(93)(94) have used a similar apparatus to examine the intermediates in the cool flame oxidation of diethyl ether and acetaldehyde. The mass-spectrometer was coupled to a high speed camera and designed to record up to 60 complete spectra per second. A certain degree of sensitivity was sacrificed for this high speed and although no free radicals could be detected some valuable kinetic data was collected.

d) Nitrogen Atom Mass-Spectrometry.

Although the mass-spectrometry of free hydrogen and oxygen atoms is relatively difficult, nitrogen atoms have been detected in relatively simple free radical mass-spectrometers. Virtually the whole of this

FIGURE 10.

Fig. 10.

DISCHARGE TUBE AND ION SOURCE BY JACKSON AND SCHIFF.

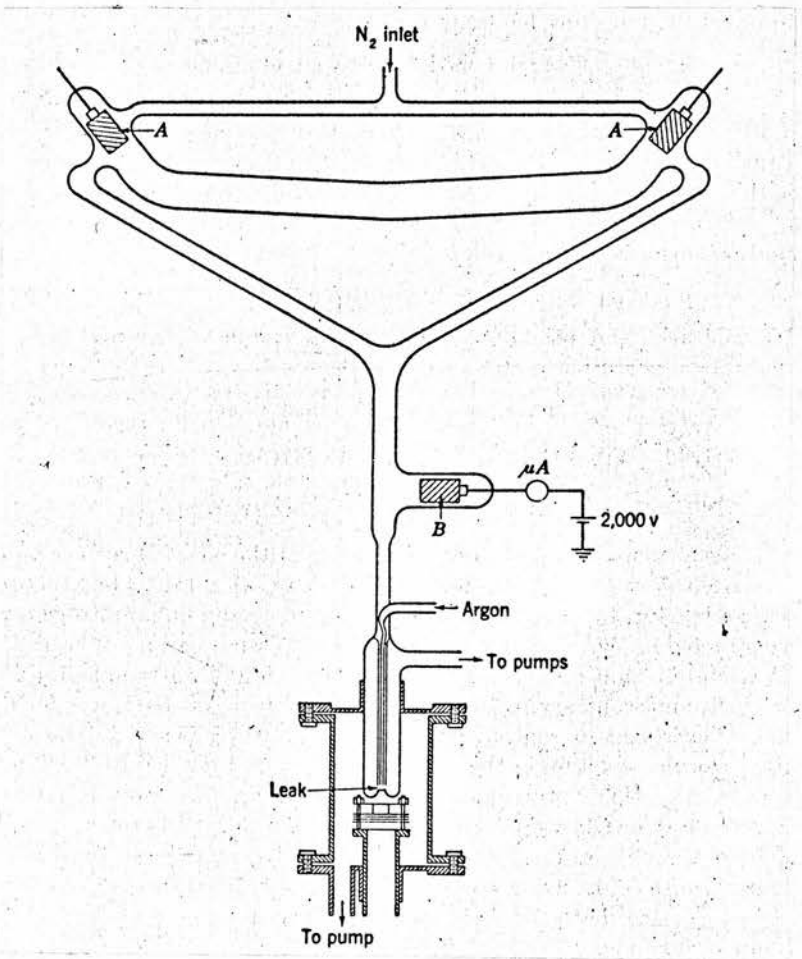

work on free nitrogen atom detection has been published by Schiff and his co-workers at McGill and Kistiakowsky et al. at Harvard.

In the experiments of Jackson and Schiff (95)(96) in 1953 a stream of active nitrogen from a condensed discharge was sampled by an orifice in a quartz cone into a modified mass-spectrometer. The experimental layout is shown in Fig. 10. Basically the mass-spectrometer was a 90^{o} Nier type instrument with the differential filament pumping system as used by Lossing. A D.C. 'electrometer' amplifier and automatic recorder provided a maximum sensitivity of 1 cm. per 3×10^{-14} amp. at a resolution of 1 in 200. The sampling leak was a 30 micron hole situated about 1.5 cm. from the ion source. Nitrogen pressures up to 3 mm. Hg. were acceptable above the leak without undue saturation of the mass-spectrometer. The discharge system was similar to the well-known Wood's tube but used an intermittent D.C. supply giving a condensed discharge. The discharge seriously interferred with the ion source electronics but an auxiliary electrode B maintained at about 2000 volts reduced this interference to an acceptable level. The glassware from the discharge tube to the ion-box was coated with a layer of meta-phosphoric acid to reduce surface recombination of the atoms.

The peak heights for 14^{+} and 28^{+} were examined at 50 eV. Whenever the discharge was activated the 28^{+} peak decreased and the 14^{+} peak increased. The relative increase in 14^{+} was apparently independent of the pulse rate but very dependent on the condition of the meta-phosphoric acid with a freshly poisoned surface giving maximum 14^{+} yield. A blank run with argon in the discharge tube showed that the 40^{+} peak height

FIGURE 11.

Fig. 11.

IONIZATION EFFICIENCY CURVES BY JACKSON AND SCHIFF FOR THE IONS Ar^+, N_2^+ and N^+.

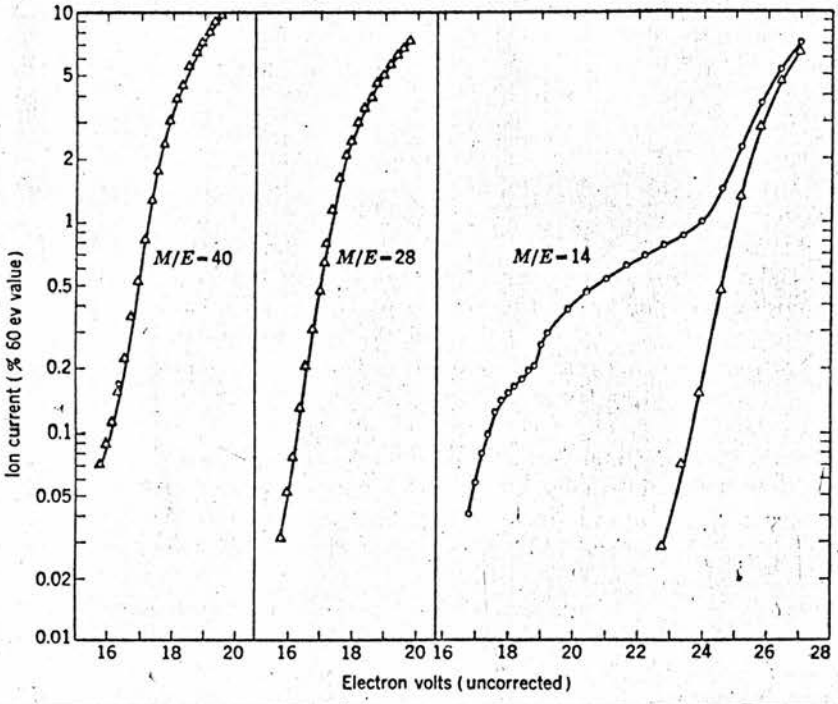

The circles represent values with the discharge.

Triangles, in the absence of the discharge.

did not change when the discharge was activated indicating that the sensitivity remained constant during these tests.

In order to identify the species at mass 14, appearance potential measurements were recorded and are shown in Fig. 11. The 28^+ curves with and without the discharge were identical but the curve for 14^+ showed a new species (A.P. 14.7 ± 0.3 eV.) in active nitrogen. This appearance potential agreed closely with the accepted value of 14.54 eV. for the spectroscopic appearance potential of ground state $N(^4S)$ atoms and clearly demonstrated the presence of nitrogen atoms in active nitrogen. The discontinuity in the 14^+ curve indicated a second species of A.P. 16.1 ± 0.3 eV. which at first was attributed to excited nitrogen atoms. An analysis of the various possible ionisation energies of the low lying metastable atoms to various ion states showed that this latter process could only be achieved by the ionisation of the $N(^2D)$ to the $N(^1S)$ ion state. This appeared to be unlikely and the appearance potential was finally attributed to the ionisation of excited N_2 or N_3 molecules. This latter molecule has been suggested as a constituent of active nitrogen by Strutt [97] and more recently by Uri and Herzberg [98].

Active nitrogen has also been investigated mass-spectrometrically by Berkowitz, Chupka and Kistiakowsky [99] and the nitrogen atom concentration related to the afterglow intensity, monitored by a photomultiplier. The essentials of the apparatus are shown in Fig.12. (p.57.). Nitrogen was dissociated in a Wood's tube powered by a 3000 volt transformer and pumped at high speed past the photomultiplier P and the mass-spectrometer. The photomultiplier was protected from the

FIGURE 12.

FLOW SYSTEM BY KISTIAKOWSKY.

Fig. 12.

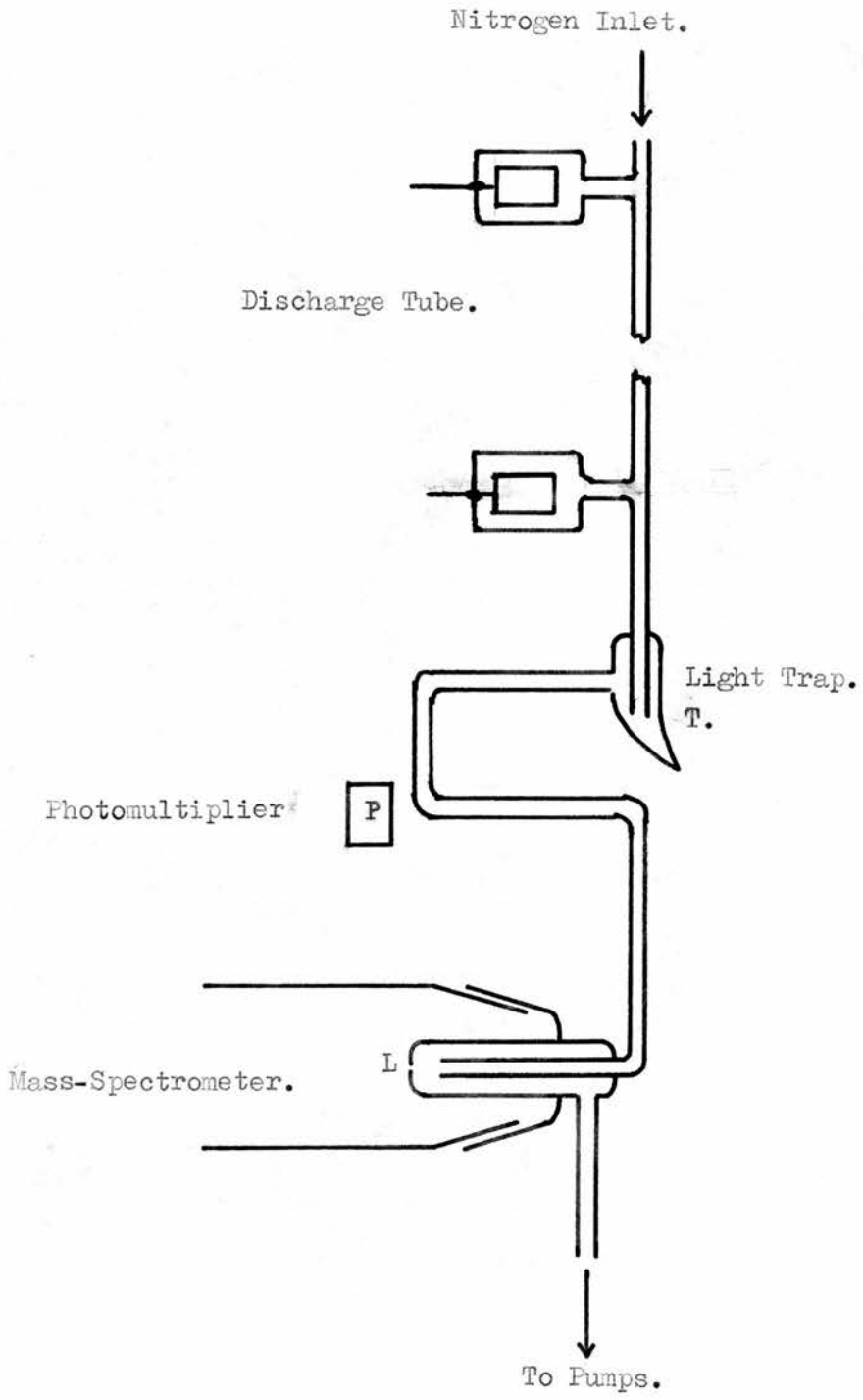

intense discharge glow by a light trap T and viewed the afterglow longitudinally down about 30 cm. of the exit tube. The exit gas stream from the photomultiplier then passed over the leak L of the mass-spectrometer positioned as near to the photomultiplier as possible. The distance from the discharge tube to the photomultiplier was about 100 cm. with the mass-spectrometer situated a further 20 cm. from the photomultiplier. The connecting tubing (1.5 cm. diameter) was thoroughly coated with meta-phosphoric acid. Nitrogen flow rates of around 1 cc. N.T.P. per sec. were used giving about 5 metres per sec. linear velocity.

The mass-spectrometer was a 60° instrument and sampled the afterglow through an orifice in a mica sheet. The ion-box had no repeller or trap and the reactive species entered through a slit in the box top. The detecting amplifier was an electron multiplier with a vibrating reed electrometer. The filament and analysing tube were differentially pumped in the usual way.

Nitrogen atoms were monitored using low energy electrons (22.5 eV.). The 14^{+} peak barely showed above background but on activating the discharge rose some 1000 times. An ionisation efficient plot showed a smooth curve of appearance potential 14.8 eV. This confirmed Jackson's and Schiff's observations [95][96] of the presence of $N(^{4}S)$ atoms in the afterglow. There appeared to be no evidence of any metastable nitrogen atoms and a similar investigation of the 28^{+} ionisation efficiency showed no trace of any metastable nitrogen molecules. From simultaneous investigations of the 14^{+} peak height and the afterglow

intensity Kistiakowsky and his co-workers clearly demonstrated that the afterglow intensity varied with the square of the $N(^4S)$ atom concentration. This clearly associated the afterglow with an atom-atom collision. Kistiakowsky was later able to conclude that the afterglow was a spectral emission of the excess energy of the recombination of two atoms, the recombination being a third body requirement and involving a short lived metastable nitrogen molecule.

In an extension of the work Kistiakowsky et al.(100)(101) introduced a reactor near the mass-spectrometer input and were able to investigate the kinetics of the reactions of atomic nitrogen with oxygen and various nitrogen oxides. The investigations were based on the principle of the stirred reactor and the nitrogen atoms were monitored with the mass-spectrometer. The Wood's type discharge tube was replaced by a 2400 Mc./sec. electrodeless discharge (125 watts) for these latter experiments. This was found to yield an equivalent flow of nitrogen atoms but with much improved stability.

e) Summary of Free Atom Mass-Spectrometry.

In general, mass-spectrometry has not been widely used in the analysis of atomic species in reaction kinetic studies. The success of free atom detection and analysis depends largely on the ability of the particular atom to survive the many surface collisions with the gas entry tube and ion-box before ionisation takes place. Nitrogen atoms being relatively stable to these collisions are readily analysed by conventional Lossing type free radical mass-spectrometers. Hydrogen and oxygen atoms on the other hand being extremely prone to recombination

require more elaborate equipment and then only yield a limited sensitivity suitable for detection but insufficient for quantitative kinetic work.

In mass-spectrometry, surface reactions on the ion-box are of importance in certain systems other than those containing free atoms or radicals. McKnight [102] has developed an ion-box for the study of corrosive gases with particular reference to uranium hexa-fluoride. In this case the gas chemically attacks the ion-box forming thin insulated films on the electrical surfaces. The films quickly build up electrostatic charges sufficient to destroy the operation of the ion source. The ion-box by McKnight was constructed out of stainless steel mesh to reduce the metal surface yet still maintain adequate electrical field requirements. It would appear that a gauze box of this type might be suitable for free atom studies having the following distinct advantages over the conventional box.

(i) Recombination reactions in the ion-box would be reduced to a minimum.

(ii) The free atoms in the sampled beam would have direct access through the gauze box top into the electron beam.

(iii) The rate of pumping through the gauze sided box would be a maximum. This would ensure that the atoms and molecules were removed as quickly as possible after their first passage through the electron beam.

A gauze ion-box system was available in the department and the preliminary stages of the experimental work of this thesis are devoted

to testing its potential in free atom work. The box had been built closely to the design by McKnight. As shown later the box was able to detect hydrogen and nitrogen atoms but with insufficient sensitivity to analyse a diffusion flame.

In the final apparatus a conventional ion-box was used. This proved fatal to hydrogen atom detection but showed extremely good sensitivity to nitrogen atoms enabling a diffusion flame several centimetres in diameter to be studied. In this way the rate constants of the important and rather controversial reactions of atomic nitrogen with nitric oxide and ethylene were investigated.

Before discussing the experimental details of these investigations it is relevant to present a summary of the existing literature on the chemistry of active nitrogen with particular reference to the reactions with NO and C_2H_4.

7. ACTIVE NITROGEN.

a) Introduction and Nature of the Afterglow.

As early as 1884 Warberg [103] noticed that when nitrogen at low pressure was subjected to an electrical discharge an afterglow was produced which persisted for some time after extinguishing the discharge. Since then the nature of this afterglow has been extensively examined and a variety of theories postulated to explain the phenomenon.

After Warberg's initial observations Lewis in 1900 [104][105] again observed the characteristic and persistent golden yellow afterglow. In 1911 Strutt [106] (later the second Lord Rayleigh) started the first systematic study of the afterglow which he termed 'active nitrogen' and suggested that many of its properties could be attributed to atomic nitrogen.

Between about 1930 and 1945 there were two main theories of active nitrogen. One of these was the Rayleigh atomic theory with the afterglow explained as an emission from the third body recombination of nitrogen atoms as suggested by Sponer [107]. The second theory was the Carlo and Kaplan [108] idea that active nitrogen consisted of a mixture of metastable atoms and molecules with the afterglow resulting from a collision of an atom with an excited nitrogen molecule.

An excellent survey of the experimental and theoretical work on active nitrogen up to 1945 was compiled by Mitra [109]. Unfortunately, this book is not readily available but the essential parts have recently been reviewed by Jennings and Linnett [110]. The book entitled 'Active Nitrogen - A new theory' suggested that the properties of active nitrogen

could be explained by assuming that the gas contained an ionised species N_2^+ and electrons. The afterglow was related to the emission from an excited nitrogen molecule formed by the interaction of N_2, N_2^+ and an electron. To quote from Mitra's book, the N_2^+ theory completely solved the problem of the nature of the active gas. Unfortunately, this was not the case and in 1953 Mitra [111] rejected the idea in favour of the now accepted atomic theory of active nitrogen.

The true active nitrogen afterglow is a rich golden yellow and can penetrate for several metres down the exit gas stream from the discharge tube. In experiments were the glowing gas is trapped in large closed vessels the glow is often visible for several hours. Thepresence of certain impurities at very low concentrations in the nitrogen stream (e.g. about ½% oxygen) greatly assist the afterglow intensity although the reason for this is not understood.(see ref.109).

The afterglow is now generally accepted to be an emission from an activated nitrogen molecule excited by the third body gas phase recombination of ground state atoms [52][110]. Since this emission is often visible for a considerable length of time it is clear that the atoms must survive many surface collisions. This is unusual considering the activity normally associated with free atoms but it is thought that the surface is deactivated towards recombination by a layer of adsorbed nitrogen molecules. Certainly it is well-known that the operation of the discharge for several hours is often necessary before the afterglow is visible, probably due to a gradual saturation of the surface with nitrogen molecules. The presence of trace impurities may assist this process in some way.

The characteristic yellow afterglow can be modified by certain impurities. Oxygen for example produces deep green afterglows which again persist after the discharge is extinguished. Tap-grease traces modify the yellow to a dark blue or purple colour (from CN emission bands) and in certain cases this has masked the true afterglow colour.

As mentioned previously, active nitrogen is known to consist mainly of atoms. Spectroscopic analysis by Tanaka [62] and mass-spectrometric studies by Kistiakowsky [99] and Schiff [95] have clearly indicated the presence of $N(^4S)$ ground state atoms and Tanaka has further detected traces of the metastable $N(^2P)$ and $N(^2D)$ atom states. Also a wide range of physical observations and chemical reactions have confirmed this idea [52][110].

A discussion of the general chemical reactions of active nitrogen is given below. The reactions of atomic nitrogen with nitric oxide and ethylene being relevant to this thesis are discussed in detail. Further relevant information may be found in reviews by Jennings and Linnett [110] in 1958 and Mannella [52] in 1961.

b) Chemical Reactions of Active Nitrogen.

(i) The Gas Phase Recombination of Nitrogen Atoms.

The third body gas phase recombination of active nitrogen has been investigated by a number of workers. The reaction is highly exothermic since a stable $N \equiv N$ bond is created, and a proportion of this exothermicity is released as afterglow emission from an excited nitrogen molecule. A discussion of the excited levels and electronic transitions involved in the reaction are beyond the scope of this report and further

details can be found in reviews by Mannella [52] and Jennings and Linnett.[110] The recombination being a third body requirement is relatively slow with an accepted rate constant of $K = 1.8 \times 10^{-8}$ $ccs^2 . mole^{-1} . sec^{-1}$. (see ref. 52).

(ii) Reaction with Oxygen.

Kistiakowsky in 1957 [100] examined the reaction of active nitrogen with molecular oxygen between 390°K and 520°K using a stirred reactor principle and analysing the nitrogen atoms with a mass-spectrometer. The primary process was shown to be $N + O_2 \longrightarrow NO + O$ with a rate constant $K = 2 \times 10^{12} e^{-6200/RT}$. ccs. $mole^{-1}$. sec^{-1}.

In 1961 Clyne and Thrush [112] using nitric oxide titration to monitor the reaction in a fast flow system obtained $K = 8 \times 10^{12} e^{-3100/RT}$. ccs. $mole^{-1}$. sec^{-1}, which agrees fairly well with Kistiakowsky's value.

(iii) Reaction with Nitric Oxide.

In 1956 Kistiakowsky [99] in his early studies of active nitrogen mass-spectrometry reported that the addition of nitric oxide to the afterglow produced a very rapid reaction which quickly removed the nitrogen atoms and emitted a continuous spectrum. A sharp boundary clearly marked the point of complete consumption of nitrogen atoms. The products of the reaction appeared to be a species of mass 44 and the reaction was thought to be:-

$$N + NO \longrightarrow N_2O^* \longrightarrow N_2O + h\nu.$$

In later work [100][101] in a more detailed study using the stirred reactor system N_2O was not detected. The only product appeared to be molecular oxygen but since this yield depended upon the size and surface

nature of the reactor it was thought that atomic oxygen played an important role. This was substantiated by the enhancement of the 16^+ peak at low nitric oxide concentrations. (The mass-spectrometric sensitivity to oxygen atoms was too low for any quantitative measurements but the 16^+ increase was detectable). The primary process was thus shown to be:-

$$N + NO \longrightarrow N_2 + O \qquad (1)$$

followed by:-

$$O + O + M \longrightarrow O_2 + M \quad \text{where M can be the wall.}$$

The primary rate constant was too great to measure but a lower limit of $K = 4 \times 10^{11}$ and later 5×10^{13} ccs. $mole^{-1}$. sec^{-1}. was evaluated. More recently in 1961 Clyne and Thrush [112] investigated the reaction over the range 476 to 755°K. The primary process was confirmed and a value $K = 3 \pm 0.6 \times 10^{13} e^{-(200 \pm 700)/RT}$. ccs. $mole^{-1}$. sec^{-1}. was obtained. In the same year Herron [113] using a mass-spectrometer similar to Kistiakowsky's obtained $K = 1 \pm 0.5 \times 10^{13}$ ccs. $mole^{-1}$. sec^{-1}.

The rate constants evaluated by these workers show a good general agreement. The theoretical collision frequency for a bimolecular process in these units is between 10^{13} and 10^{14} such that the reaction proceeds at about 1 in every 10 collisions. The secondary reactions which can take place after theprimary step are very important and form the basis of the NO titration technique first described by Spealman and Rodebush.[114] At low NO concentration a blue radiation is observed and has been identified as the nitric oxide $A^2\Sigma$ and $B^2\Pi$ transitions to the ground state $X^2\Pi$ [52][115] which are mainly in the ultra-violet but overlap

slightly into the blue-violet region. These main electronic transitions require energies of 125 and 130 Kcal./mole. respectively [116] and suggest that the NO excitation is associated with a highly exothermic reaction such as a bond formation step. In this way the process has been identified as the reaction between the oxygen atoms from equation (1) and nitrogen atoms:-

$$N + O + M \longrightarrow NO\ (B^2\pi,\ A^2\Sigma) + M \qquad (2).$$
$$\longrightarrow NO\ (X^2\pi) + M + h\nu.\ (\text{blue})$$

A variety of workers have confirmed this mechanism and more recently Winkler [117] has calculated the rate constant as $K = 1.8 \times 10^{15}$ $ccs^2.\ mole^{-2}.\ sec^{-1}$.

At higher NO concentrations reaction (1) exchanges N for O almost instantaneously. Reaction (2) becomes negligible and a new reaction involving the green or white air afterglow emission and identified as an excited NO_2 emission [52][118] is produced by:-

$$O + NO \longrightarrow NO_2^* \longrightarrow NO_2 + h\nu.\ (\text{white-green})$$

The emission of NO_2 has been studied by a variety of workers especially in upper atmosphere studies [119]. Unfortunately, the knowledge of the NO_2 electronic levels is still very poor but it is known that the emission involves relatively sharp bands (6000 to 7600 Å) superimposed on an apparently continuous emission.

The change of emission colour when nitric oxide has been fully consumed by reaction with nitrogen atoms has been used to estimate the atom flow rate in the well-known titration technique [52]. Nitric oxide is added at low concentration to the flow system. The yellow nitrogen

afterglow fades and as the input rate of nitric oxide is gradually increased the blue emission appears. At still higher nitric oxide injection rate the blue changes suddenly to the white-green afterglow. At this point the input rates of nitric oxide and nitrogen atoms are equivalent.

(iv) Reaction with NO_2 and N_2O.

Kistiakowsky examined the reactions of active nitrogen with NO_2 and N_2O using the stirred reactor system described earlier. The reaction with N_2O was relatively slow [100] with $K = 2.5 \times 10^6$ ccs. $mole^{-1}$. sec^{-1}. In studies with equimolar amounts of nitric oxide and nitrous oxide Kistiakowsky was able to conclude that the reaction between oxygen atoms and N_2O was also slow with $K = 2 \times 10^8$ ccs. $mole^{-1}$. sec^{-1}.

In the studies of $N + NO_2$, the reaction was complex [101] and only a tentative mechanism was suggested. In more recent work Clyne and Thrush [120] have examined the reaction at 1.26 to 6.32 mm. at temperatures up to 708°K and have clarified the primary processes as:-

$$N + NO_2 \longrightarrow N_2O + O \qquad (3).$$

$$N + NO_2 \longrightarrow 2NO^* \longrightarrow 2NO \qquad (4).$$

where $K_3/K_4 = 0.47$.

(v) Reaction with Organic Compounds.

The reactions of active nitrogen with a variety of saturated and unsaturated hydrocarbons have been investigated by a number of workers. Generally the main product is HCN together with small percentages of related hydrocarbons, traces of cyanogen and sometimes ammonia. The almost quantitative yield of HCN has been used as a method for

estimating nitrogen atom flow rates usually by reaction with ethylene (see ref. 52, 110). Ethylene reacts very rapidly and the HCN is trapped out of the gas stream and analysed in the usual way. The amount of HCN collected over a period of time gives the active nitrogen flow rate assuming a stoichiometric loss of one N to one C_2H_4 molecule.

The mechanism of the reaction was first suggested by Evans, Freeman and Winkler [121] and is now generally accepted. The primary process is:-

$$N + C_2H_4 \longrightarrow [C_2H_4N] \longrightarrow HCN + CH_3 + 62 \text{ Kcal./mole.} \quad (5)$$

The reaction involves a change of spin from 3 unpaired electrons ($N(^4S)$) to 1 unpaired electron in CH_3 and also a carbon-carbon transfer of a hydrogen atom. It is thought that the intermediate $[C_2H_4N]$ has a relatively long life but has never been detected as such even in high pressure systems where it might be stabilised by collisions.

The primary process (5) is then followed by:-

$$CH_3 + N \xrightarrow{M} HCN + 2H + 10 \text{ Kcal./mole.}$$

with many other minor processes occurring such as:-

$$N + [C_2H_4N] \xrightarrow{M} C_2H_4 + N_2$$

$$\xrightarrow{M} 2C_2N_2 + 2H_2$$

$$2[C_2H_4N] \xrightarrow{M} 2C_2H_4 + N_2$$

In 1961 Herron [122] investigated the reaction, confirmed the primary process and obtained a rate constant $K = 5.8 \times 10^{10}$ ccs. $mole^{-1}$. sec^{-1}. The technique involved a mass-spectrometer similar to Kistiakowsky's for the analysis of the nitrogen atoms. In the same year Dunford [123] using a crude diffusion flame method computed $K = 9.6 \times 10^{10}$ ccs. $mole^{-1}$. sec^{-1}. These values are in good general

agreement considering the experimental difficulties in such investigations. The reaction between active nitrogen and ethylene thus appears to be some 50 to 100 times slower than the reaction with nitric oxide.

In recent years the validity of the NO and C_2H_4 titration techniques has been questioned by a variety of workers. The controversy has arisen mainly from experiments where the same atom concentration has been analysed by the two different methods. The NO technique reproducibly indicates nitrogen atom flow rates much higher than expected from the equivalent HCN formation data. Unfortunately, other physical methods of analysing nitrogen atoms have not been sufficiently reliable to determine which titration technique is correct. Verbeke and Winkler [73] have suggested that the discrepancy arises from excited nitrogen molecules present in the active gas which can react with NO and thus give high titration readings. Recent work by Back and Mui [124] using $N^{15}O$ failed to detect any evidence for a reactive N_2 species.

FIGURE 13.

EXPERIMENTAL DISCHARGE TUBE.

Fig. 13.

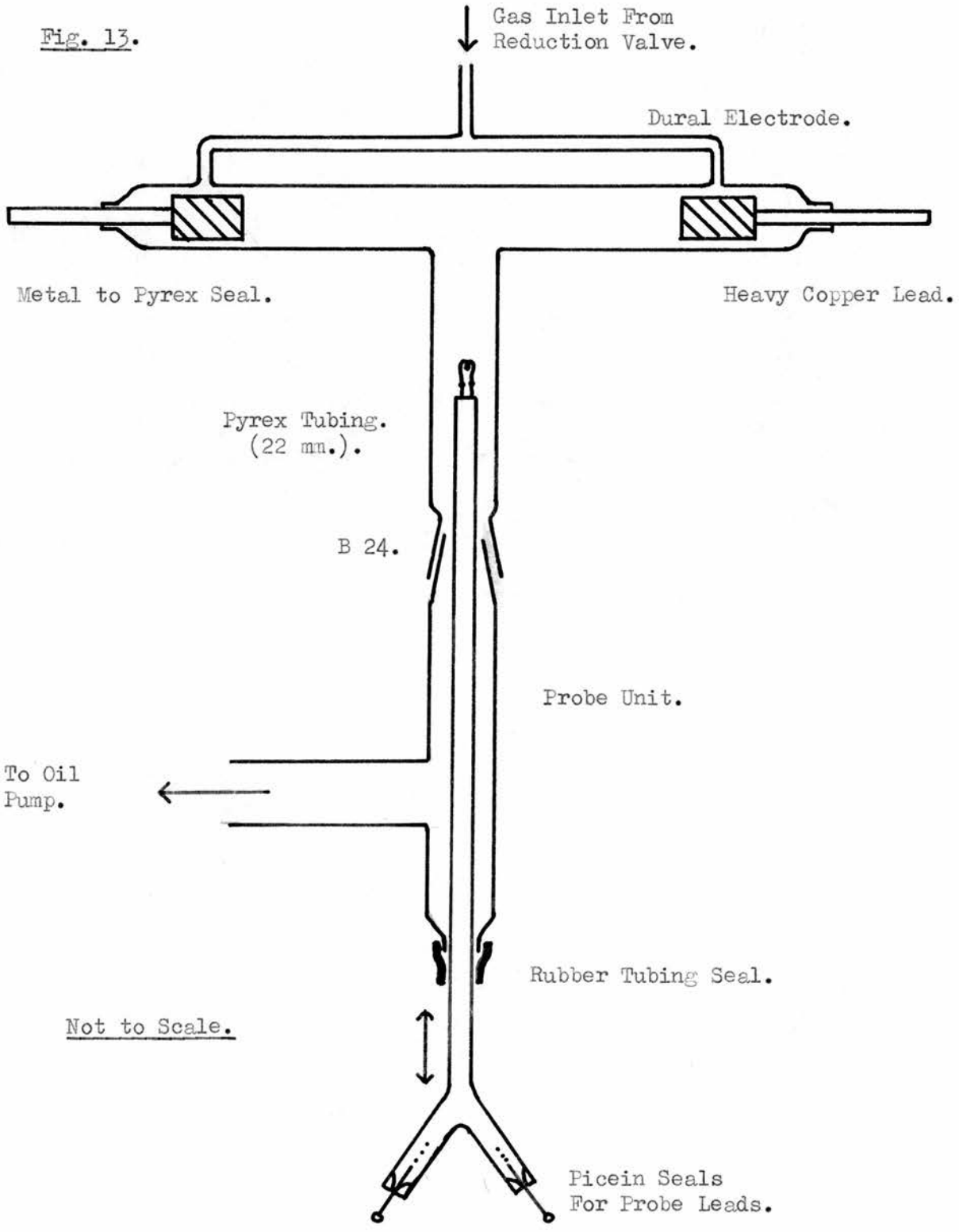

Not to Scale.

8. PRELIMINARY INVESTIGATIONS USING DISCHARGE TUBES.

a) General Discharge Tube and Detection Equipment.

Since there was little experimental experience available in the department on the production and detection of free atoms, a very simple Wood's type discharge tube [26] with a hot wire detector [30] was constructed. Essentially this consisted of two duraluminium electrodes 80 cm. apart, sealed into a length of 22 mm. pyrex glass tube as shown in Fig. 13. The exit tube from the centre of the discharge tube contained a movable probe unit, the actual detector being a small spiral of platinum wire (39 s.w.g.) which could be partially heated by an external E.M.F. when necessary. Discharge power was provided by a 6000 volt, 1000 watt transformer fed from the A.C. mains via a 0 to 250 volts Variac.

Discharges were tested in both nitrogen and hydrogen and could be produced at pressures between 10^{-2} and 5 mm. Hg. The striking potential necessary for a series of pressures in nitrogen is shown in Fig. 14, a minimum value occurring at about 0.5 mm. Even at this pressure however the discharge was so intense that the glass near the electrodes tended to melt and the power could only be maintained for intervals of about 20 seconds. This was sufficiently long to permit several important observations and experiments to be made.

b) General Experimental Observations.

The system was studied with either hydrogen or nitrogen flowing at 0.5 to 1 mm. pressure at a flow rate of 0.5 ccs. N.T.P. per second. In nitrogen the platinum probe glowed a dull red about 0.5 inch. from the

FIGURE 14.

Fig. 14.

The Relationship between the Striking Potential and the Nitrogen Pressure for a Wood's type Discharge Tube.

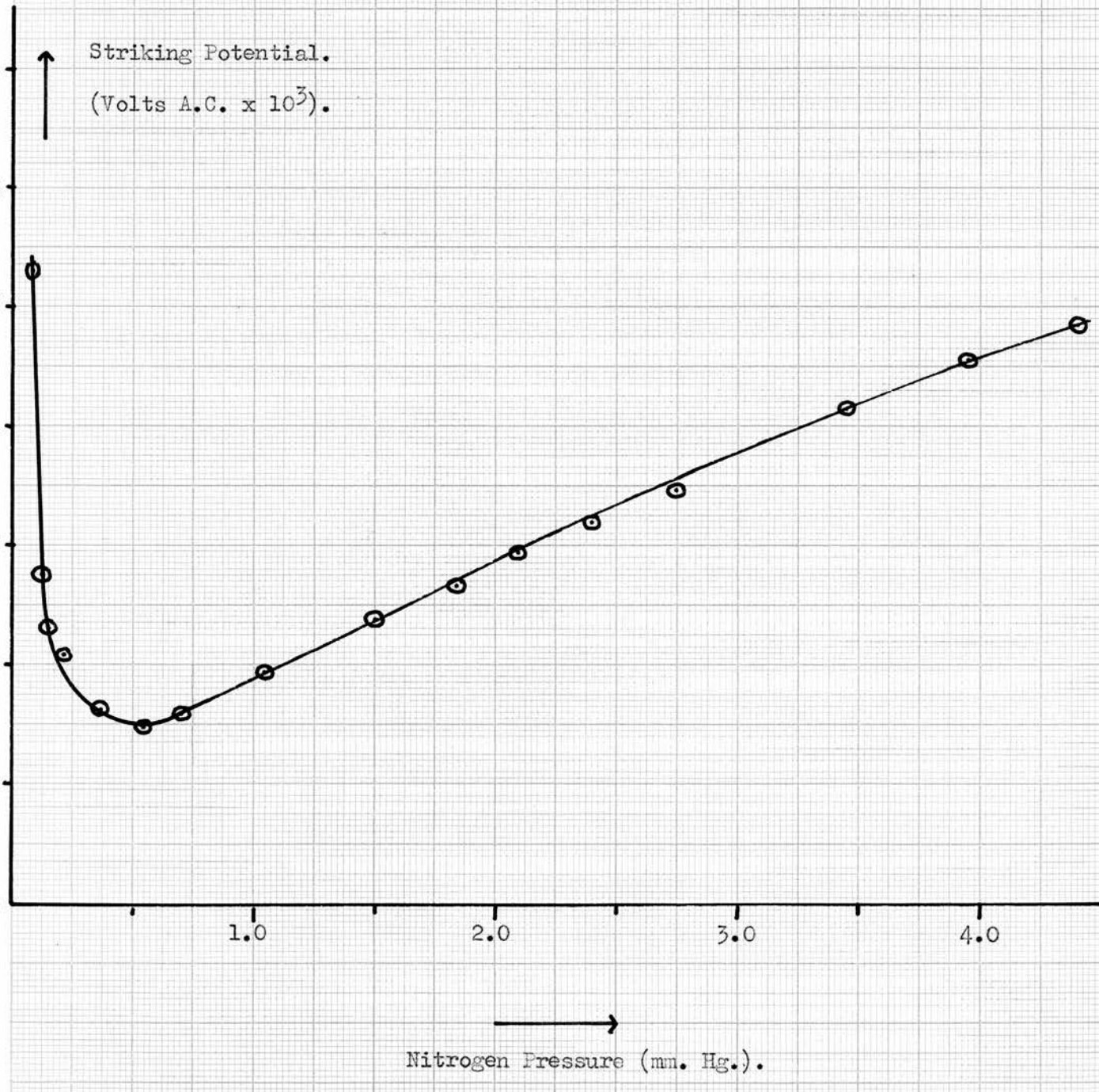

discharge and if biased by an external E.M.F. could visually detect atoms as far as 5 inches down the tube. It was found necessary to flash clean the detector from time to time as on occasions no activity was apparent even with the detector a few millimetres away from the discharge. After flash cleaning the platinum would glow distinctly in the atom stream. This seemed valid evidence that the temperature rise of the probe was a catalytic property rather than thermal energy carried by the gas from the hot discharge tube. No yellow afterglow was visible even in a darkened room but mixtures of oxygen (10 to 20%) produced deep green afterglows which persisted for several seconds after the discharge was extinguished and could be followed down the gas stream to the pumps.

In hydrogen the discharge was less intense, no afterglows were visible and no catalytic activity could be detected even near the discharge or after repeated flash cleanings of the probe.

c) The Effect of Various Wall Coatings.

The discharge tube was removed and coated with meta-phosphoric acid as suggested by Wartenberg and Schulze [46] and now used widely [99] as a wall inhibitor and was applied as follows:-

Sufficient meta-phosphoric acid was added to hot water and boiled gently until the solution was syrupy yet still quite mobile. The discharge assembly was warmed and the hot solution poured into it, swirled round the required areas, drained and then the deposit dried under vacuum. This gave a firm crystalline deposit of meta-phosphoric acid on the discharge tube and exit lines.

With a discharge in hydrogen the probe response was immediate. The platinum probe became red hot three inches from the discharge without external aid and atoms could be detected as far as six inches from the discharge with external probe biasing. In the region near the discharge the probe melted on several occasions and had to be replaced.

In nitrogen meta-phosphoric acid gave increased atom concentrations but to a much smaller extent. Other wall inhibitors were examined with both nitrogen and hydrogen discharges. These included teflon [48], water vapour [26], dri-film [50][51], hydrofluoric acid [45], potassium chloride [47] and sodium and magnesium phosphate [47] but these were little better than clean pyrex glass.

Although it was now possible to produce and detect nitrogen and hydrogen atoms, they could not be produced for any appreciable length of time due to the intense heat developed near the electrodes. This was corrected by using a modified discharge tube built to the design by Lawrence and Edlefson [125] and is shown in Fig. 15.

d) Discharge Tube by Lawrence and Edlefson.

Two closely fitting hollow electrodes were sealed into a pyrex U-tube (50 cm. long and 3 cm. O.D.). The closely fitting electrodes removed any electrical arcing near the electrodes although the reason for this is not fully understood. The U-tube was fitted into a brass water jacket and cooling water circulated at high speed. The electrodes being conduction cooled through the glass remained comparatively cool.

The detector was modified, the platinum spiral now being replaced by a square of platinum foil (1 mm. square and .004 inch thick) spot-

FIGURE 15.

welded to a fine thermocouple junction. This was much more sensitive than the spiral but more prone to poisoning.

The discharge tube could be operated for long periods but it was soon evident that meta-phosphoric acid coatings were not suitable for long term operation. The output of hydrogen atoms dropped considerably as the acid gradually dried out under the hot and low pressure conditions of the discharge tube and when once dry the coating easily broke away from the walls. Attempts to keep it moist by introducing moist hydrogen had little or no effect on the drying out process even with relatively high water vapour concentrations.

Even with the improved detector, no hydrogen atoms could be detected unless the walls were coated with meta-phosphoric acid. The efficiency of a coated tube would probably be rather erratic and in later work any sputtering from the walls when a mass-spectrometer leak was sampling the active species would be most undesirable. Nitrogen atoms, however, could be produced in steady concentrations in untreated pyrex discharge tubes and could even be passed through relatively small bore nozzles without appreciable loss as would be necessary in a Diffusion Flame experiment.

However, the main disadvantage with this type of tube was its physical dimensions. It would probably produce adequate atom concentrations but was much too large and heavy to be conveniently accommodated over the mass-spectrometer so it was decided to investigate other discharge tube equipment.

DISCHARGE TUBE BY LAWRENCE AND EDLEFSON.

Fig. 15.

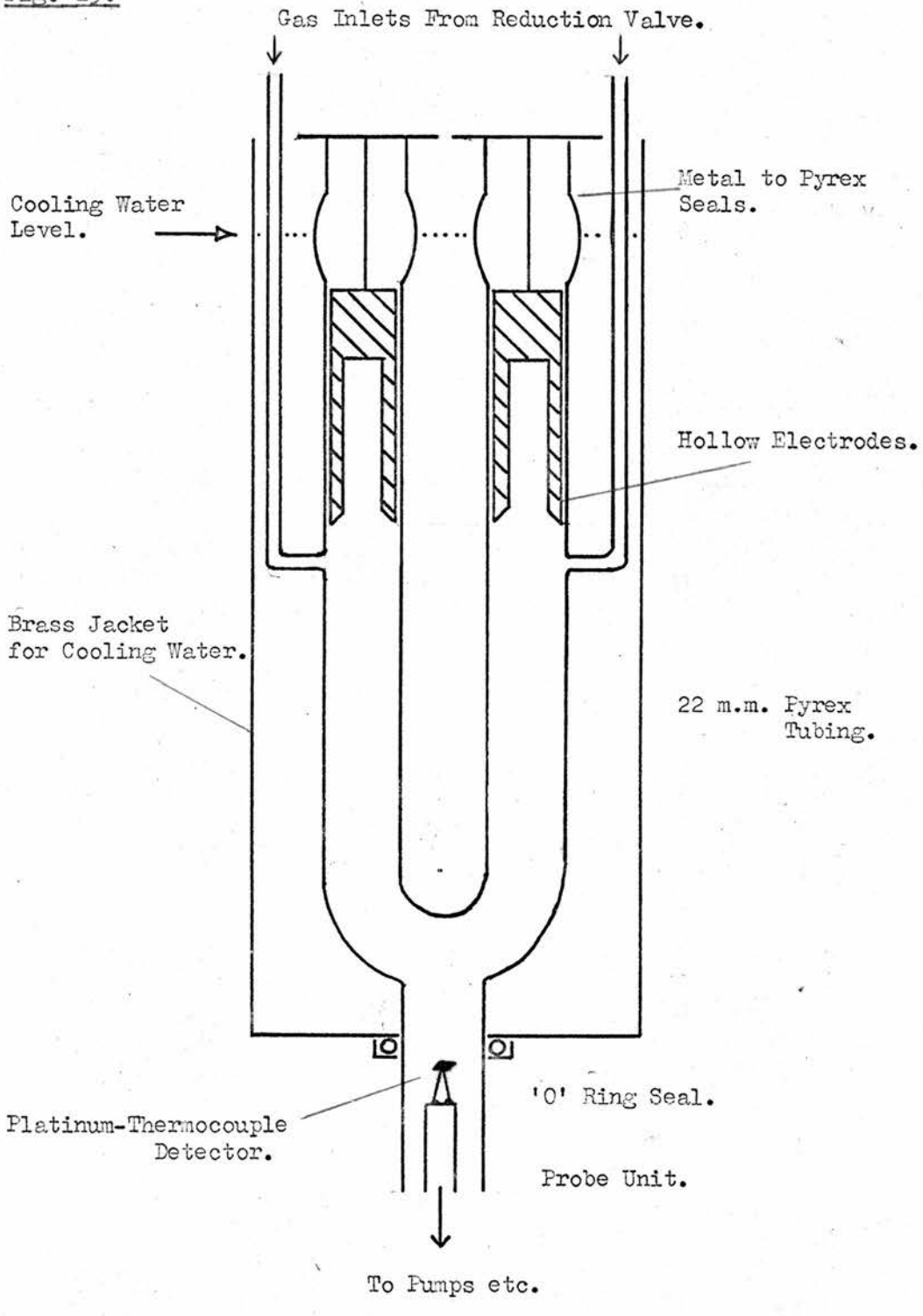

9. PRELIMINARY ELECTRODELESS DISCHARGE INVESTIGATIONS.

a) Initial Tests with Radio-Frequency Diathermy Unit.

The radio-frequency, or electrodeless discharge is known to produce high concentrations of free atoms and is much more efficient than the A.C. mains type (36)(37)(38)(126). Furthermore, since the discharge system is more efficient, cooling is relatively easy and the tubes are generally quite simple in construction.

For preliminary work a 250 watt Radio-Frequency Medical Diathermy unit was borrowed and the electrodes placed each side of a straight pyrex tube (22 mm.) carrying nitrogen at 1 mm. pressure at the same flow rate as used in the previous experiments. On activating the radio-frequency (R.F.) unit a discharge was produced which gave as many atoms as the Lawrence and Edlefson tube although using much less power. Again, poisoned probe experiments showed that the detector heating was catalytic and not thermal or R.F. induction heating.

This test was very encouraging and a Canadian Philco Transmitter was purchased capable of producing 300 watts at 2 to 12 megacycles per second. This was purchased complete with speech modulation equipment and it was first necessary to modify it for carrier wave only.

b) Methods of R.F. Power Coupling and Transmitter Tuning Procedure.

The transmitter power could be coupled to the discharge tube by either an Electrostatic (E.S.) or Electromagnetic (E.M.) method as shown in Fig. 16A and 16B. In either case the system consisted of a resonance circuit tuned to the transmitter frequency and load. The

FIGURE 16.

Fig. 16.

TYPICAL COUPLING METHODS FOR R.F. DISCHARGES.

A. ELECTROMAGNETIC.

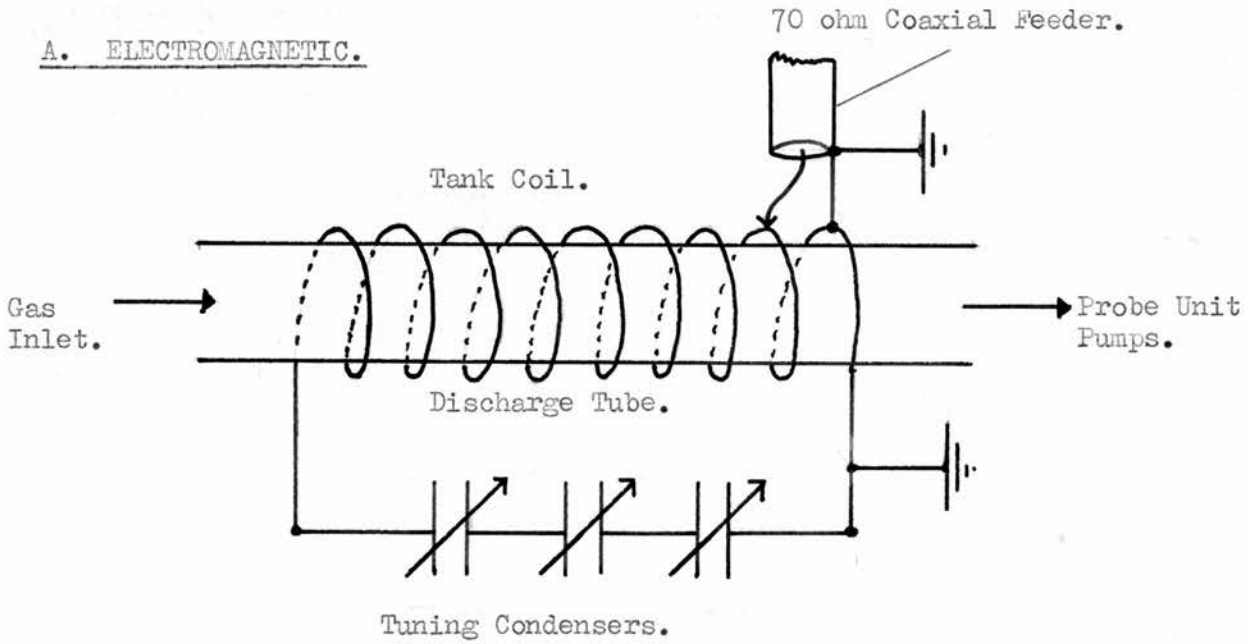

B. ELECTROSTATIC.

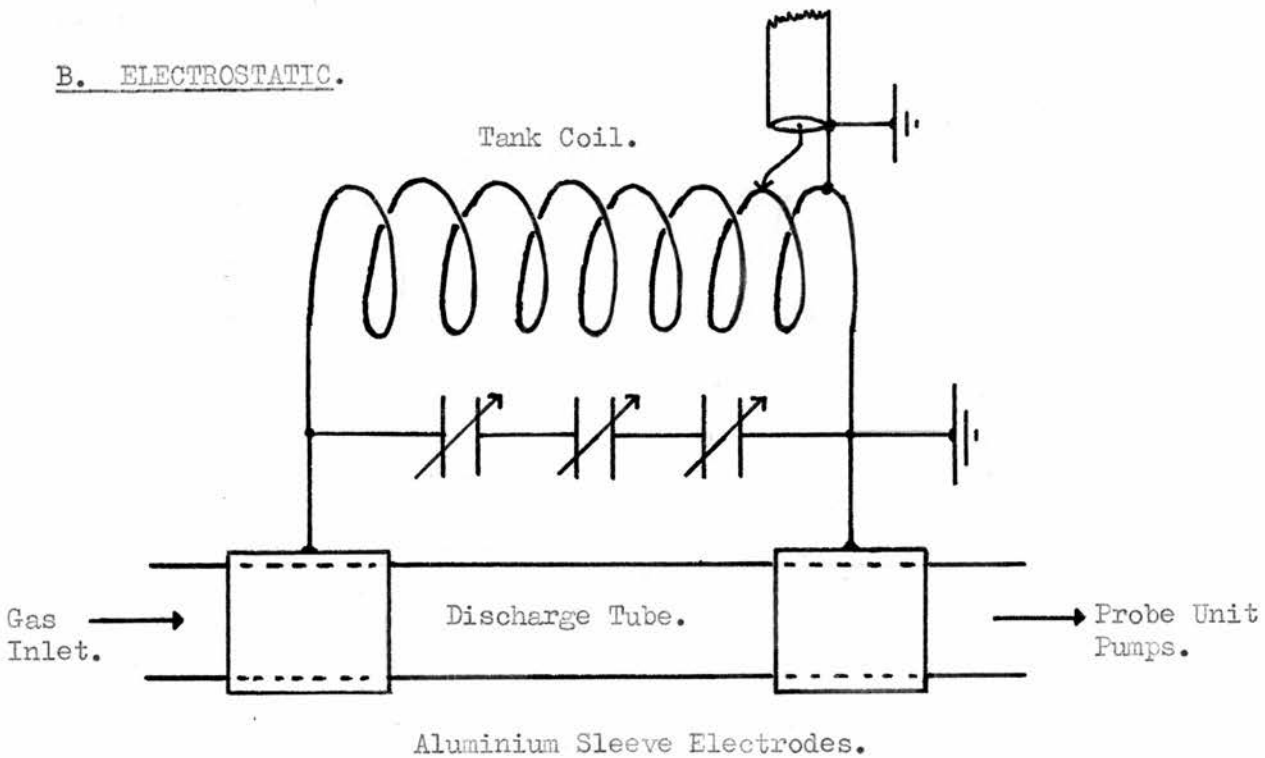

tank coil (about 1.5 by 8 inches) was generally about 30 turns of heavy copper wire (1 mm. diameter) with several variable tuning condensers across it in series, although the actual coil dimensions were not critical. The use of several tuning condensers was found necessary since the condensers available were not high voltage working. The three condensers in series proved to be adequate and had sufficient capacity for tuning purposes. The pyrex discharge tube was then either fitted through the coil for E.M. coupling or from each end of the coil by sleeve electrodes for E.S. coupling.

The transmitter contained a connection for a 70 ohm coaxial feeder line. Since the tank circuit is essentially a high impedance circuit the coupling had to be effected via an impedance matching transformer. It was usually adequate to attach the two ends of the coaxial feeder across one or two turns of the tank coil to provide the correct matching.

It was found beneficial during these tuning procedures to use a 70 ohm resistive load capable of dissipating 300 watts. This was generally three 100 watt bulbs in parallel. The tuning procedure then became as follows:-

The bulbs were fixed directly to the transmitter output and the transmitter tuning condensers adjusted to give the correct matching for this load such that at full power the cathode and screen meters each indicated 30 milliamps. A length of 70 ohm coaxial cable could now be placed between the transmitter and the bulbs without altering the tuning to any appreciable extent. The bulbs were then removed and the discharge unit fitted directly to the coaxial line (see Fig. 16) and tuned to

resonance by the tuning condensers (the resonance position shown either by the transmitter meters or by a neon indicator lamp held near the coil or by the discharge intensity). The impedance matching transformer was now adjusted by altering the coaxial feeder tapping point on the tank coil until the transmitter showed the correct loading when turned up to full power. The conditions for maximum power transfer now applied and there was no danger of damaging the transmitter components by operating the unit out of tune.

A transmitter frequency of 8.5 megacycles per second was used in all of the work described in this thesis. This frequency was chosen such that the main carrier wave and harmonics would not interfere with local transmissions. All of the discharge equipment used was carefully screened by earthed copper mesh to comply with the interference regulations laid down by the G.P.O.

c) Experimental R.F. Water-Cooled Discharge Tube.

Preliminary experiments with straight pyrex discharge tubes showed that although the R.F. discharge was much more efficient than the A.C. mains type there was still considerable heating of the tube in the discharge glow regions. Large air blowers reduced this heating but it was found to be more practical to use a narrow water jacket around the discharge tube. This made negligible difference to the discharge intensity but was more than adequate to cool the tube. A diagram of the experimental discharge tube and probe system is shown in Fig. 17. and the same tube could be used for either E.M. or E.S. coupling experiments.

FIGURE 17.

EXPERIMENTAL WATER-COOLED R.F. DISCHARGE TUBE.

Fig. 17.

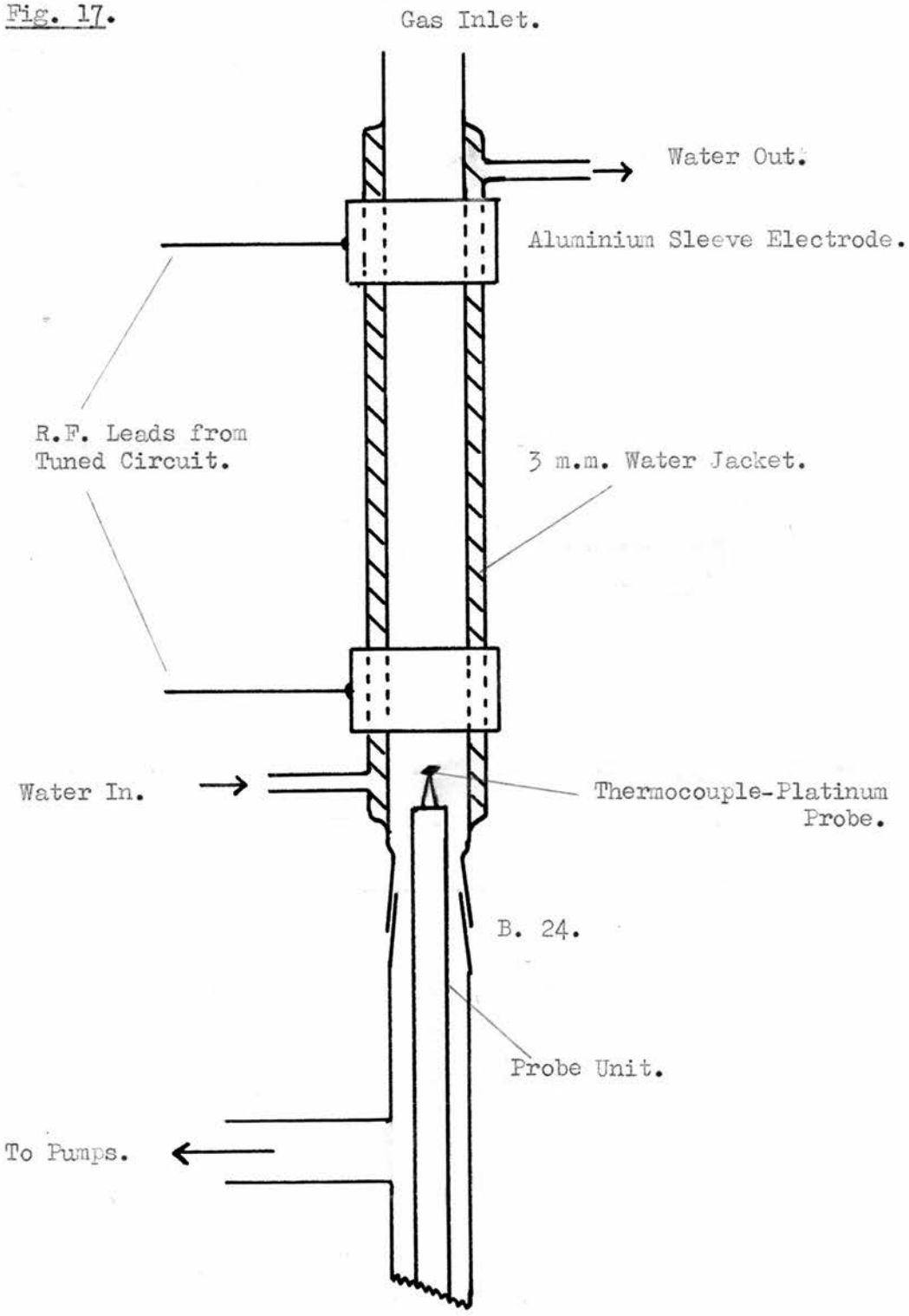

d) Experimental Observations.

Discharges could be produced readily between 10^{-3} and 3 mm. Hg. pressure with either type of coupling but the higher limit could be extended to 5 mm. Hg. using E.S. coupling with the electrodes close together. In both coupling methods the discharge spread along the tube and attempts to confine the glow to the electrode regions with earthed sleeves showed little or no improvement. At 10^{-1} mm. Hg. the spread was about 1 metre each way from the discharge tube but at 1 mm. Hg. the spread was only a few inches.

Discharges were tested in either nitrogen or hydrogen flowing at the same flow rate as before. No hydrogen atoms could be detected in an uncoated tube but the application of meta-phosphoric acid considerably reduced the discharge intensity with both E.S. and E.M. couplings (probably by the formation of conducting paths in the moist acid). Even so, hydrogen atoms could be detected up to a few inches from the discharge front.

In nitrogen, atoms were formed very readily even in an uncoated tube. Also in a darkened room a faint golden yellow glow was visible in the exit tube and after several hours running and with careful adjustment of the discharge power the afterglow penetrated about one metre down the exit tube. This condition gave the greatest activity of the probe unit. On heating a few inches of the exit tube with a gas torch the glow refused to pass this point for several hours indicating

the importance of surface activity in this work. Additions of 10 to 20% oxygen produced vivid green afterglows visible for several seconds after extinguishing the discharge.

e) Wall Coatings with R.F. Discharge Tubes.

The effect of various wall inhibitors was again tested with both nitrogen and hydrogen discharges. As in previous experiments only meta-phosphoric acid gave any noticable increase in the concentration of atoms but it quickly dried out in the discharge tube and then its efficiency was reduced and became variable.

FIGURE 18.

EXPERIMENTAL MASS-SPECTROMETER HEAD.

Showing Gauze Box and 2,000 volt Terminal Block.

Fig. 18.

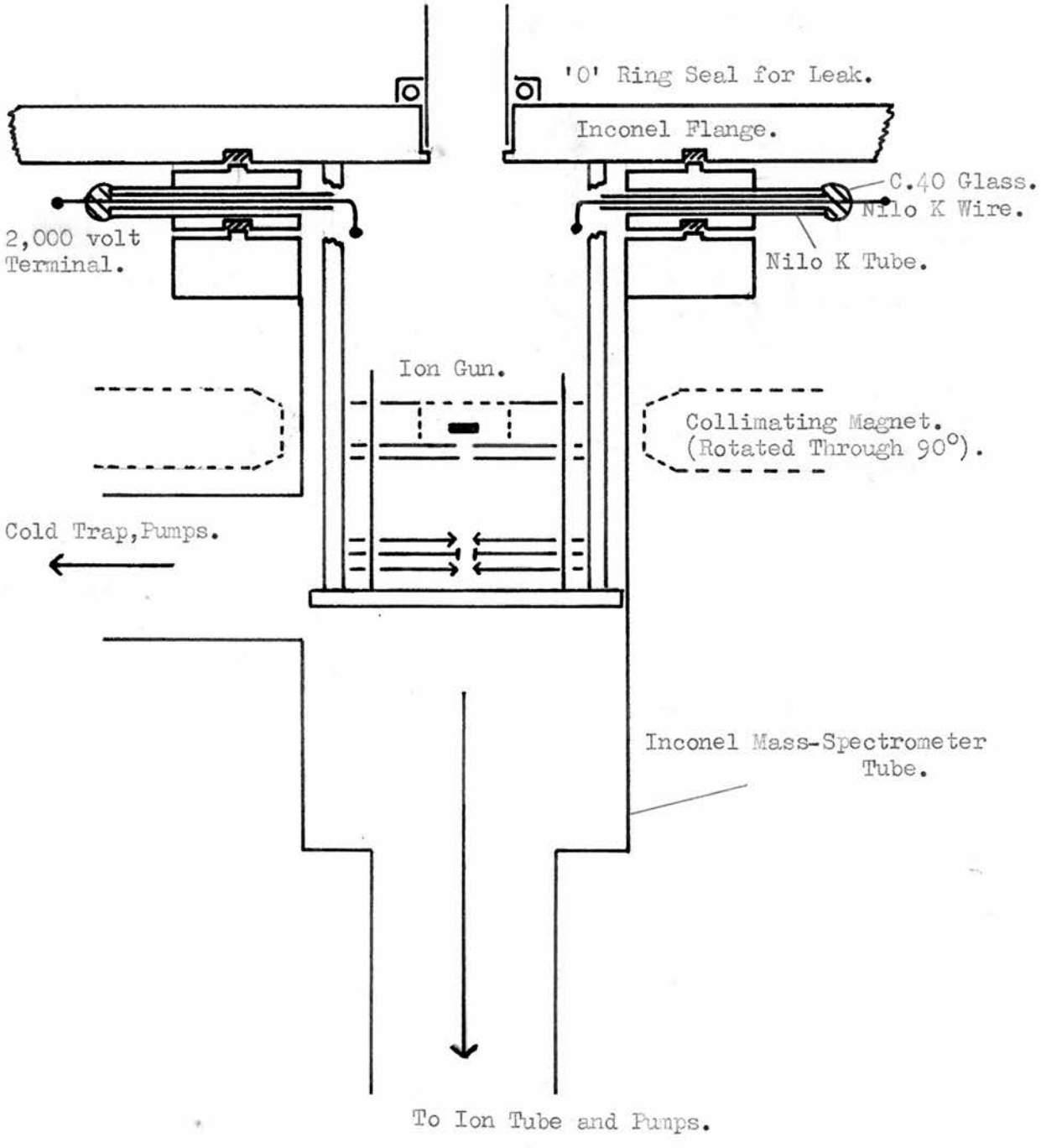

10. PRELIMINARY DEVELOPMENT OF THE MASS-SPECTROMETER.

a) General Modifications.

The existing mass-spectrometer was a 60° Nier type instrument complete with all associated electrical equipment. It had been designed and used for studies of stable molecules and had a tortuous gas entry path, with the ion-gun situated some 8 inches from the top flange which made it quite unsuitable for work with free atoms.

For the analysis of atoms and other short lived species it is necessary to provide a short and practically collision free (line of sight) path from the leak to the ion-chamber and it was considered easier to construct a new head unit rather than attempt to modify the existing one. The experimental layout of the new head is shown in Fig. 18.

Essentially, this consisted of a large inconel plate (9 inch diameter and 0.5 inch thick) with the upper surface carefully machined so that a reaction vessel could be fixed directly to it with a 'Gaco' synthetic rubber seal for future work. The plate, containing a 1 inch diameter hole for the gas inlet leak, served as the main head flange and was bolted to the existing mass-spectrometer tube with phosphor-bronze studs such that it clamped a brass terminal ring into place as shown. The brass washer carried the 10 ion-gun and ion-acceleration leads into the head. These were evenly spaced around the washer and consisted of a length of Nilo-K wire sealed into a short length of C 40 glass tube. The glass tube was then sealed into a length of thin Nilo-K tube protruding from the washer. This gave a seal which would easily withstand

2000 volts but the two leads carrying the 6 amps to the filament overheated on test and were replaced by stranded nickel wire except for the few millimetres of Nilo-K required for the seal itself. The nickel having a greater electrical conductivity than the Nilo-K remained relatively cool. The seals could be replaced if necessary without too much trouble and were generally painted over with silicone varnish when in place. This latter treatment rendered them adequately vacuum tight.

The experimental ion-gun unit was fixed to a small inconel plate bolted to four inconel pillars protruding from the main flange. The electrical leads were joined inside the mass-spectrometer with small stainless steel barrel connectors so that the gun could be readily removed as a unit for repairs and modifications. A series of accurately machined washers on the pillars allowed the ion-gun to be fixed as near to the top flange as possible. In practice this was limited by the external collimating magnet fouling the head flange but at this point the electron beam was about 1 inch below the top plate and this was considered adequate.

b) The Gauze Box.

An experimental ion-gun unit was available in the department [25] and was used for the preliminary work. It had been successfully used on previous occasions in the study of certain unstable materials and had a gauze ion-box to reduce wall interference. It had been built closely to a design suggested by McKnight [102] for the analysis of corrosive gases such as uranium hexafluoride.

A gauze box system would seem to be of value with work on free atoms.

FIGURE 19.

REALIGNMENT OF MASS-SPECTROMETER ION 'OPTICS'.

Fig. 19.

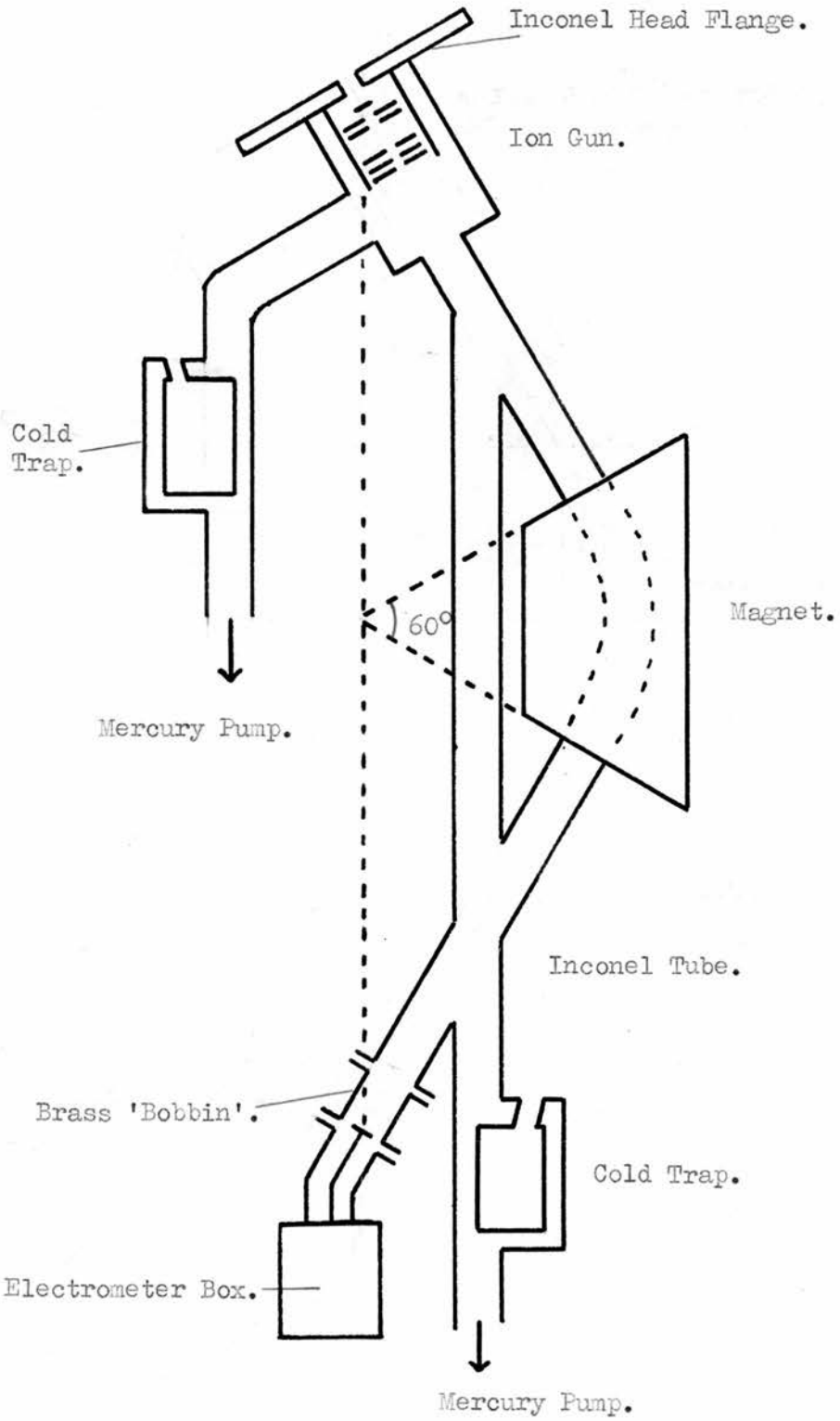

Recombination reactions on the box walls would be reduced and a much higher rate of pumping than in a conventional box could be maintained. Larger leak sizes could be tolerated and this could result in enhanced atom to molecule sensitivity.

The ion-gun assembly consisted of a pointed filament (tungsten ribbon .003 inch thick) protruding through a 3 mm. hole held at box potential. The electrons emitted from the hot filament tip travelled down a so-called channel formed by the gauze sides of the box and were collected at a trap held slightly more positive than the box. An external magnet (200 gauss) collimated the electrons in a spiral path down the channel. There was not a bottom to the box and the ions were drawn out by a drawout plate situated immediately below the box. A repeller electrode was not used and the resulting loss in sensitivity was partially corrected by the more powerful drawout system. The ion beam was focused and accelerated through 1840 volts by a conventional plate system. In all cases the plates were stainless steel insulated from one another by ceramic washers.

c) Realignment of the Mass-Spectrometer Ion 'Optics'.

Before the mass-spectrometer could be tested it was necessary to realign the Nier type ion focusing which had been upset by the repositioning of the electron beam. This was corrected by inserting a brass 'bobbin' to lengthen the collecting end of the mass-spectrometer tube, and by readjustment of the main magnet. This is shown in Fig. 19. with the theoretical Nier type focusing conditions shown in dotted lines.

The mass-spectrometer gas inlet was blanked off with a glass tube

FIGURE 20.

REVISED ION GUN FOR LOW ELECTRON VOLTS.

Showing Electron Accelerating Plate and Mild Steel Pole Pieces.

Fig. 20.

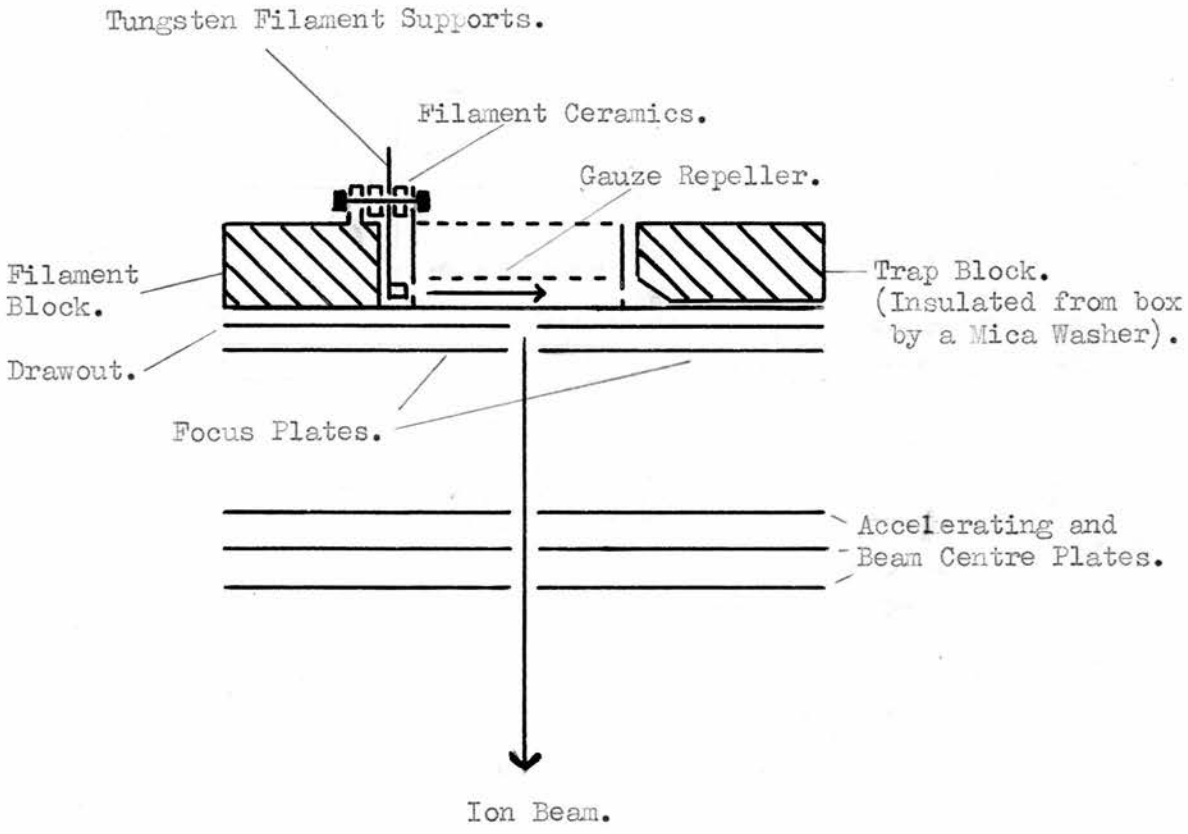

NOTE:- The filament unit and box plate have been rotated through 90° for convenience.

and the unit evacuated. At high electron volts the gun responded extremely well giving more than adequate resolution, good peak shape and a sensitive background scan even though the Phillip's gauge indicated a low background pressure. Below about 40 eV. the filament circuit lost control and the filament current rose sharply and could only be brought back into control by raising the electron volts. Also in the 40 to 50 eV. region the drawout plate potential disturbed the electron beam and the gun had to be operated at reduced sensitivity. Above 50 eV. the electrons had sufficient energy such that the optimum drawout conditions could be applied without disturbing the electron beam.

d) Modified Ion-Gun for Low Electron Volt Working.

Fig. 20. shows a modified gun designed to operate at low electron volts. The box was again gauze sided but had a conventional plate bottom such that the drawout potential now penetrated through a narrow slit in the box bottom as in a conventional head. A stainless steel gauze repeller was fitted directly over the electron beam and insulated from the box by a thin mica washer. The filament unit was modified, the filament now being only slightly curved and held as close as possible to a slit in the acceleration plate held at box potential. This close separation was found necessary for working at low electron volts in stabilising circuits where the trap current controls the filament temperature.

Essentially the electron source is equivalent to a diode valve and should obey the general diode characteristics. The difference is that in the mass-spectrometer case the diode plate has a slit in it and the

FIGURE 21.

TYPICAL DIODE CHARACTERISTICS.

Fig. 21.

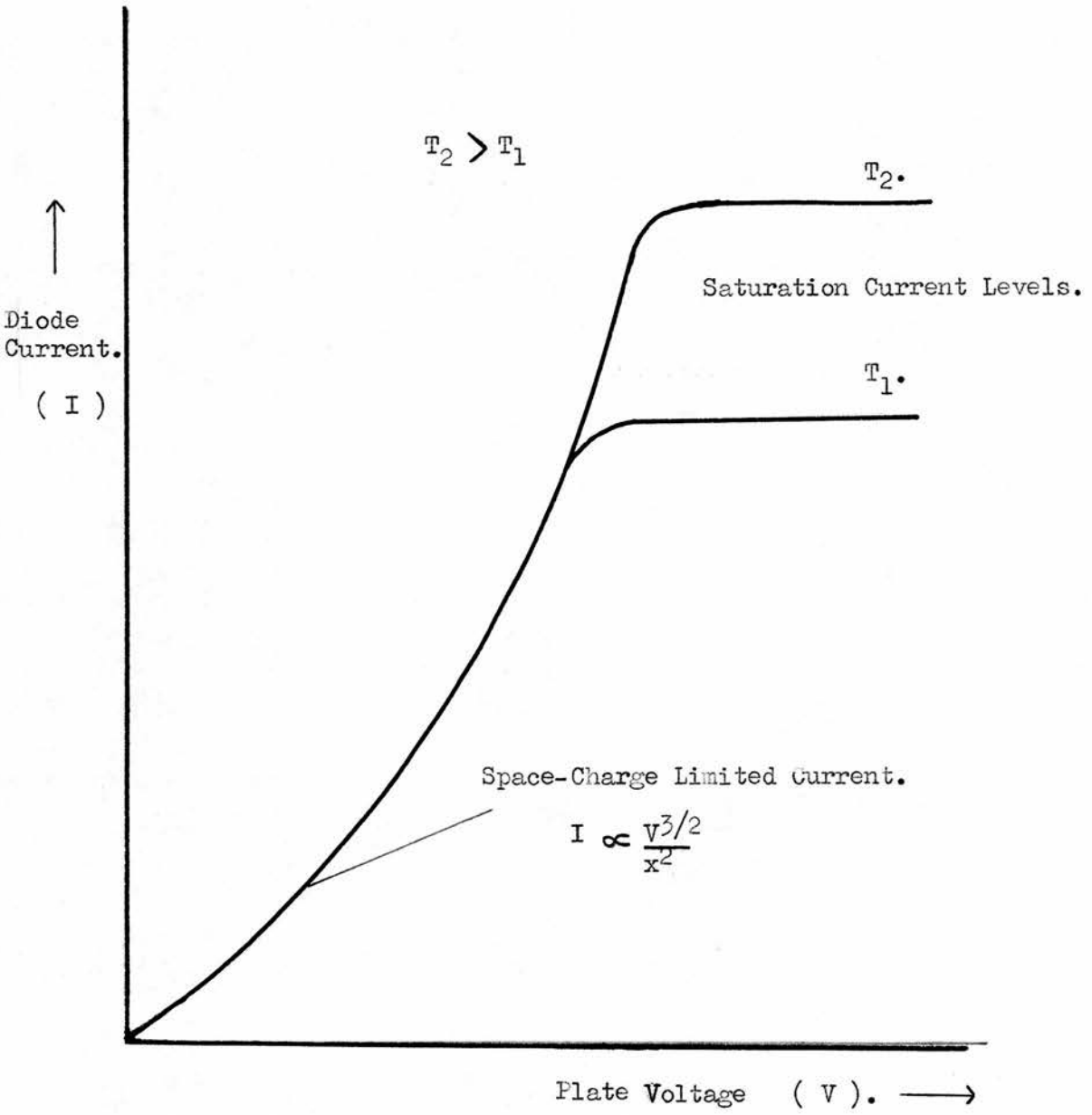

portion of the plate current which penetrates this slit, aided by the collimating field produces the trap current.

e) Filament and Diode Characteristics.

Fig. 21. shows a typical diode characteristic graph for two different filament temperatures [127][128]. For a mass-spectrometer filament to stabilise it must operate on the 'saturation current' part of the graph where a temperature change can produce a significant trap current alteration. If at low electron volts the filament becomes 'space charge limited' then stability is lost since a rise in the filament temperature cannot increase the trap current.

In the 'space charge limited' region where the plate potential is shielded from the filament by a mass of electrons Child's law [129] holds, namely:- $I \propto \frac{V^{3/2}}{X^2}$

where I is the plate current, V the plate voltage and X the inter-electrode separation. Thus if X is reduced the current rises more sharply for given plate voltages and the saturation levels occur at lower plate potentials.

In practice the filament ribbon could not be fixed too near the acceleration plate since as soon as the filament heated up a short circuit developed to the box. Generally filaments were constructed leaving about .005 inch gap between the filament and the plate.

The effective collimating magnetic field strergth was also increased by introducing mild steel pole pieces into the head (see Fig. 20. page 90). One of these served as the filament mounting block

FIGURE 22.

EXPERIMENTAL R.F. DISCHARGE TUBE FITTED OVER MASS-SPECTROMETER.

Fig. 22.

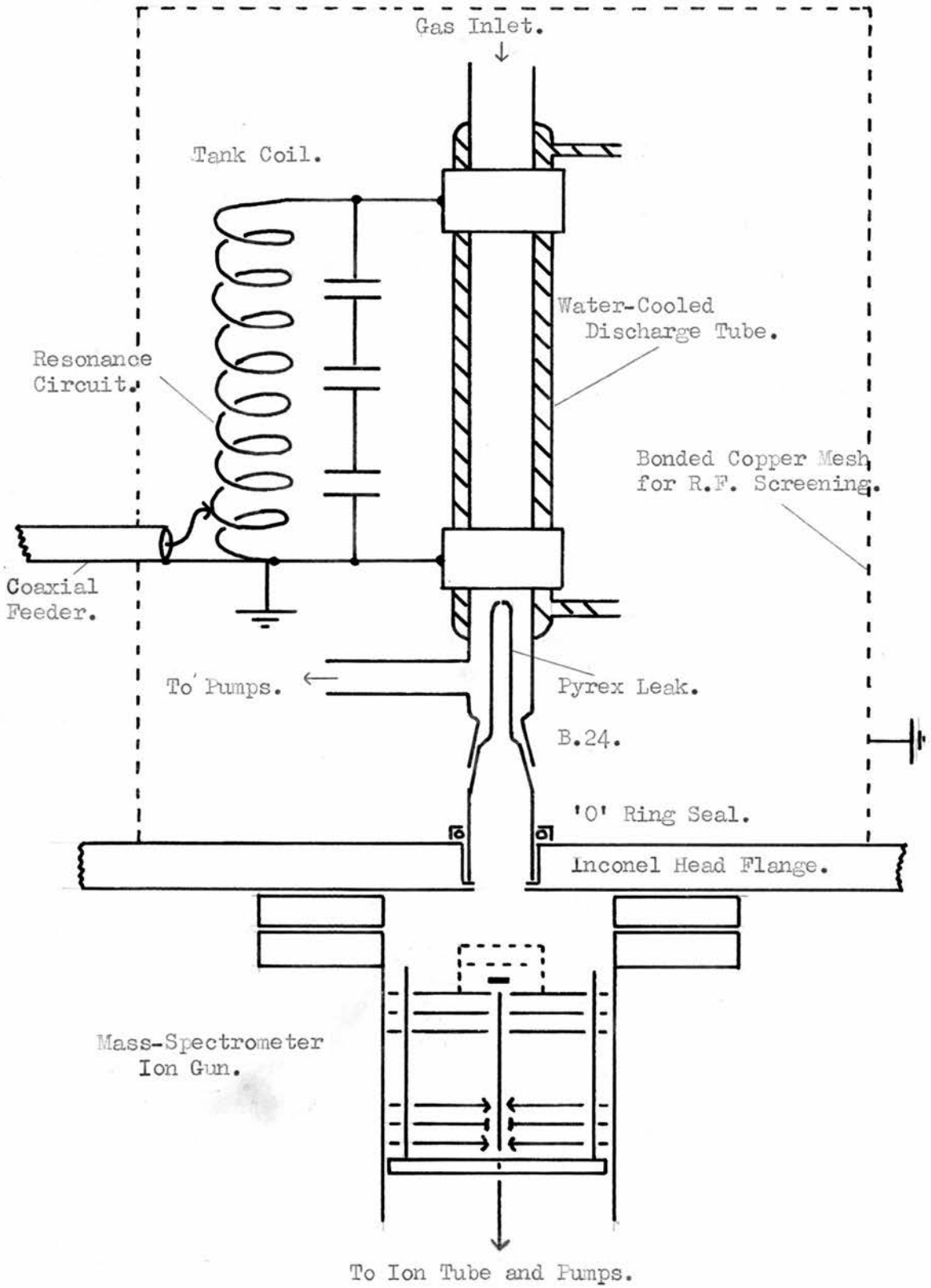

and the other, insulated from the box with a mica washer became the trap. The latter contained a nichrome inset to act as a Faraday cage for electron trapping. Experiments with a field strength meter showed that the magnetic flux in the electron beam region increased from 200 to 350 gauss by the addition of the pole peices. It also removed the necessity for sensitive external adjustment of the collimating magnet.

f) Experimental Observations.

The head was again assembled and the mass-spectrometer evacuated. The response at low electron volts was immediate and the unit would control over the range permitted by the control deck (11 to 85 eV.). The total emission remained more or less constant over this range at 400 μ amps giving a trap of 40 μ amps. Generally as the filament aged the total emission gradually rose to about 800 μ amps but would still control over the whole range. Again, a background scan indicated that resolution was quite adequate (1 in 150) and it now seemed appropriate to mount a discharge system over the head and examine the atomic species formed in the discharge.

g) Experimental R.F. Discharge Tube over the Mass-Spectrometer.

Fig. 22. shows an experimental R.F. discharge tube fitted over the mass-spectrometer head. The leak was fused onto an extended B 24 cone and the other end sealed into the inconel head plate with an O-ring seal. The condenser type discharge tube could then be piecin sealed onto the leak unit and this greatly assisted its construction. The leak was carefully made as follows.

FIGURE 23.

Fig. 23.

CONSTRUCTION OF THE MASS-SPECTROMETER LEAK.

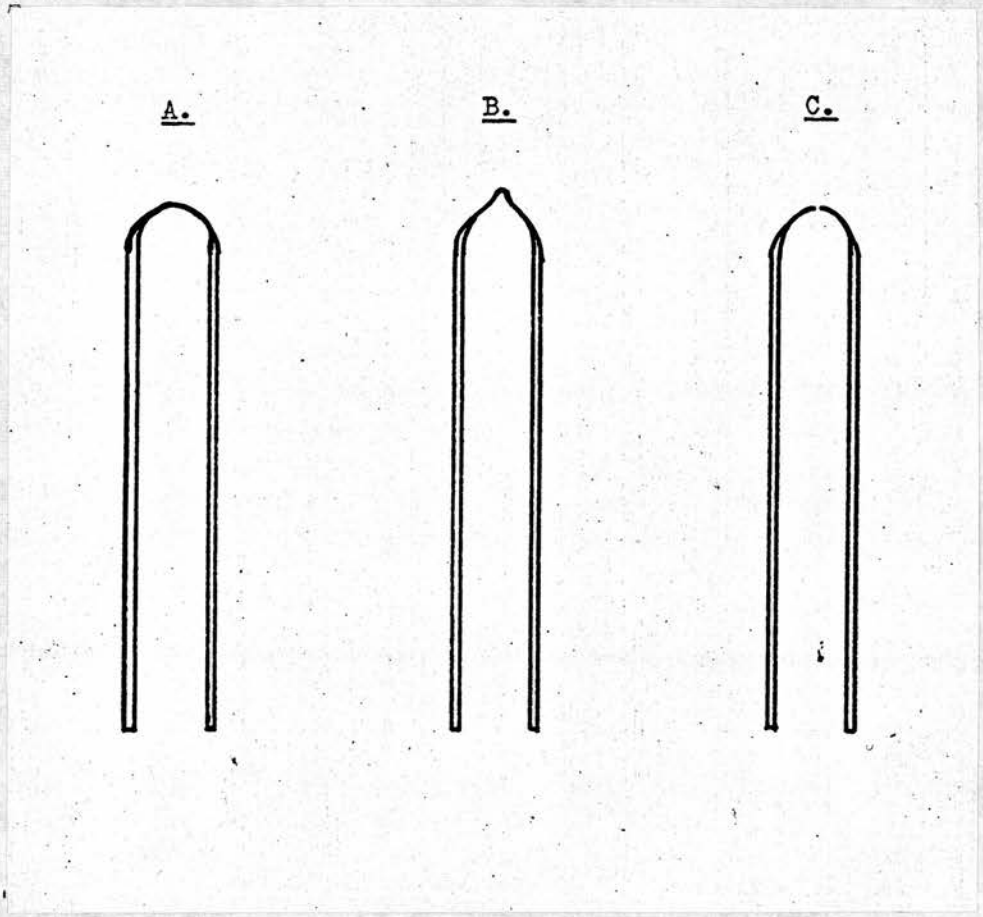

h) Construction of the Mass-Spectrometer Leak.

A pyrex glass tube (6 mm.) was sealed off at one end and carefully pulled down and blown out until the end was wafer thin (see Fig. 23A). The tip was then warmed and pulled out with a sharp glass rod (Fig.23B). The tip was now carefully ground until a leak the correct size and shape was formed (Fig. 23C). With care a leak of .006 inch diameter was constructed and fitted as explained above.

i) The Vibrating Reed Electrometer.

The basic sensitivity of the mass-spectrometer was increased by replacing the existing D.C. amplifier with a vibrating reed electrometer. This was an Ekco unit type N616B having a theoretical sensitivity some 200 times greater than the existing amplifier but zero instability did not permit its use on the most sensitive ranges. The unit had switching facilities for 10^8, 10^{10} and 10^{12} ohm resistors with associated voltage measurements of various ranges between .003 and 3 volts. A backing off unit could inject up to 90 volts into the electrometer input such that both large and small peak heights could be determined without undue resistor changing. The electrometer output was fed to an automatic recording potentiometer.

During the preliminary installation of the unit it was apparent that the normal method of coupling the unit to the collector by a coaxial line was quite inadequate. Any slight vibration or tremor induced a capacity change in the cable and this gave enormous oscillations in the output meter reading. This was corrected by strapping the vibrating reed unit to the bottom of the mass-spectrometer

DIAGRAM OF THE REVISED EARTHING SYSTEM.

Fig. 24.

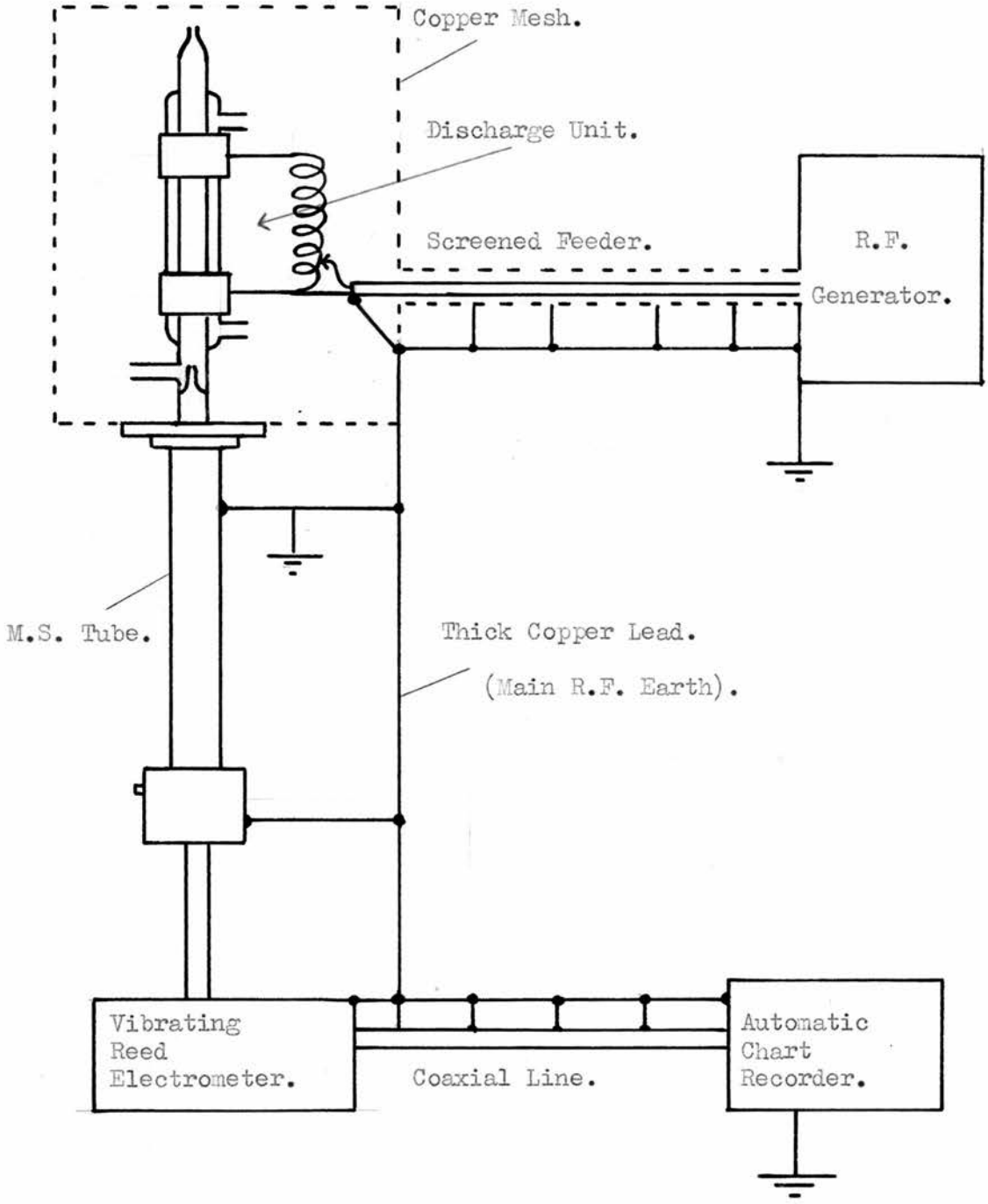

tube and connecting the unit to the collector with stout copper wire screened by a 2.5 inch diameter brass tube. This virtually eliminated all vibration troubles and the zero stability was about ± 0.25 mv. on the 100 mv. range on the 10^{12} ohm resistor but the 30 and 3 mv. 10^{12} ohm ranges were unusable due to random instrument noise.

j) R.F. Interference with the Mass-Spectrometer Electronics.

The discharge tube was coupled to the transmitter feeder line by an electrostatic coupling (see Fig. 22. page 94) and the unit built into a cage of earthed copper mesh to meet the G.P.O. interference regulations.

Nitrogen or hydrogen could be pumped through the discharge tube at pressures near 1 mm. Hg. and the leak positioned to sample gas from the discharge glow regions. It was found that the R.F. discharge produced considerable electrical interference with all the mass-spectrometer equipment. The magnet and filament currents changed slightly but the electrometer reading oscillated from one end of the scale to the other on all ranges and all resistors, such that the operation of the mass-spectrometer under these conditions was quite impossible.

k) Revised Earthing System.

Experiments with additional earthing sometimes showed a distinct improvement in the interference level and in other cases just the opposite. It was decided to revise the whole earthing system of the electronic equipment and to connect each unit together with one heavy copper earthed lead. Fig.24. shows a block diagram of the revised earthing system.

This immediately reduced the interference to a fraction of its

FIGURE 25.

Fig. 25.

ELECTROMETER BACKGROUND WITH AND WITHOUT THE DISCHARGE.

On the illustrative traces given below a 10 inch chart was used, such that on the 10 mV. range 1/10 inch is equivalent to 0.1 mV.

1. 10^{10} ohms Resistor.

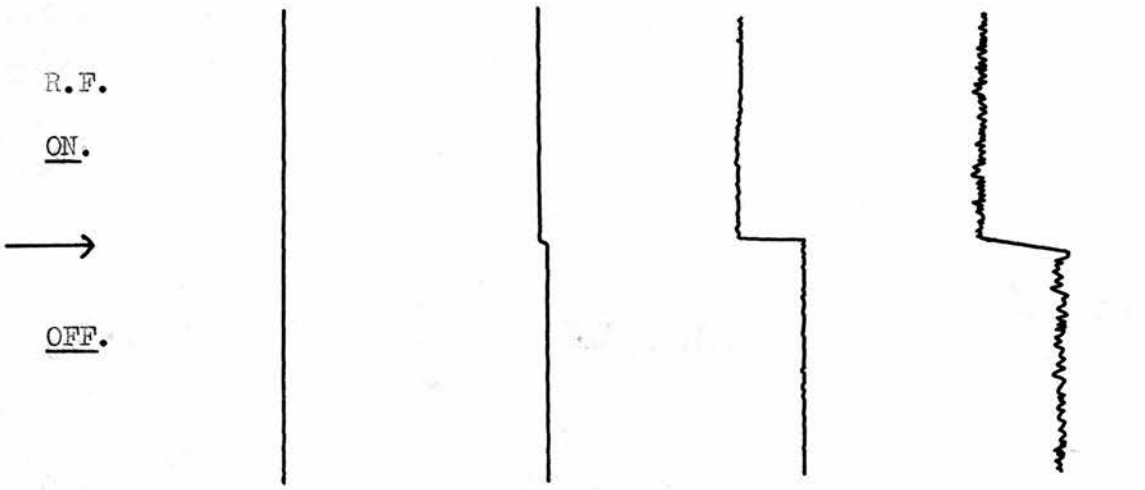

Range:- 300 mV. 100 mV. 30 mV. 10 mV.

2. 10^{12} ohms Resistor.

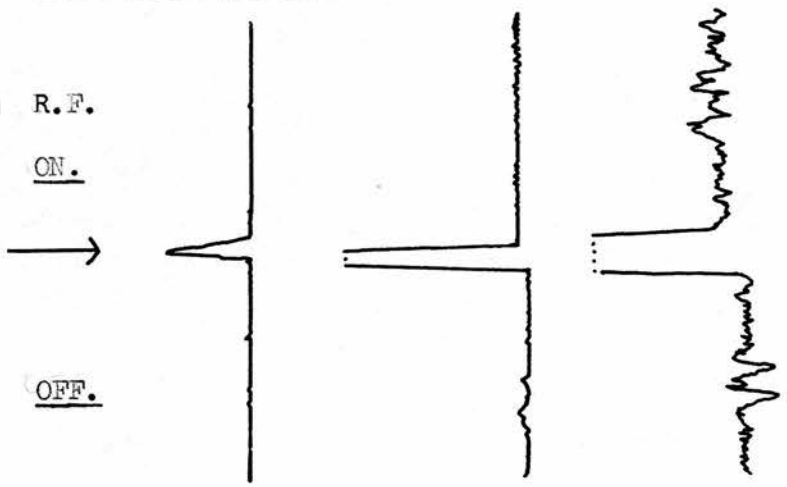

Range:- 300 mV. 100 mV. 30 mV.

original value and with careful positioning of the earthed leads the interference in the electrometer was negligible even on the very sensitive ranges. Fig. 25. shows an electrometer trace on the 10^{10} and 10^{12} ohm resistors with and without the discharge. In fact the discharge produced so little disturbance to the electronics that the mass-spectrometer would drift only slightly off a peak as the discharge was activated.

l) R.F. Interference with the Mass-Spectrometer Sensitivity.

Although there was no R.F. electrical interference with the mass-spectrometer it was soon obvious that a sensitivity change occurred whenever the discharge was activated. With the discharge on, peak heights both from the gas sampled from the discharge tube and from background material appeared as about 0.75 of their value in the absence of the discharge. There was no change in resolution and little change in the focus conditions. On certain occasions however when the discharge failed to strike although thefull R.F. field was available, the peak heights remained unchanged until the gas actually struck. From this it was inferred that the effect was transmitted in some way by the ionised gas. Possibly the R.F. field carried by the ionised gas penetrated the mass-spectrometer head through the hole in the head flange and affected the ion-gun potentials resulting in a loss of sensitivity.

m) The All Metal Leak.

The head was removed and the glass leak replaced by a complete metal leak. This consisted of a brass unit which could be 'Gaco' rubber sealed to the main inconel flange as shown in Fig. 26A. A thin 5 mm.

FIGURE 26.

MODIFIED MASS-SPECTROMETER LEAKS.

Fig. 26.

A. Copper Foil Leak.

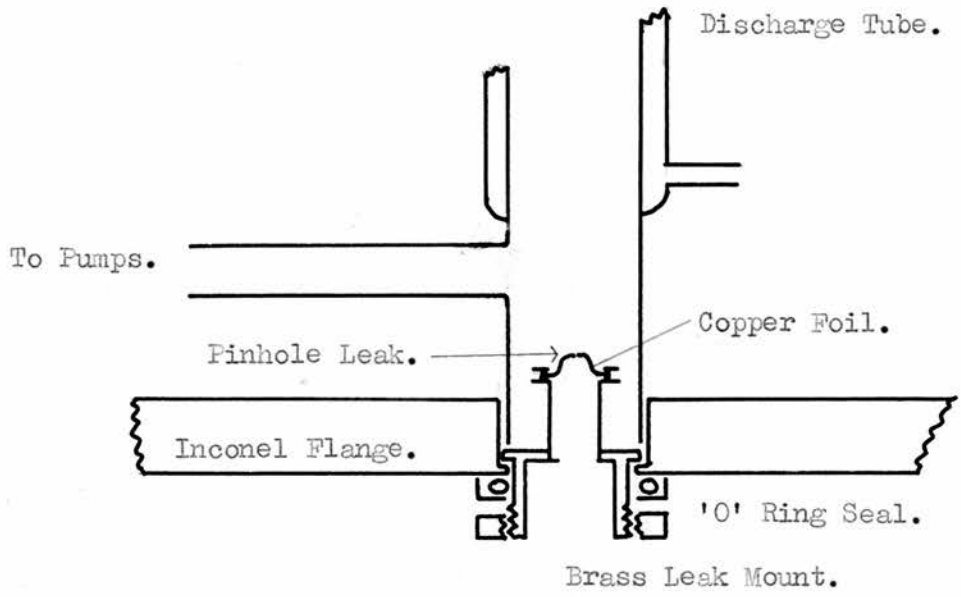

B. Slender C.40 Glass Leak.

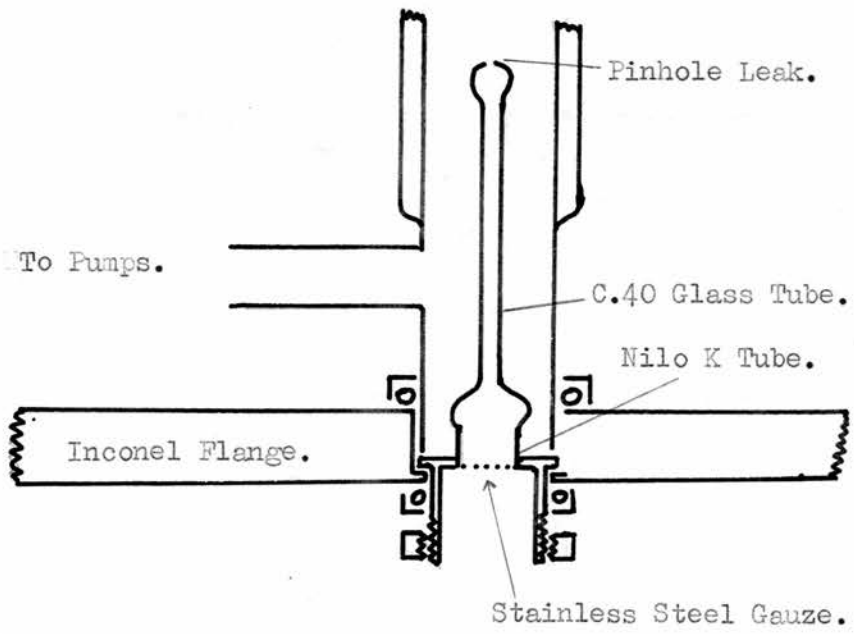

brass tube protruded from the unit and on top of this was hard soldered a piece of copper foil (.004 inch) which was compressed into a hump by a ball-bearing and punctured with a fine needle to give a .006 inch hole. This gave a metal leak of the correct size and also enabled the discharge tube to be mounted much nearer to the head as there was now no need for the B 24 joint.

With the complete metal leak there was no loss of sensitivity on activating the discharge, and peak heights, shapes and resolution were identical with and without the discharge.

n) Preliminary 14^+ Investigations.

With the transmitter off, a steady flow of nitrogen at 1 mm. Hg. was maintained in the discharge tube. The mass-spectrometer was tuned to the 14^+ peak at 50 eV. and then the electron volts decreased. The main 14^+ peak due to $N_2 \xrightarrow{e} N^+ + N + e$ dropped sharply at about 27 eV. but there was still a residual background signal of 500 mv. on 10^{12} ohms above deflect zero even at 23 eV. This background dropped to 100 mv. when the discharge tube was evacuated.

With nitrogen present at 1 mm. Hg. pressure and the background signal backed off to the 300 mv. range a distinct rise of about 30 mv. (at 23 eV.) was apparent whenever the discharge was activated. No equivalent rise could be detected in the 1^+ peak in a similar experiment with hydrogen.

This seemed to indicate the presence of a mass 14 species in nitrogen whenever the discharge was activated but it was evident that

much greater sensitivity would be necessary before a diffusion flame could be analysed. Kistiakowsky however in his experimental nitrogen atom mass-spectrometer obtained adequate sensitivity using a complete ion-box assembly (99)(100)(101). The box was isolated from the mass-spectrometer tube apart from small pumping holes and consequently operated at relatively high box pressures. Apparently the nitrogen atoms were sufficiently long-lived to survive the many hundreds of wall collisions that were necessary before ionisation. This form of box could probably give good results in nitrogen atom detection but the solid walls would be fatal to hydrogen atoms where the recombination coefficient on metal surfaces is almost unity.

MODIFIED MASS-SPECTROMETER HEAD UNIT.

Showing the complete box and the differential filament pumping.

Fig. 27.

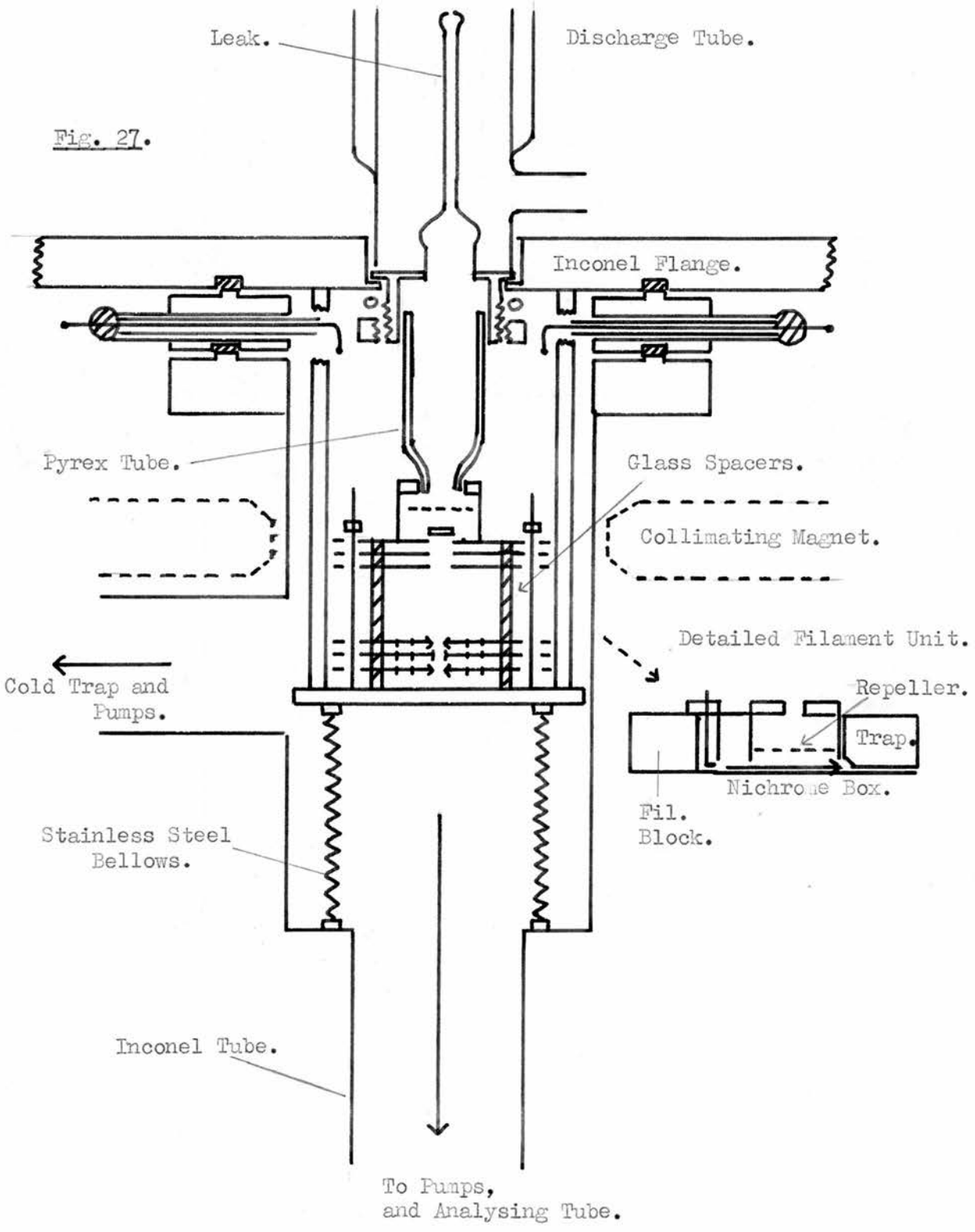

FIGURE 27.

11. THE MODIFIED MASS-SPECTROMETER (COMPLETE ION BOX).

a) The Complete Box and Differential Pumping System.

The head was removed and modified with a view to examining nitrogen atoms alone and its construction is shown diagramatically in Fig. 27.

The gauze box was replaced with a complete nichrome unit. The mild steel filament block was shortened so that the filament could be set back about 0.25 inch from the box and pumped separately. The gas sampled by the leak was directed into the ionisation box by a funnel shaped piece of glass tube, one end of which fitted tightly into the brass filament mount and the other end into a nichrome block on the box top. After passing through the box the gas diffused down the drawout and acceleration plate slits (this latter diffusion was assisted by small holes drilled as shown) and was directed into the mass-spectrometer tube by a stainless steel bellows fixed to the small inconel flange. The ion-chamber was isolated from the filament section by circular glass washers clamped between the plates such that the only access from one region to the other was via the small entrance slit for the electron beam. The filament and ion-tube regions were pumped separately by independent mercury pumps backed by their own oil pump. The filament region was thus maintained at a very much lower pressure than the box so that any 14^+ from dissociation of nitrogen on the hot filament would be reduced to a minimum.

b) The Modified Leak.

The leak was also modified, the copper leak now being replaced by

a slender C 40 glass tube (2 inch long and about 3 mm. I.D.) glass blown onto a Nilo-K tube silver soldered onto the leak block (see Fig. 27B. page 102). A smaller leak size of .003 inch was made in the tip of the C 40 tube by the method described earlier. The smaller leak size was chosen since the original leak (.006 inch) would probably have produced too high a pressure in the box in view of the restricted pumping. A stainless steel gauze was soldered over the bottom of the brass leak block to prevent the R.F. field penetrating into the head.

c) Experimental Observations.

The mass-spectrometer was again evacuated and tested. The gun operated identically with the gauze unit. It would stabilise over the whole range of electron volts and gave adequate resolution (1 in 150). With 1 mm. of nitrogen in the discharge tube the 28^{+} peak height at 50 eV. was about 200 mv. on the 10^{8} ohm resistor. The background 14^{+} at 25 eV. was still suprisingly large at 300 mv. on the 10^{12} ohm resistor above deflect zero but on activating the discharge the peak height rose to over 800 mv. This immediately dropped back to 300 mv. on extinguishing the discharge and was very reproducible and varied with the discharge power.

This was extremely encouraging but the high background above deflect zero was rather alarming. The introduction of complete differential filament pumping had failed to alter this background appreciably and it seemed unlikely that the background was derived from nitrogen atoms formed on the hot filament diffusing back into the box.

A scan however soon showed that the background was not specific to

FIGURES 28 and 31.

Fig. 28. THE MODIFIED ION COLLECTING SYSTEM.

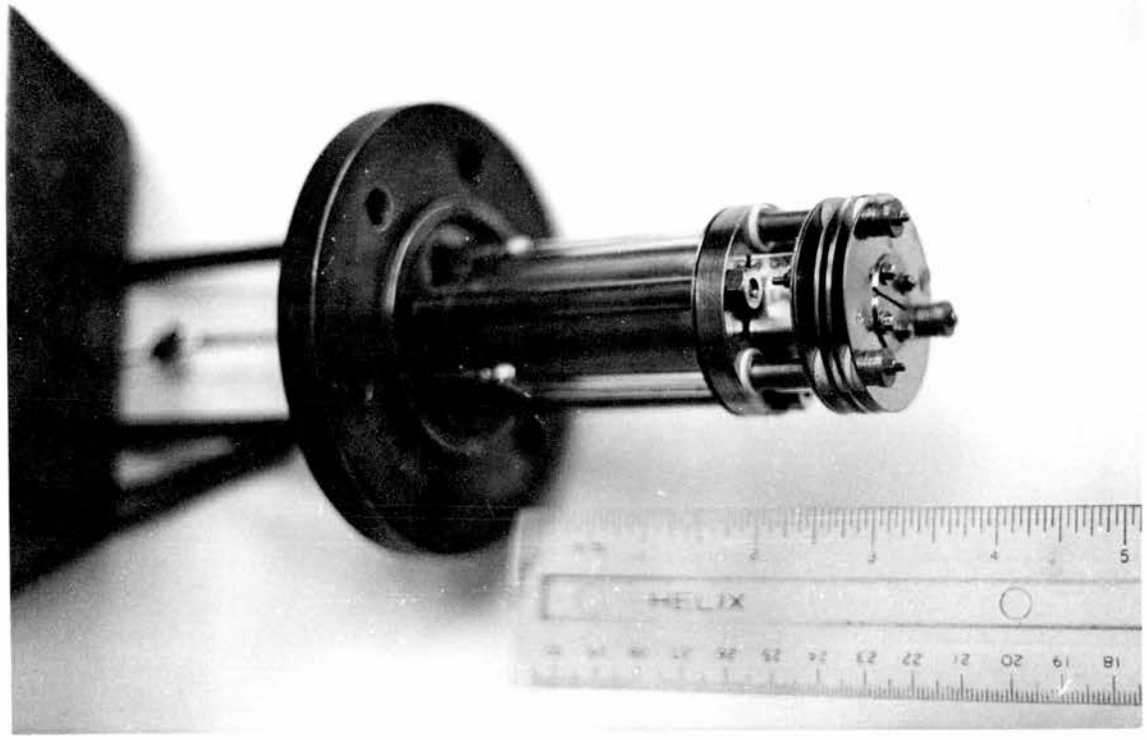

Fig. 31. THE ELECTRON SUPPRESSOR GRID.

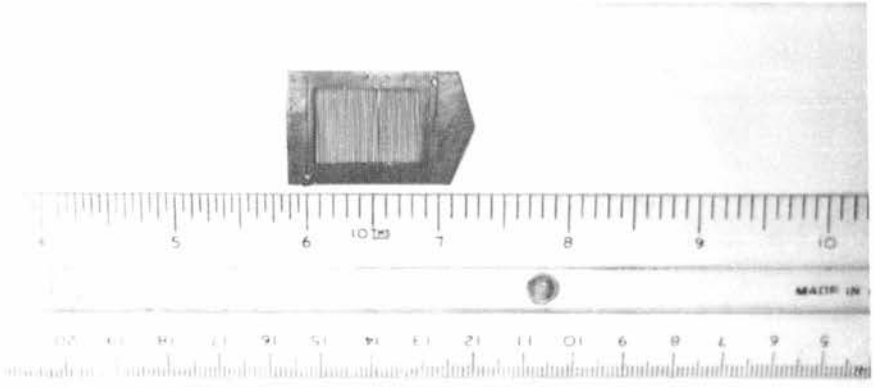

the 14^+ peak but appeared at a position corresponding to about 5^+ as the mass-spectrometer scanned from 1^+. Up to this point the background and deflect zero were identical and it seemed to suggest that as soon as any appreciable ion currents began to penetrate the ion-tube the background rose above deflect zero. The rise increased with greater discharge tube pressure and this suggested that it was probably caused by ion-molecule interactions in the mass-spectrometer tube which were pronounced due to the very high sensitivity and working pressure of the unit.

It was found however that the mass-spectrometer had not reached saturation pressure and showed a linear response of output signal with nitrogen pressure up to 2.5 mm. Hg. Above this pressure the peak height decreased with increasing nitrogen pressure.

In modern high sensitivity and high resolution mass-spectrometers ion-molecule interactions are generally accepted and more refined collecting systems are used to overcome this trouble (130). An ion-molecule collision results in a loss of some or all of the kinetic energy of the ion. Thus, if a potential barrier maintained at box potential is applied near the collector, all ions which have lost a certain fraction of their kinetic energy will be rejected. In this way a differential collecting system can be operated.

d) The Modified Collecting System and the Effect on the 14^+ Background.

The collecting system of the mass-spectrometer was removed and modified to form an electron lens system as suggested by Craig (131). The modified unit is shown in Fig. 28. and presented diagramatically

FIGURE 29.

MODIFIED ION COLLECTING SYSTEM.

Fig. 29.

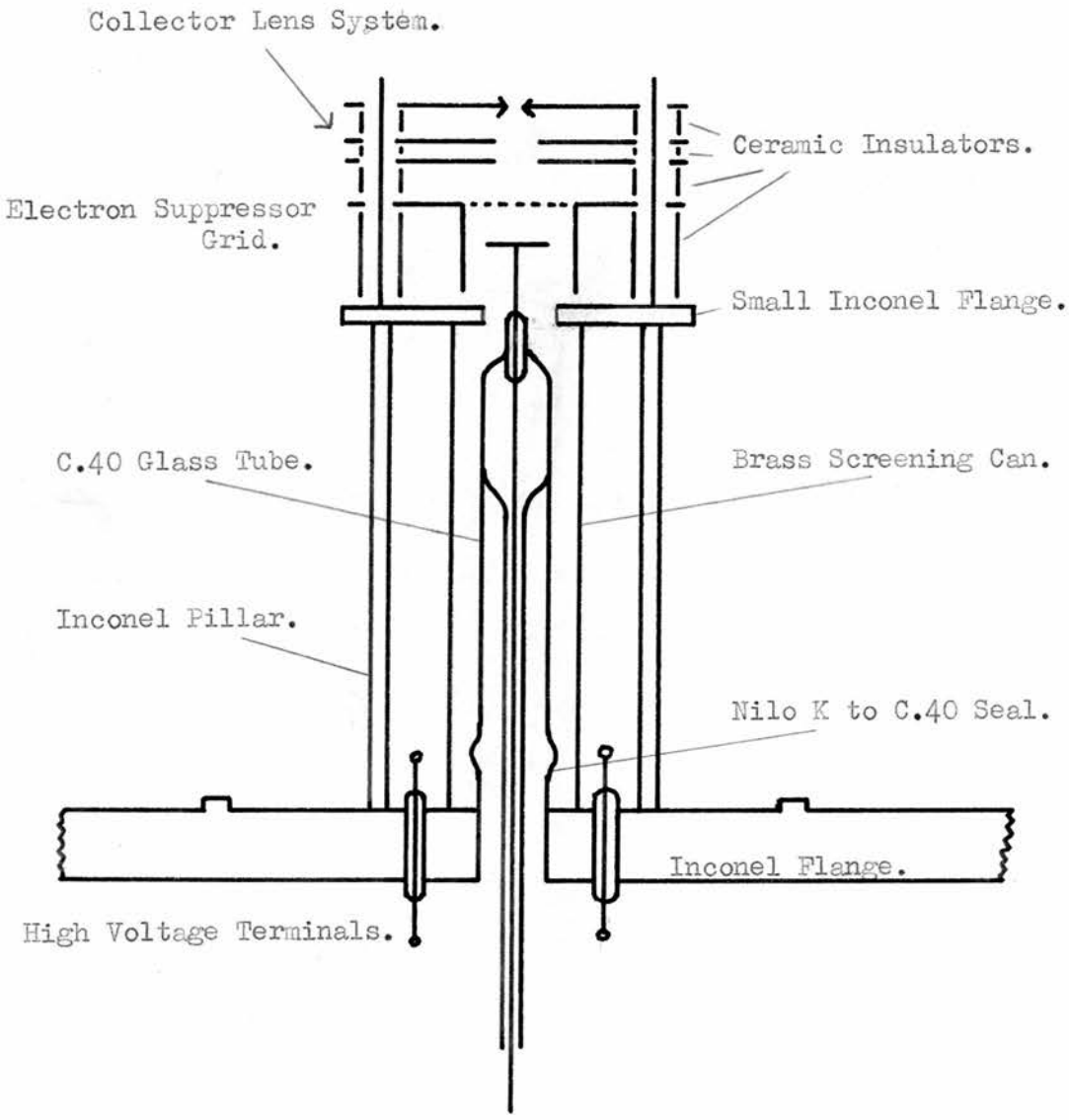

FIGURE 30.

MODIFIED ION COLLECTING SYSTEM.

Electrode Dimensions.

Fig. 30.

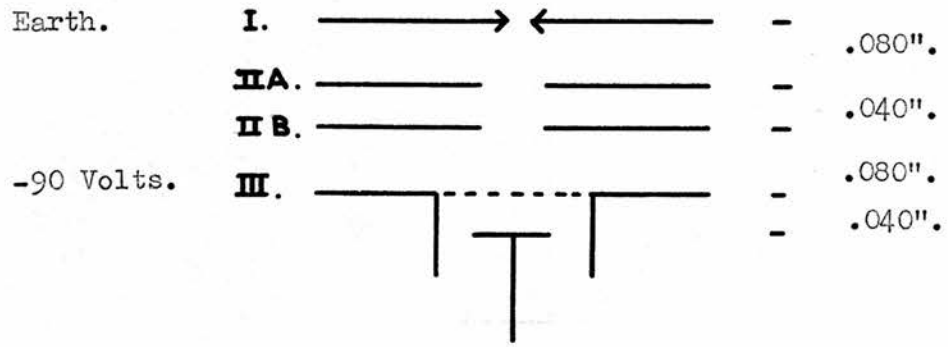

Electrode.	Thickness.	Slit-Width.	Slit-Length.
I.	.080".	.025".	.6".
II A.	.080".	.180".	.8".
II B.	.080".	.180".	.8".
III.	.080".	.6".	.8".

in Fig. 29. The electrode dimensions (see Fig. 30.) were as near as possible to those suggested by Craig.

Essentially the unit consisted of a knife-edge slit (electrode I) held at earth potential and separated from the collector plate by two insulated stainless steel plates (electrodes IIA and IIB) held at potentials V_{IIA} and V_{IIB} near box potential, and forming the main electron lens. An electron suppressor grid was held between plate IIB and the collector and consisted of a rectangular slit covered with a grid of fine nickel wire (.004 inch thick and spaced .012 inch apart). The grid was made by carefully winding the wire onto a brass former which had been toothcombed by an eccentric cutter on an automatic feed lathe, (see Fig. 31. p. 108). The grid was maintained at -90 volts with respect to earth. By suitable adjustment of potentials V_{IIA} and V_{IIB} the collecting system could be used as (i) a collector with an adjustable slit width or (ii) a rejector of ions which have lost a certain fraction of their kinetic energy.

Since there was already adequate resolution, the main concern was to use the unit as an ion energy discriminator. Craig suggests that in order to reject all ions which have lost 1/90th or more of their kinetic energy that $V_{IIA} / V_{IIB} = 1.28$ where V_{IIB} is just insufficient to cut off the peak.

The modified collecting system was assembled and tested. Various test voltages were applied to the two main electrodes. For preliminary experiments V_{IIA} was set at 1740 volts by backing off 100 volts of the 1840 box volts, and V_{IIB} made variable over the range 1840 to 2340 volts

FIGURE 32.

14^+ Peak Scans showing the background above deflect zero and the general peak shape and intensity with and without the discharge.

Fig. 32.

(i) Original Collecting System.

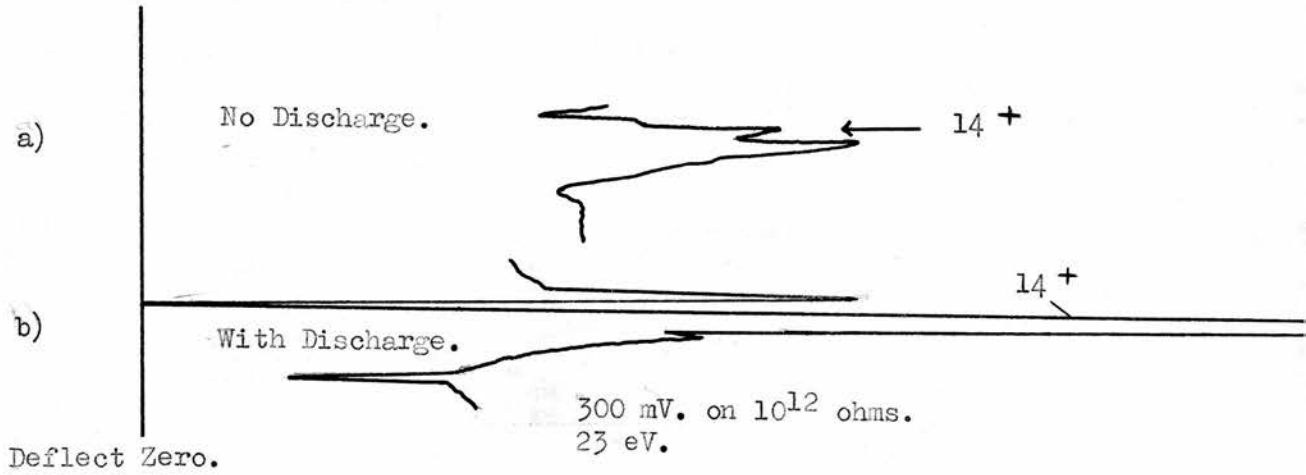

(ii) Modified Collecting System.

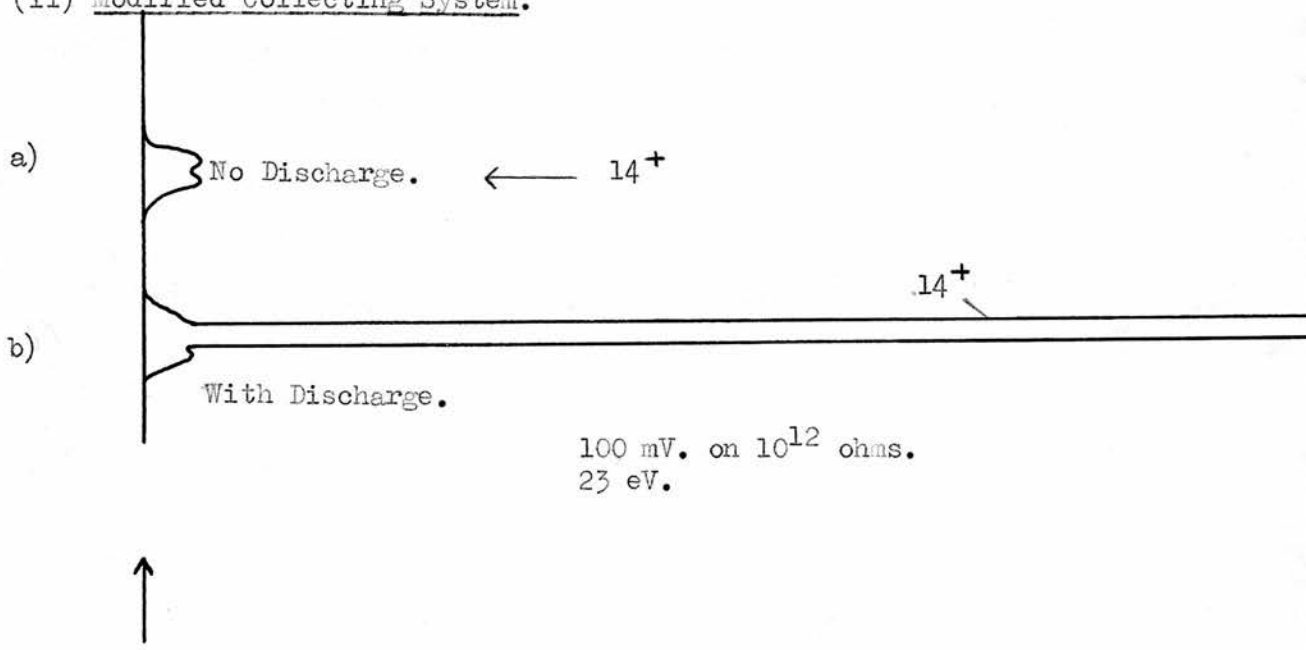

with batteries assisted by the box volts.

As V_{IIB} was gradually increased from 1840 the peak height remained constant up to 2220 volts and then suddenly dropped to zero. V_{IIB} was then adjusted to have the maximum voltage before the cut-off point occurred.

The response on the 14^+ background with nitrogen at 1 mm. Hg. in the discharge tube was immediate and astonishing. The background and deflect zero were virtually identical and a trace of the 14^+ background with the old and revised collecting systems is shown in Fig. 32 (i) and (ii). Also shown are the traces of the 14^+ peak with the discharge activated. Note that in Fig. 32 (ii) the scans are three times as sensitive as Fig. 32 (i).

FIGURE 33.

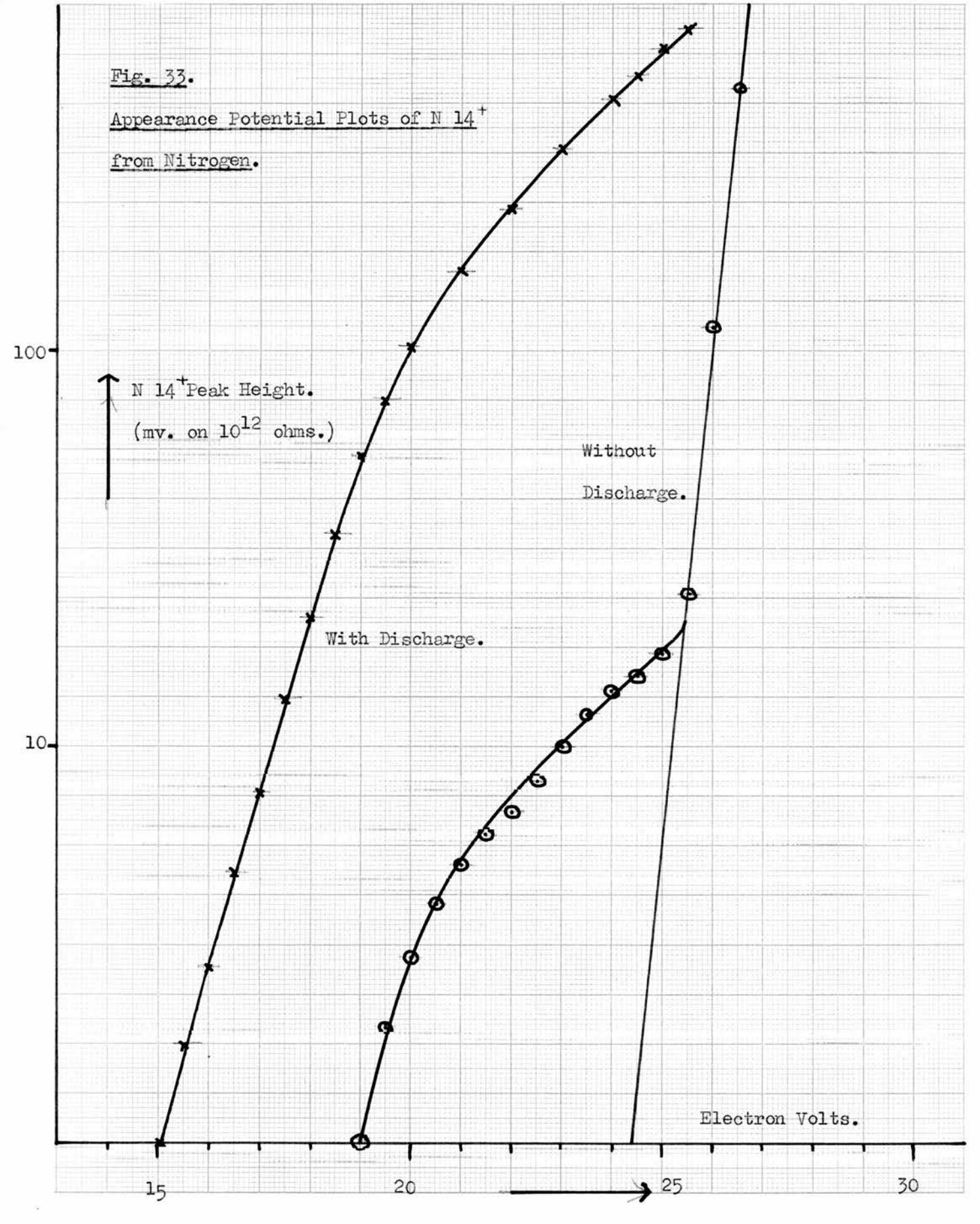
Fig. 33.
Appearance Potential Plots of N 14+ from Nitrogen.
100
10
N 14+ Peak Height.
(mv. on 10^12 ohms.)
Without Discharge.
With Discharge.
Electron Volts.
15
20
25
30

12. THE APPEARANCE POTENTIAL OF THE 14^+ PEAK IN THE DISCHARGE.

Fig. 33 shows the experimental appearance potential graph of the 14^+ peak with and without the discharge. The electron volts scale has been corrected slightly so that the appearance potential of argon agrees with the theoretical value of 15.75 eV.[132]. The experimental appearance potentials of 14^+ from nitrogen atoms and from electron impact on nitrogen molecules, obtained from Fig. 33. are tabulated below and are compared with other existing data. The difference between these two ionisation potentials is clearly the nitrogen bond dissociation energy and this is also shown below.

	APPEARANCE POTENTIALS (eV).		D_{N_2} (eV).
	$N \longrightarrow N^+ + e$	$N_2 \longrightarrow N^+ + N + e$	
Accepted Values.	14.54 ∅	24.3 *	9.76 ∅
Kistiakowsky [99][100].	14.8	24.3	9.5
Jackson and Schiff [95][96]	14.7 0.3	-	-
This Work.	15.05	24.4	9.35

∅ Spectroscopic values [132][133].

* Electron impact data [132].

On the whole these values are in good agreement but the experimental appearance potential of 14^+ from nitrogen atoms is slightly larger than the spectroscopic value. As a result the experimental $N \equiv N$ bond dissociation energy is less than the accepted spectroscopic value of 9.76 eV.

The 14^+ appearance potential curve without the discharge shows a small peak below the appearance potential of N^+ from molecular nitrogen (24.4 eV.). The magnitude of this peak could be varied by adjusting the potentials of the ion lens in the collecting system, suggesting that the peak was caused by incomplete removal of the scattered ions near the collecting electrode. With careful adjustment of the ion lens potentials the peak height could be reduced almost to zero as is shown in the trace in Fig. 32, page 113. Generally, the peak height was of the order of a few millivolts on the 10^{12} ohm resistor at 23 eV. In future work the 14^+ increase above this background value was used for measuring nitrogen atom concentrations.

With the discharge activated the appearance potential curve of 14^+ is extremely smooth, indicating the presence of a single species, presumably ground state $N(^4S)$ nitrogen atoms, although higher electronic states if present in small amounts would probably not be apparent.

In a similar experiment with hydrogen in the discharge tube at 1 mm. Hg. with the electron energy turned just below the threshold of $H_2 \longrightarrow H^+ + H + e$ at 18.05 eV. [132] only a slight increase in the 1^+ peak was observed when the discharge was activated. The maximum rise detected was about 3 mv. on the 10^{12} ohm resistor.

FIGURE 34.

DIFFUSION FLAME APPARATUS.

Fig. 34.

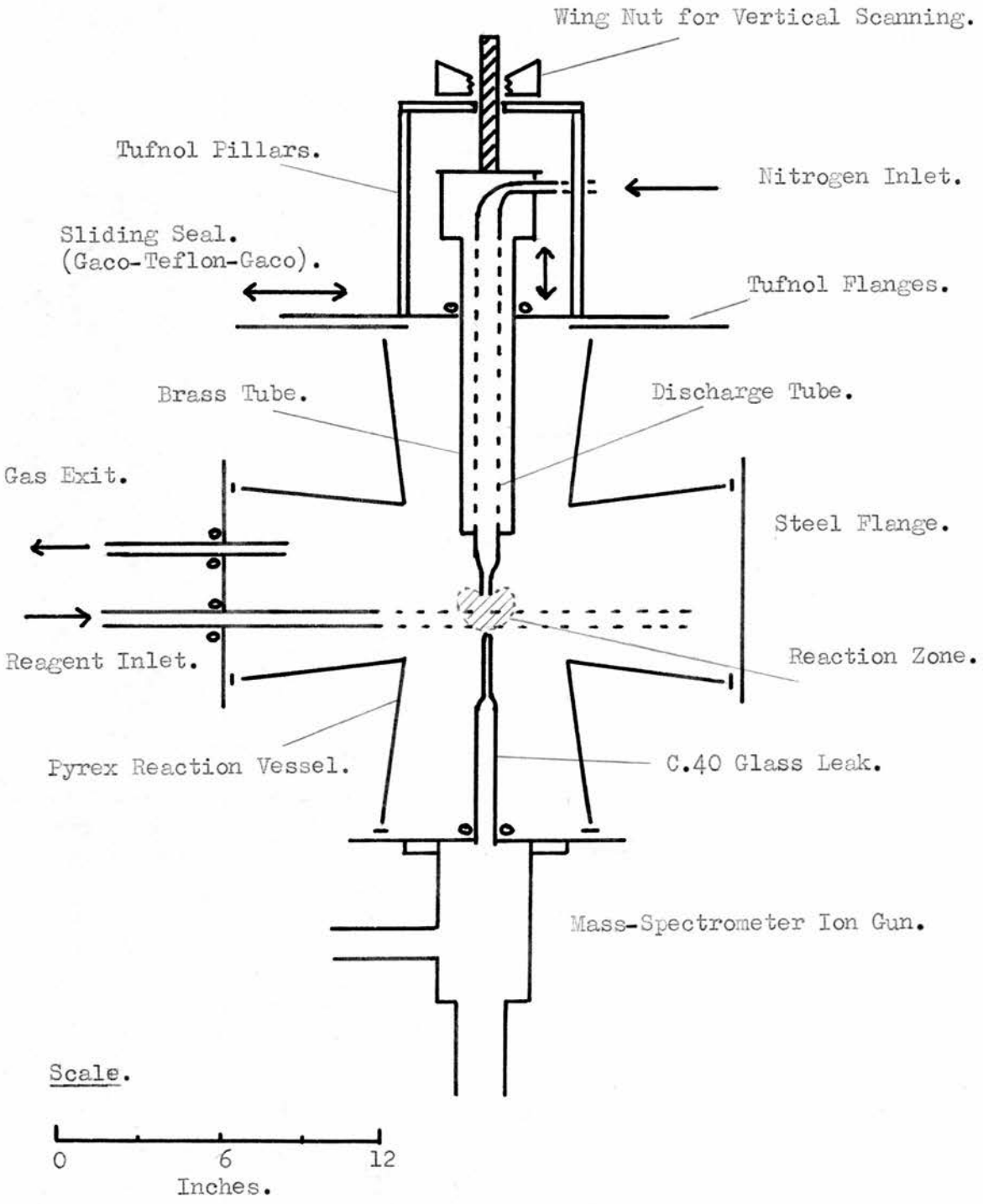

13. PRELIMINARY DIFFUSION FLAME APPARATUS.

a) Description of Apparatus.

It was now possible to produce and detect nitrogen atoms in moderate quantity even after sampling them through a long slender probe. The next stage in the research seemed to be the construction of a diffusion flame apparatus over the mass-spectrometer and its related gas handling system. The two essential points about the apparatus were:-

(i) The reaction vessel had to be fitted immediately above the mass-spectrometer so that the diffusion flame (expected size a few centimetres in diameter) was situated as near to the ion-chamber as possible.

(ii) Some form of accurate scanning of the flame was necessary, preferably in both vertical and horizontal directions. Since the mass-spectrometer leak could not be moved this necessitated moving the nozzle and discharge equipment.

The layout of the apparatus is shown in Fig. 34. The reaction vessel was a commercial pyrex cross 18 inches high with six inch diameter ends, having an estimated volume of about 40 litres. One end of the cross was sealed to the machine inconel head flange of the mass-spectrometer with a greased 'Gaco' rubber sheet washer. The two horizontal arms of the cross were blanked off with mild steel plates again 'Gaco' sealed to the glass cross. One of these end pieces contained two holes fitted with O-ring seals on to glass tubing to serve as the main nitrogen exit line and the reagent injection line.

A more detailed diagram of the discharge and scanning system is

FIGURE 35.

DETAILED DIAGRAM OF DISCHARGE ASSEMBLY AND SCANNING SYSTEM.

Fig. 35.

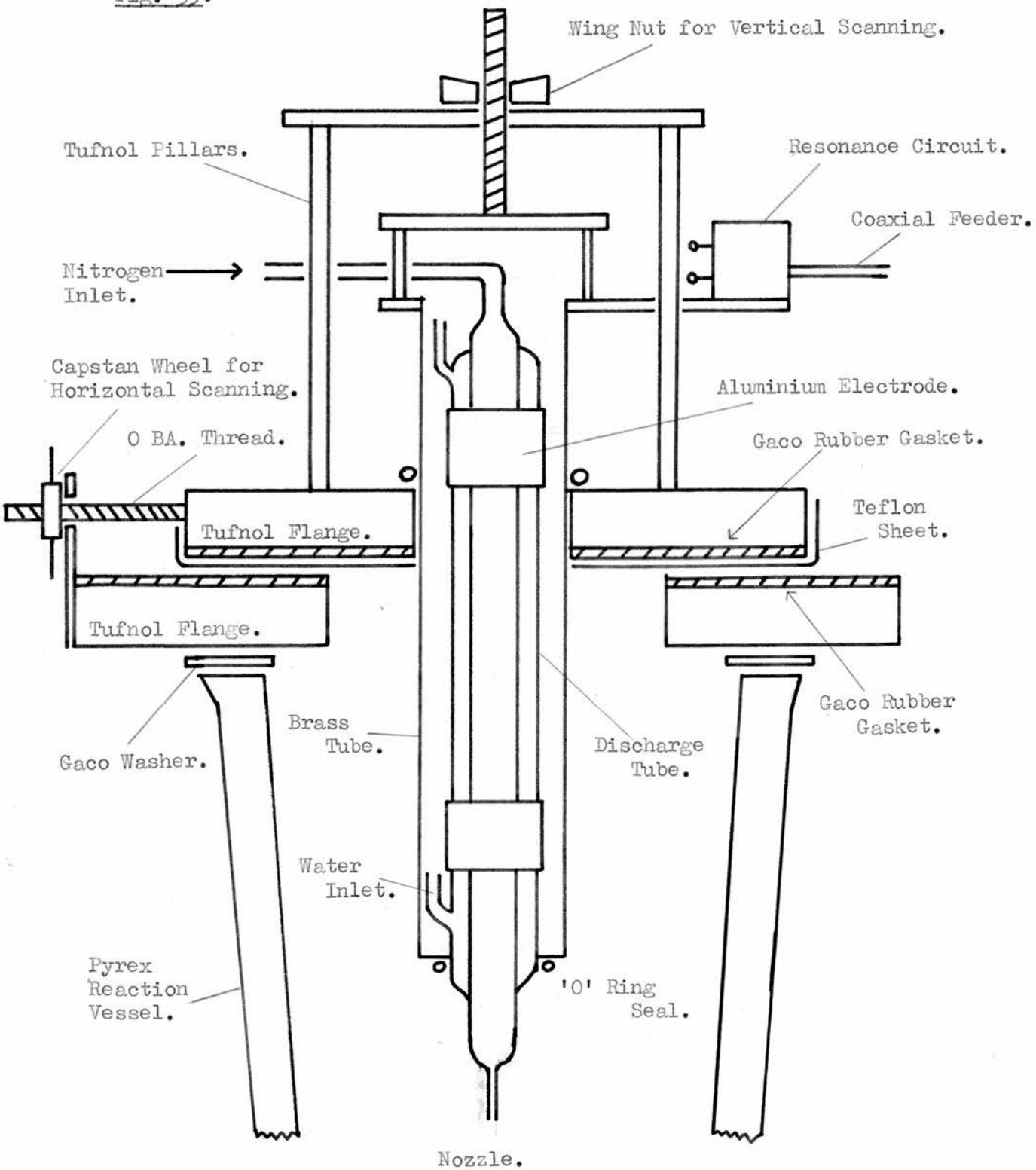

Not to Scale.

shown in Fig. 35. A water cooled thin walled pyrex condenser acting as the discharge tube was carefully 'Gaco' sealed and clamped into a brass tube (15 inches long and 2.25 inches diameter). Radio-frequency power was coupled to the tube by electrostatic linking as shown. Attempts to use electromagnetic coupling proved disastrous since an earthed metal tube around an R.F. coil acts as a series of complete loops around the coil and shorts out the R.F. energy. In tests, the brass tube became extremely hot and violent shocks were experienced if it was accidentally touched. This condition also gave considerable interference with the mass-spectrometer electronics. With the electrostatic coupling there was no power loss in the brass and in fact the large capacity to earth provided by the earthed tube proved beneficial since less capacity was needed in the resonance circuit for tuning purposes.

The resonance circuit consisted of the usual tank coil and condensers and was strapped to a bakelite support fixed to the brass tube. As a result when the brass tube was moved for scanning purposes the resonance circuit moved with it since any relative movement of the circuit components could seriously affect the output of nitrogen atoms by altering the tuning position.

For vertical and horizontal scanning the brass tube was fitted into a sliding flange system which for convenience of construction and lightness had been made out of tufnol. Essentially the unit consisted of two tufnol blocks, one 18 x 12 x $\frac{3}{4}$ inch. containing a central rectangular hole $2\frac{3}{4}$ x $6\frac{1}{2}$ inch. for the brass tube, and the other block

FIGURE 36.

Fig. 36.

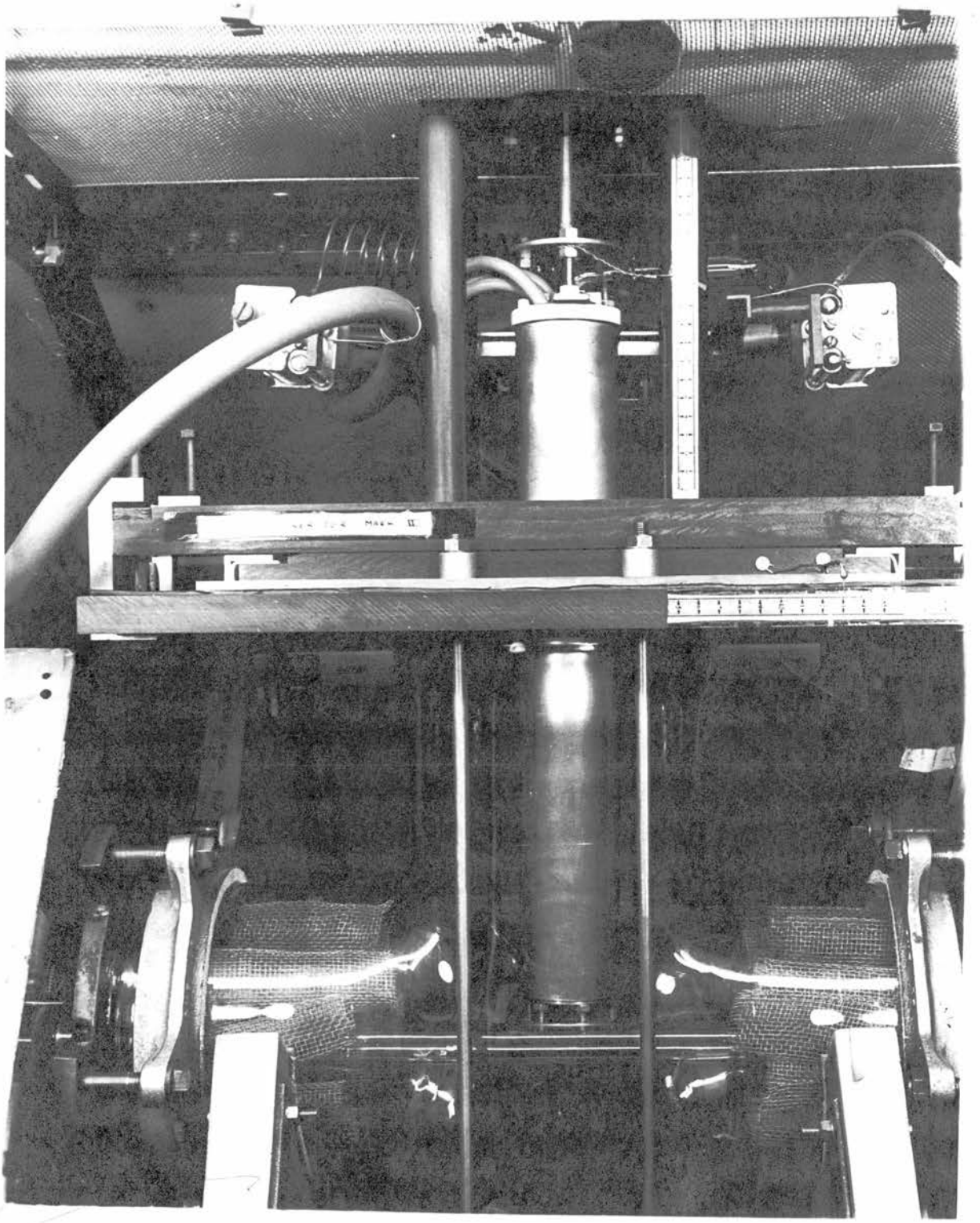

12 x 6 x $\frac{3}{4}$ inch, 'Gaco' rubber sealed to the brass tube, could slide across the larger flange and was held in a track by two tufnol guides running the length of the main block. In the original design a sheet of greased 'Gaco' rubber ($\frac{1}{8}$ inch. thick) was bolted to each block for the seal. However, the friction between the greased surfaces was too great for easy operation. This trouble was overcome by inserting a sheet of teflon (1/32 inch. thick) between the 'Gaco' sheets and bolting it to the smaller sliding block.

For vertical scanning the brass tube could slide in and out of the O-ring seal on the tufnol block and a bridge system of tufnol pillars allowed the tube to be raised and lowered by operating a wing nut as shown.

For horizontal scanning the sliding action was operated by a capstan wheel threaded onto an OBA. screwed rod fixed to the sliding part. The OBA. thread having a pitch of 1 mm. gave a very easy and accurate method of scanning. Centimetre scales and pointers fixed to the horizontal and vertical movements indicated the scanning position giving the relative probe-nozzle distance. Each scale could be read to within 0.1 mm. but in the more common horizontal scanning the capstan wheel permitted even more accurate settings to be made, but this was seldom necessary.

The sampling leak was the same slender C40 glass leak (.003 inch) as used in previous experiments but was now glass blown onto a length of 28 mm. C40 glass tube and 'Gaco' sealed into the head flange as shown. The distance from the ion-box to the leak orifice was about

FIGURE 37.

THE GAS HANDLING SYSTEM. Fig. 37.

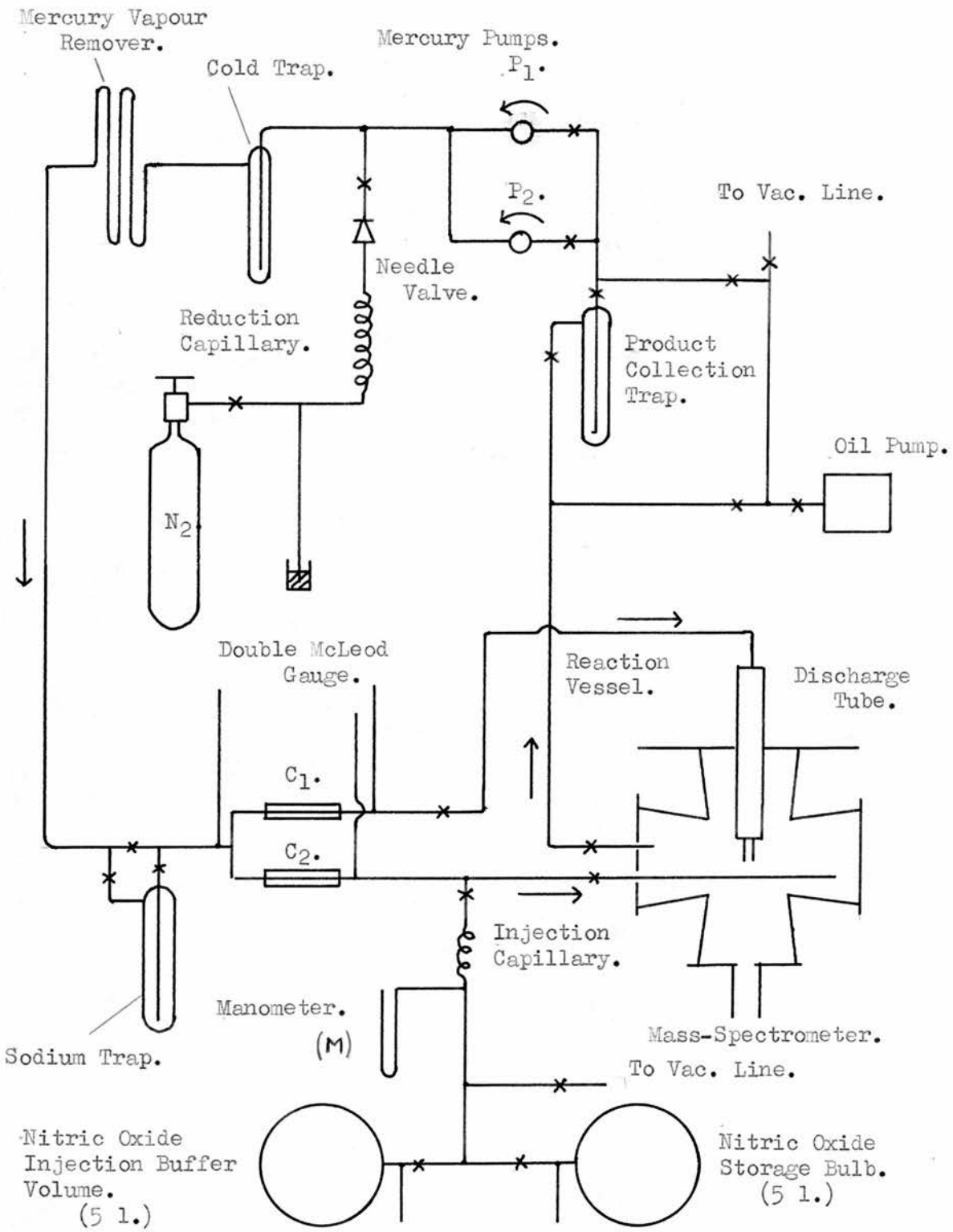

6 inches. The discharge tube nozzle was a one inch length of 4 mm. internal diameter pyrex glass tubing and the scanning facilities permitted a zone of 4 cm. radius to be analysed in vertical and horizontal directions.

A photograph of the completed apparatus is shown in Fig. 36.

b) The General Gas Handling System.

The general gas handling system is shown in Fig. 37. It was constructed so that either a circulation or an injection and flow through to waste system could be used. This latter system was necessary when using reagents which are not easily condensed from the exit gases. Commercial grade nitrogen (0.15% oxygen) was used throughout these experiments and gave much more reproducible atom concentrations than oxygen-free nitrogen. Nitrogen, from the cylinder, was regulated at one atmosphere pressure by a mercury valve and injected into the system via a needle valve and 8 metres of fine capillary for extra control. The nitrogen flow was then divided by calibrated capillaries C_1 and C_2 such that about half of the nitrogen flowed down the discharge tube via C_1 and the other half flowed down the reagent injection line via C_2 to ensure a certain degree of premixing of the reagents before entering the reaction vessel. The exit gas, taken from the opposite side of the cross then passed through several cold traps for product removal and analysis and then either to waste via an oil pump or back round the system via one or two large mercury circulation pumps in parallel.

The discharge tube was coupled to the gas handling system by flexible tubing. In preliminary work P.V.C. tubing was used but this

collapsed after a while and was replaced by heavy walled rubber tubing which proved more reliable.

With all the 'Gaco' seals carefully greased the cross could be evacuated to almost 10^{-6} cm. Hg. and when isolated from the pumps and with continuous operation of the sliding seals would still be better than 5×10^{-3} cm. Hg. after one hour. This was quite adequate since 4/5ths of the gas leaking into the cross would be nitrogen. On a circulation system the oxygen could be controlled by the sodium trap fitted in the circulation line and on the injection system where the reaction vessel was continually flushed out with nitrogen the oxygen concentration would be extremely small.

14. PRELIMINARY DIFFUSION ZONE EXPERIMENTS.

a) Preliminary Vertical and Horizontal Scans.

It was first necessary to obtain the correct nozzle flow rate, slow enough to give an approximately spherical diffusion zone but fast enough to provide adequate nitrogen atoms for analysis.

Since it was very easy to scan vertically and horizontally over the zone it was decided to set up a spherical state experimentally by trial and error and then to compare this with Heller's [14] suggested limits for v/D, where v is the nozzle velocity and D the diffusion coefficient of nitrogen atoms into molecular nitrogen. Nitrogen was injected into the reaction vessel and pumped to waste via the main oil pump and the nitrogen injection valve adjusted to give a pressure of 1 mm. Hg. in the reaction vessel. This gave more than adequate nitrogen atoms beneath the nozzle (1.5 volts on the 10^{12} ohm resistor at 23 eV.), but trial scans showed the nitrogen atom concentration to decrease four times faster horizontally than vertically, indicating a long and narrow diffusion zone issuing from the nozzle. The pumping speed was reduced and for convenience the auxiliary oil pump was removed and the exit nitrogen pumped to waste down the vacuum line by the vacuum line oil pump. This was a smaller pump and the vacuum line introduced more restriction to the gas flow. The nitrogen input was reduced to give an operating pressure again of 1 mm. Hg., the flow rate being about a third of its original value.

The nitrogen atom concentration under the nozzle was now much lower (500 mv. on the 10^{12} ohm resistor at 23 eV.), but was still sufficient

FIGURE 38.

Fig. 38.

Vertical Scan over the Diffusion Zone.

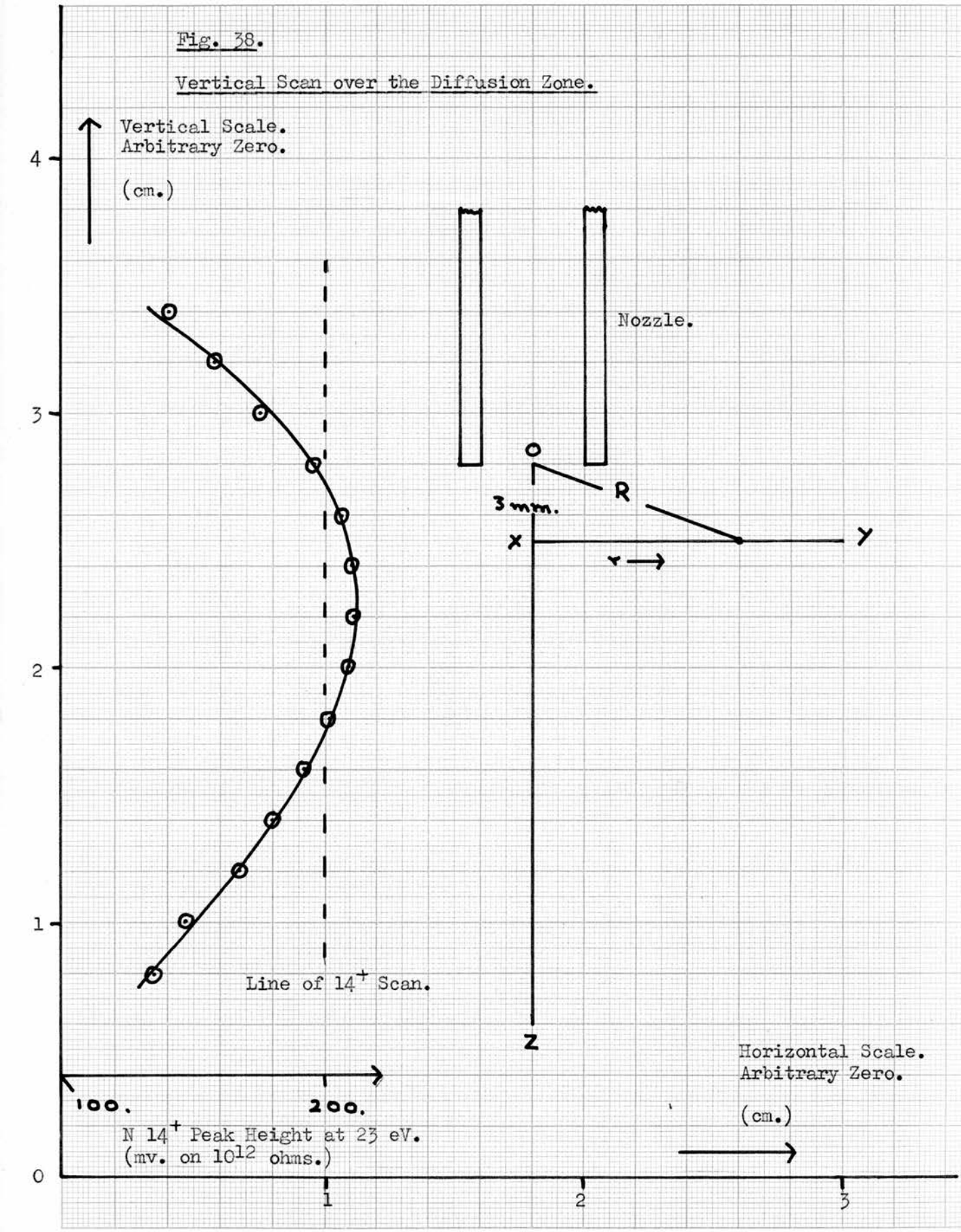

for a flame analysis.

A scan in the two directions now showed a remarkably similar decrease, and a vertical scan a few millimetres from the nozzle is shown in Fig. 38. As can be seen the graph is quite smooth but there must certainly be some distortion produced in the regions behind the nozzle where diffusion is somewhat restricted. This will be even more apparent when actually sampling from these regions as there is the added restriction of the probe.

It was considered that for horizontal analyses a scan at a vertical distance of 3 mm. below the nozzle (XY in Fig. 38.) would give a good representation of flame nature and the majority of future scans were performed in this position.

A typical horizontal scan is shown in Fig. 39A. Quite clearly the nitrogen atom concentration was not falling to zero in the peripheral regions of the zone. This suggested that the atoms were not being effectively destroyed on the reaction vessel walls and the background atom concentration in the reaction vessel could rise gradually to a value in this case equal to approximately one half of the nozzle concentration. This was undesirable since the curves of the decrease of 14^+ would be the composite graphs of:-

(i) The outward decrease of 14^+ from the nozzle by diffusion.

(ii) The general build up of 14^+ throughout the reactor to a steady state value.

b) The Effect of Copper Mesh on the 14^+ Scans.

For convenience in handling later data, it was decided to remove

FIGURE 39.

Fig. 39.

The Effect of Copper Mesh on the $N\ 14^{+}$ in the Reaction Zone.

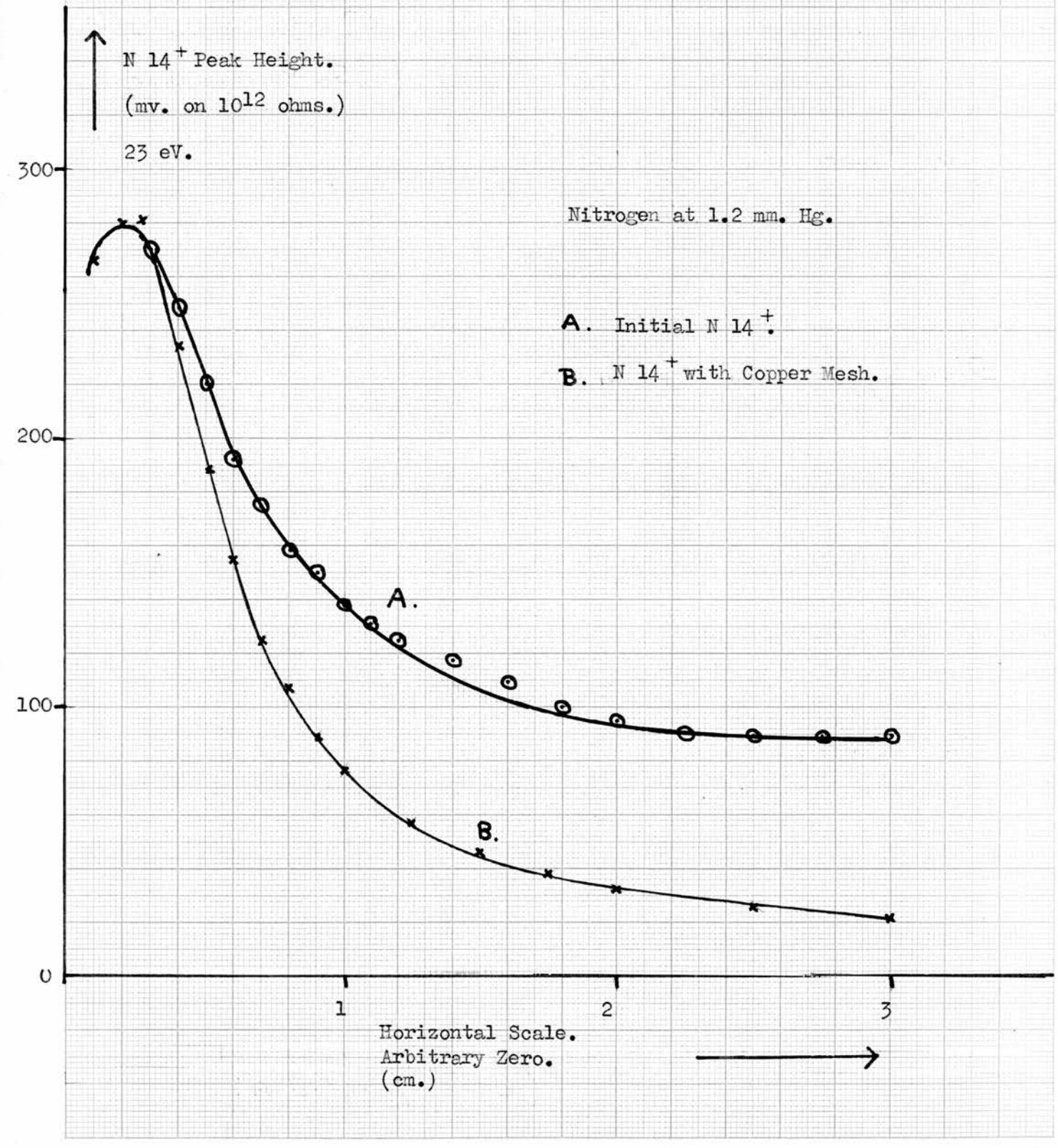

FIGURE 40.

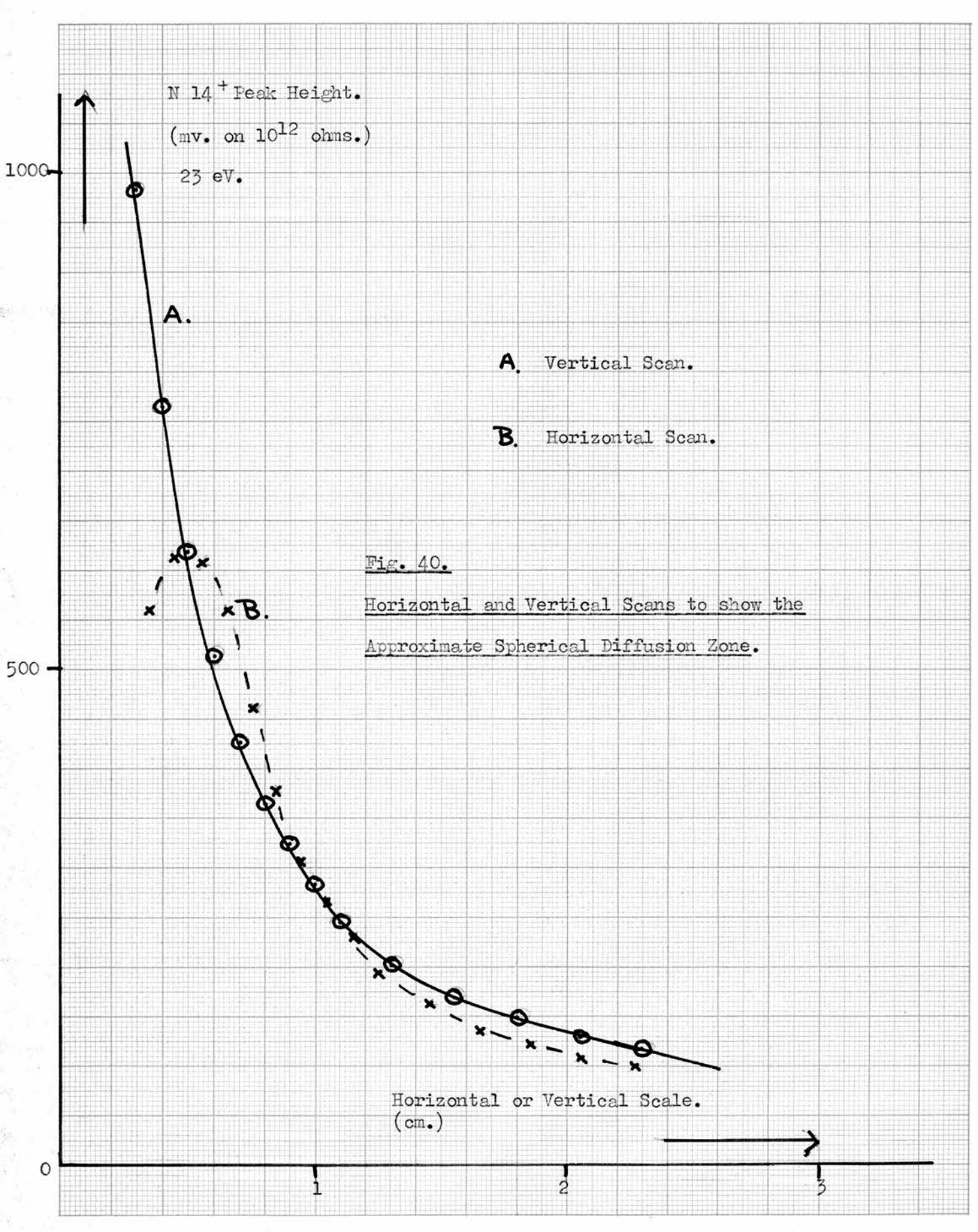

Fig. 40.

Horizontal and Vertical Scans to show the Approximate Spherical Diffusion Zone.

the 14^+ background and the reaction vessel base and ends were packed with clean copper mesh rolled into spirals and packed as tightly as possible. The copper mesh having a much greater recombination efficiency than pyrex reduced the peripheral atom concentration to an acceptable level as shown in Fig. 39B. A comparison of horizontal and vertical scans to show the spherical uniformity of the diffusion zone is shown in Fig. 40.

c) Some Relevant Diffusion Theory and its Application to Experimental Data.

From the theory of steady state spherical diffusion [134], the ideal case being a point source of diffusion the concentration N of nozzle reagent at a distance R from the source is given by the general equation:-

$$N = A + B/R$$

where A and B are constants for a particular temperature.

Clearly then, the curves shown in Fig. 40. should obey this inverse law assuming that:-

(i) The third body recombination of nitrogen atoms ($K = 1.8 \times 10^{-8}$ $ccs.^2\ mole^{-2}.sec^{-1}$.) [52] would be much too slow to give any appreciable loss of nitrogen atoms.

(ii) The response of the mass-spectrometer to nitrogen atoms is linear. The operation of a mass-spectrometer requires a box pressure of about 10^{-5}mm. Hg. where the recombination of nitrogen atoms would be entirely surface recombinations and the rate of loss would be proportional to the concentration of nitrogen atoms, so that the assumption of a linear response of peak height to sampled N is quite reasonable.

FIGURE 41.

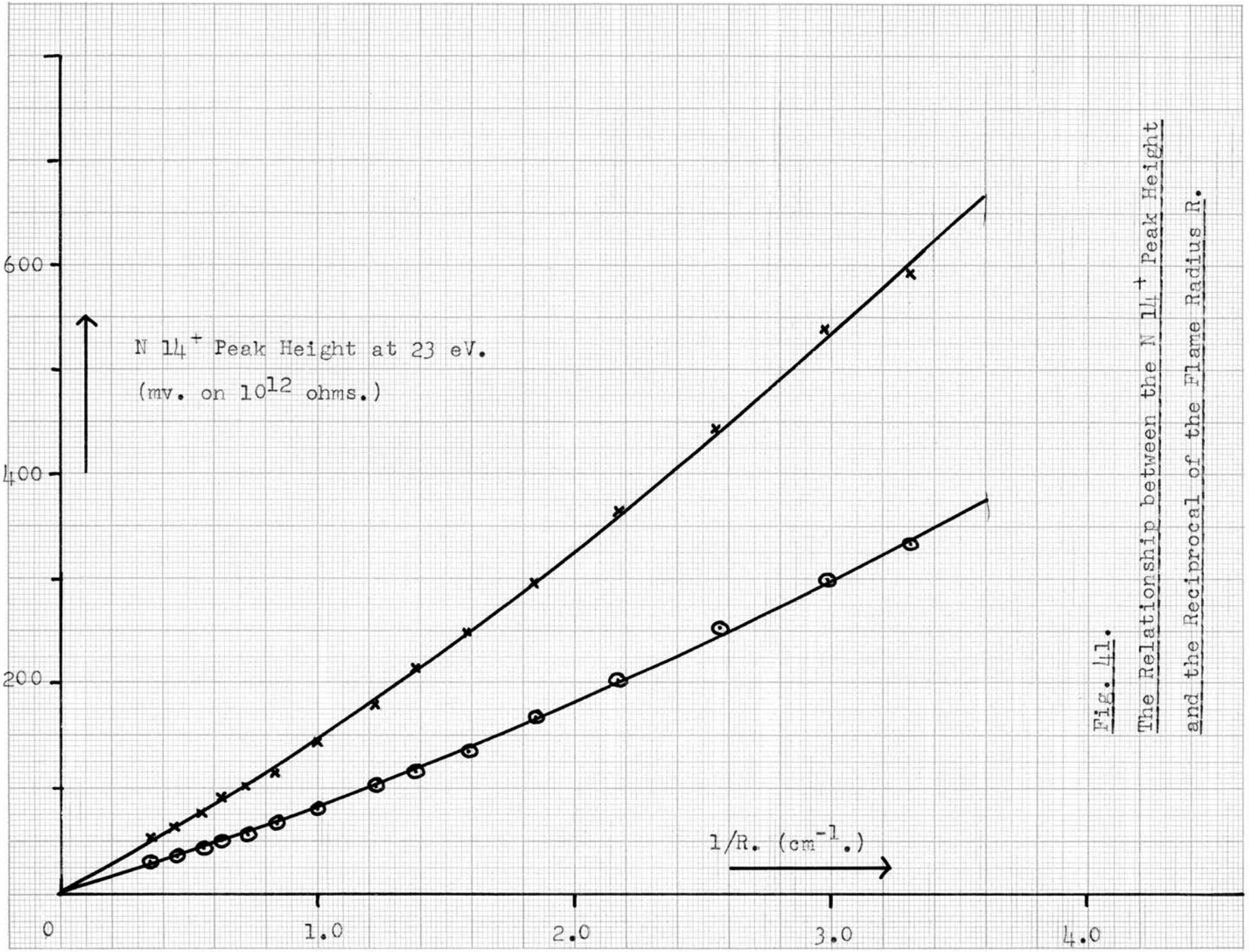

Fig. 41.

The Relationship between the N 14^+ Peak Height and the Reciprocal of the Flame Radius R.

As mentioned previously the scans over the diffusion zone were performed in a horizontal direction, 3 mm. below the nozzle (XY in Fig.38 page. 128.). However, the point source of nitrogen atoms is in the best approximation the centre of the plane of the nozzle tip (Point O in Fig.38). For any probe position in the XY plane the true sampling distance R may be calculated from the horizontal distance r by $R^2 = r^2 + OX^2$ where OX = 3 mm.

Fig. 41. shows two horizontal scans of the 14^+ peak height plotted against 1/R, using different initial nitrogen atom concentrations to show the reproducibility of these plots. In each case the graph shows some general deviation from linearity. However considering the disturbance to the diffusion zone by the relatively large nozzle and sampling probe the linearity is surprisingly good.

d) Flow Rate Calibrations and Experimental v/D values.

The production of a spherical diffusion zone had been set up experimentally by adjusting the flow rate down the nozzle until horizontal and vertical scans showed an equivalent decrease in the 14^+ peak height with distance from the nozzle. It now seemed of interest to compare the v/D value for these conditions with those suggested by Heller [14]. This required a knowledge of the flow rate through the discharge tube and the diffusion coefficient D of nitrogen atoms into molecular nitrogen under the temperature (22°C) and pressure (1.2 mm.Hg.) conditions of the experiment.

The gas flow was calculated by calibrating the two flow capillaries C_1 and C_2 (see Fig. 37. page 124.). These were calibrated experimentally

FIGURE 42.

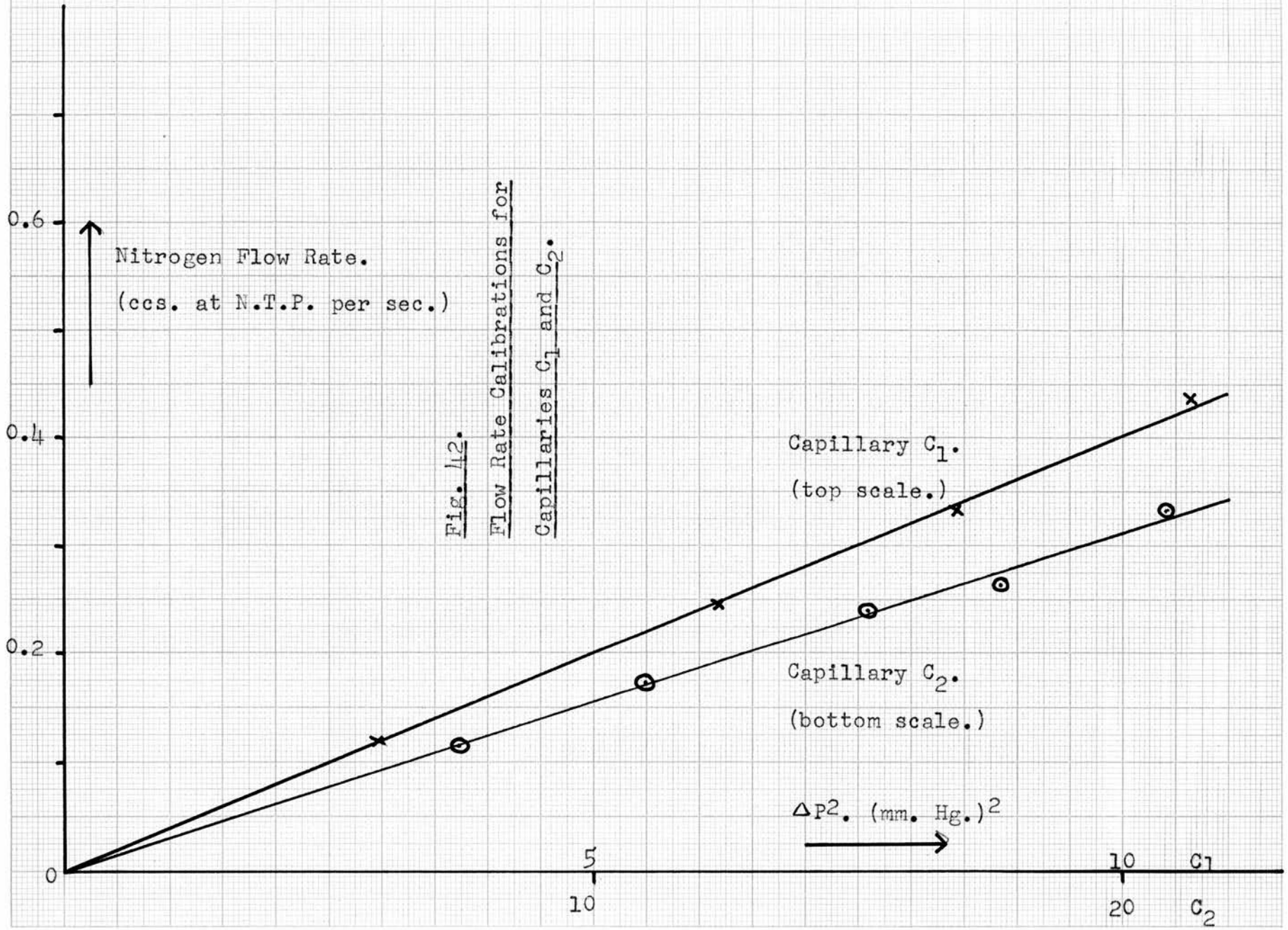

Fig. 42.

Flow Rate Calibrations for Capillaries C_1 and C_2.

by passing known volumes of dry nitrogen from a gas burette through each in turn and recording the pressure drop with a double McLeod gauge. This is shown in Fig. 42. with a linear plot of $\Delta P^2_{N_2}$ against the flow rate, the units of the flow rate being ccs. at N.T.P. per sec. for convenience.

From the calibration data the flow conditions of the previous experiments were calculated. With nitrogen at 1.2 mm. Hg. in the reaction vessel at 22°C the total nitrogen flow rate was 0.5 ccs. at N.T.P. per sec. with 0.3 ccs. at N.T.P. per sec. of this flowing down the discharge tube. This gave a calculated nozzle velocity of about 1500 cm./sec. and using the only experimentally available value of D obtained by Young (135) as 234 $cm^2. sec^{-1}.$ at 1.2 mm.Hg. the value of v/D becomes 6.4 $cm^{-1}.$ The value of D is open to criticism and a more reliable value of 595 $cm^2. sec^{-1}.$ is calculated from collision theory in a later section. This new value gives v/D equal to 2.5 $cm^{-1}.$ which is outside the limits of $5 < v/D < 12$ suggested by Heller, and apparently nozzle flow rates several times larger should be used. However, previous experiments had shown that these increased flow rates gave considerable deviation from spherical zones and it seems that the limits of Heller are not directly applicable to the large bore nozzles used in this work.

It seemed reasonable to rely on the experimental evidence for the spherical nature of the diffusion zone and virtually all of the future work was done under these conditions. If the collection traps were

kept clean and the injection needle valve carefully adjusted it was found that the flow rates and working pressure of the reaction system could be reproduced accurately from day to day. This ensured that all the subsequent runs were performed under good spherical zone conditions.

FIGURE 43.

Fig. 43.

The Appearance Potential of $N\ 14^{+}$ from Nitric Oxide.

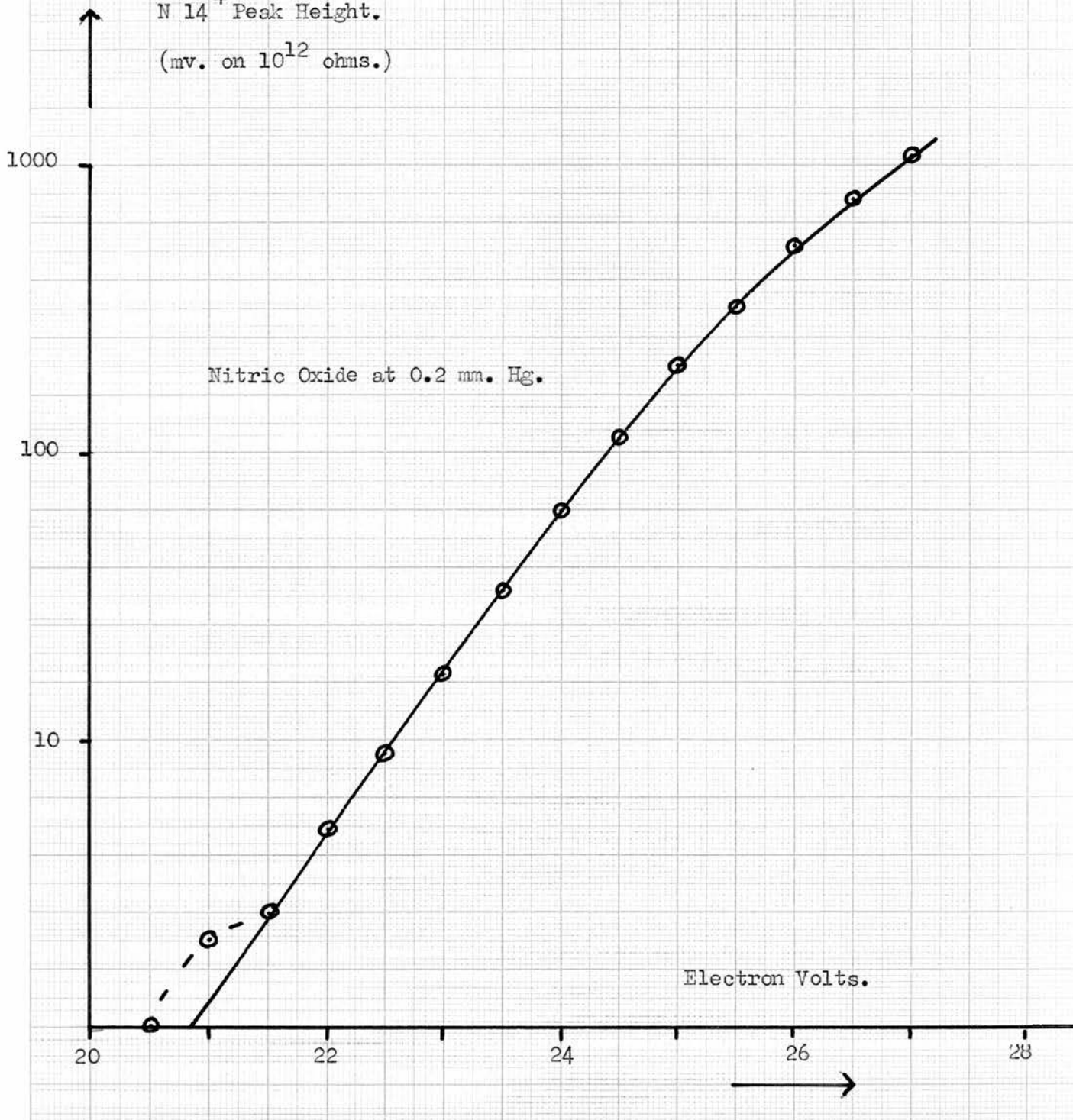

15. PRELIMINARY EXPERIMENTS WITH NITRIC OXIDE.

a) Preparation and Mass-Spectrum of Nitric Oxide.

Nitric oxide was produced by the action of acidified ferrous sulphate on sodium nitrite, by the method given in Inorganic Syntheses [136], as a colourless gas condensible with liquid air to a green liquid (B.Pt. -151.7°C). Before use it was purified by several trap to trap distillations retaining only the middle fraction in each case. Mass-spectrometric analysis showed the main impurity to be N_2O (0.15%), but this was considered sufficiently pure for this work.

The mass-spectrum of NO showed a peak at mass 14 presumably by pyrolysis of NO on the hot filament and at first it was thought that this might interfere with the determination of the nitrogen atom concentration.

Fig. 43. shows the appearance potential and order of magnitude of the 14^+ peak from NO in the reaction vessel at 0.2 mm. Hg. As can be seen at 23 eV there is a peak height of about 10 mv. on the 10^{12} ohm resistor. In a reaction with nitrogen atoms the NO pressure would be very much less than 0.2 mm. Hg., probably of the order of 10^{-3} mm. Hg. so that the contribution of nitric oxide to the 14^+ peak height would be negligible.

b) Mass-Spectrometric Calibrations of N_2, NO, N_2O and O_2.

Before any detailed study could be made of the N + NO reaction it was first necessary to investigate the sensitivity of the mass-spectrometer to NO and compare this with the corresponding N_2 sensitivity as standard. It was found more convenient to monitor the NO 30^+ peak

FIGURE 44.

Fig. 44.

Calibration Data for NO, N_2O and O_2.

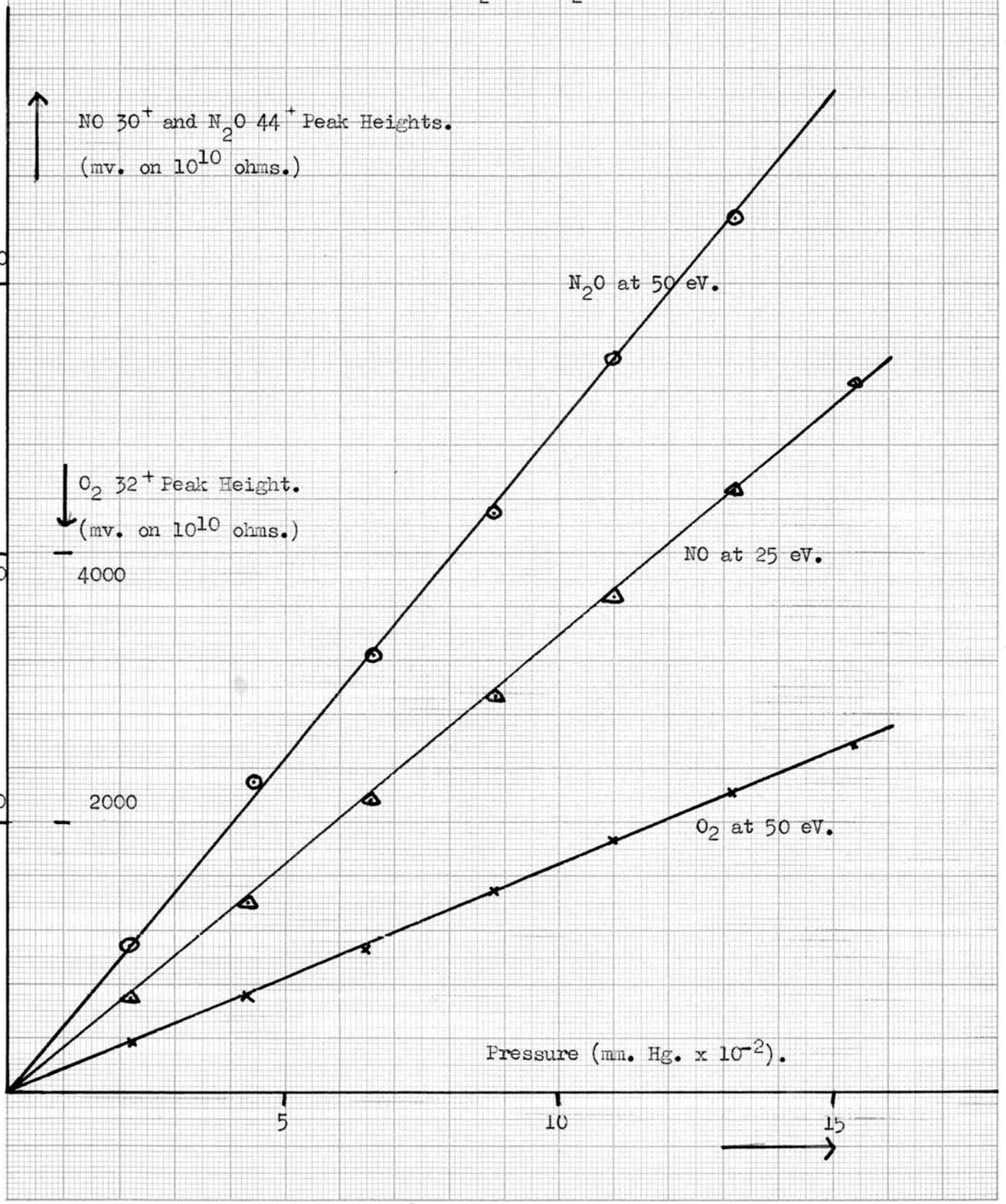

FIGURE 45.

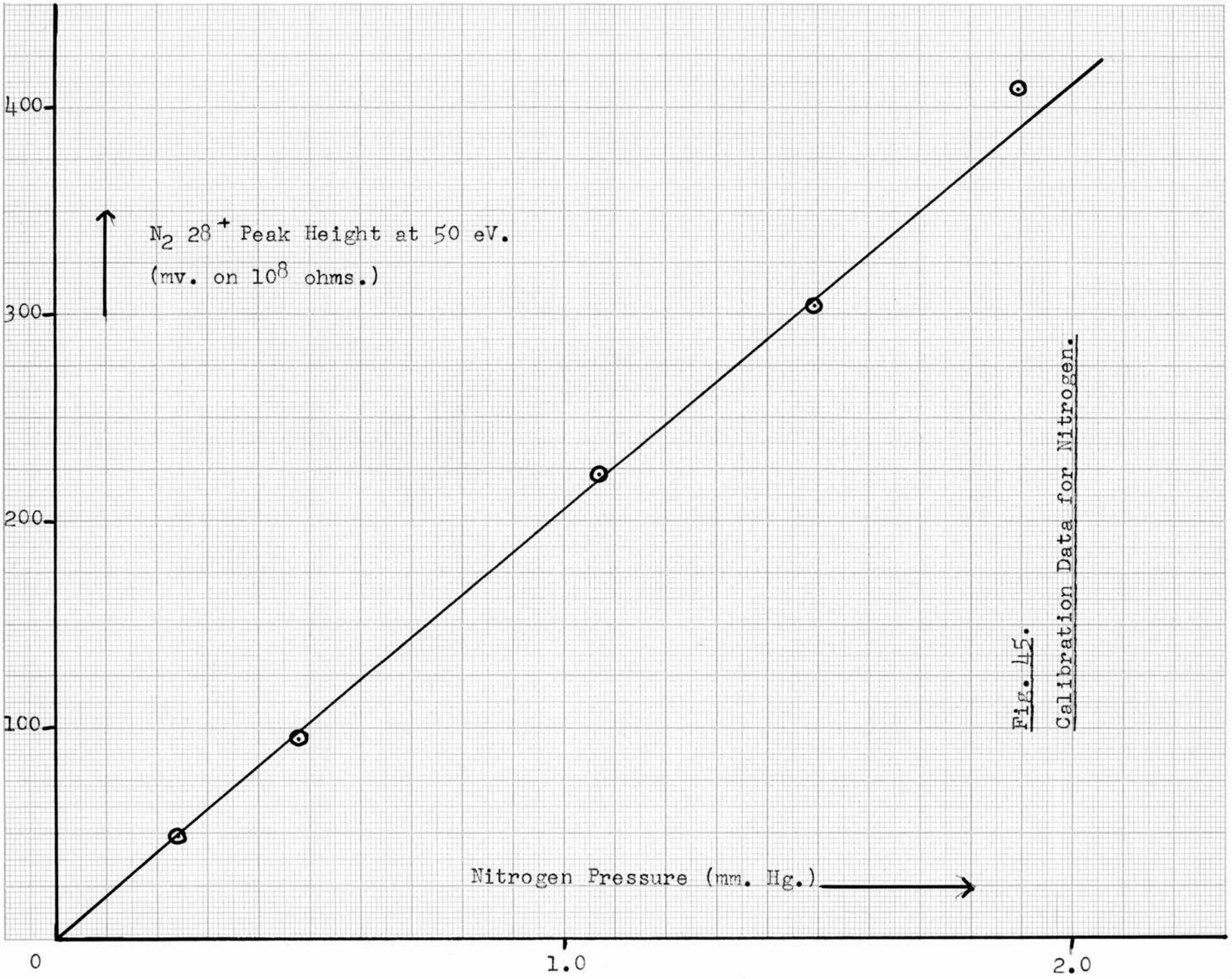

Fig. 45.
Calibration Data for Nitrogen.

at 25 eV rather than at high eV. This did not alter the 30^+ peak appreciably but reduced the large N_2 28^+ peak (200 mv. on the 10^8 ohm resistor at 50 eV.) and hence assisted the resolution of the 30^+ peak.

The calibrations were performed at low NO pressures in the presence of 1.2 mm. Hg. of nitrogen. This gave a more accurate calibration since the ion-box and filament would be operating under similar conditions to those of an actual run. This was effected by injecting aliquots of NO from a calibrated volume into the reaction vessel and mixing with a circulation pump. The peak height was recorded against the NO pressure and is shown in Fig. 44. Also shown are the equivalent data for N_2O and O_2 used later in product analysis and calibrated in a similar manner. The NO and O_2 sensitivities were almost identical and for convenience the O_2 scale is reduced as shown. All three sensitivities were corrected to the standard N_2 sensitivity shown in Fig. 45. This is linear up to 2.5 mm. Hg. but after this point the peak height begins to level out (not shown) indicating saturation of the mass-spectrometer. For pressures above 2.5 mm. Hg. a smaller leak orifice would be necessary.

c) Nitric Oxide Injection System.

The essential details of the nitric oxide injection system are shown on the circulation diagram (see Fig. 37. page 124.). As mentioned earlier the nitrogen input was divided by the two calibrated capillaries C_1 and C_2 such that about half of the gas flowed down the discharge tube and the remainder flowed directly into the reaction vessel and contained the NO injection line. This ensured a certain degree of mixing before the NO entered the reaction vessel. The NO was stored in a 5 litre

reservoir and injected via a long length of narrow bore capillary. A manometer M gave an indication of the injection rate but for accurate calculations the NO flow rate was determined from the total N_2 flow rate and the relative N_2 and NO pressures in the reaction vessel as indicated by the mass-spectrometer. The injection capillary was chosen empirically such that NO partial pressures between 10^{-4} and 10^{-1} mm. Hg. could be produced in the reaction vessel, the reservoir maintaining this supply steadily over at least one half hour.

d) The Effect of Nitric Oxide on the 14^+ Peak Height in the Reaction Zone.

For preliminary work the discharge was activated and the leak positioned to sample nitrogen atoms from a point about 5 mm. from the nozzle where the atom concentration had dropped to about one half of the nozzle value. Additions of very small pressures of NO gave an immediate reduction of the 14^+ peak height and the reaction was so fast that NO could not be detected. The atom concentration decreased even further as the NO injection rate was carefully increased and the NO 30^+ peak appeared. With 10^{-3} mm. Hg. of NO in the reaction vessel the reaction zone had reduced to about one half of its original size. No visible radiations could be seen during these tests even in a darkened room with the discharge glare shielded but this is not surprising considering the low concentrations of NO and N. However, if the NO pressure was increased to 10^{-1} mm. Hg. a distinct green glow appeared over the whole of the reaction vessel and was not confined to the nozzle areas. If the NO injection was now cut off so that the NO pressure in the reaction vessel gradually decreased the green glow

FIGURE 46.

Fig. 46.

A Typical Horizontal Scan to show the Effect of NO on the $N\ 14^+$ Peak Height in the Reaction Zone.

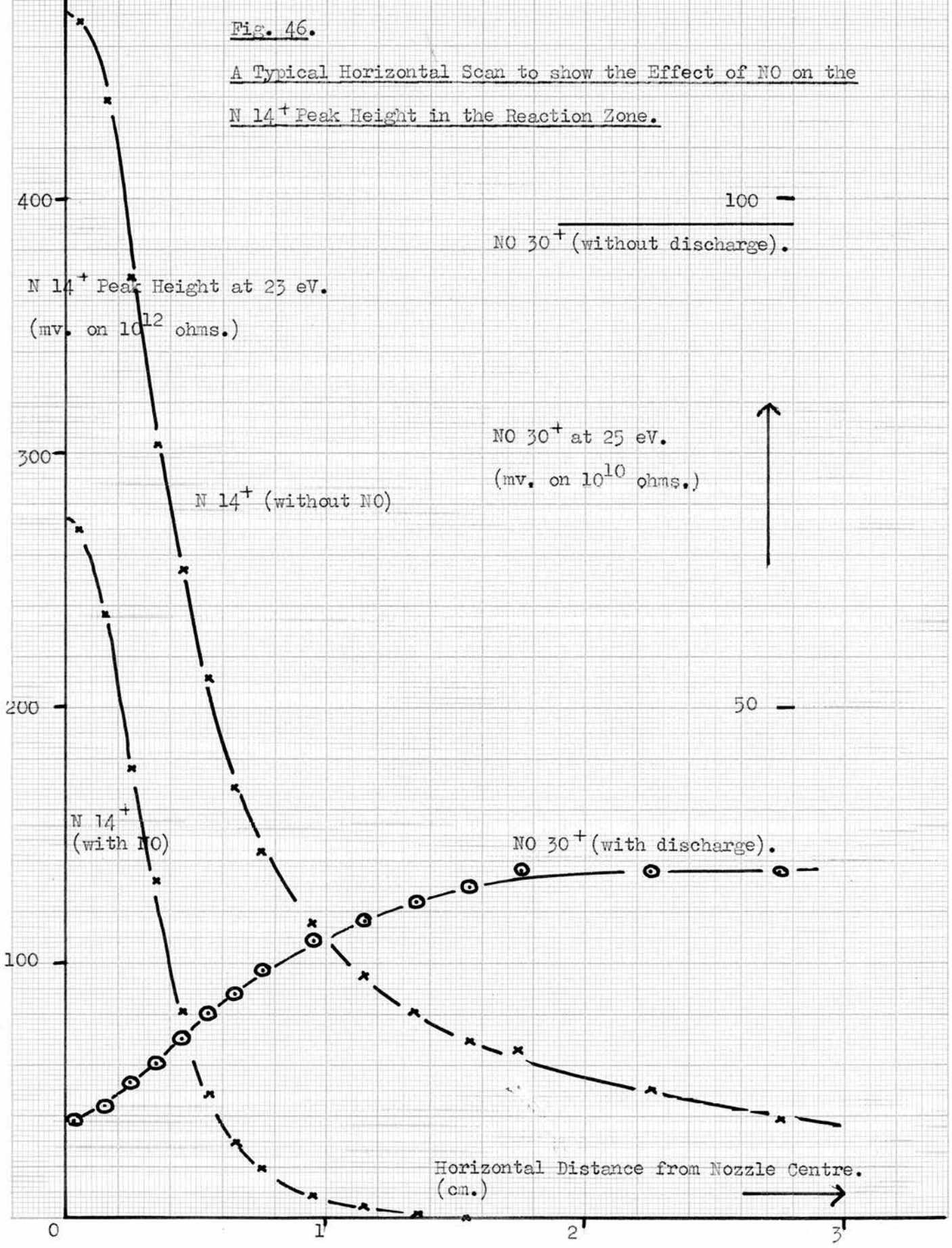

FIGURE 47.

Fig. 47.

The Effect of NO on the N 14$^+$ Peak Height

Plotted against the Flame Radius R.

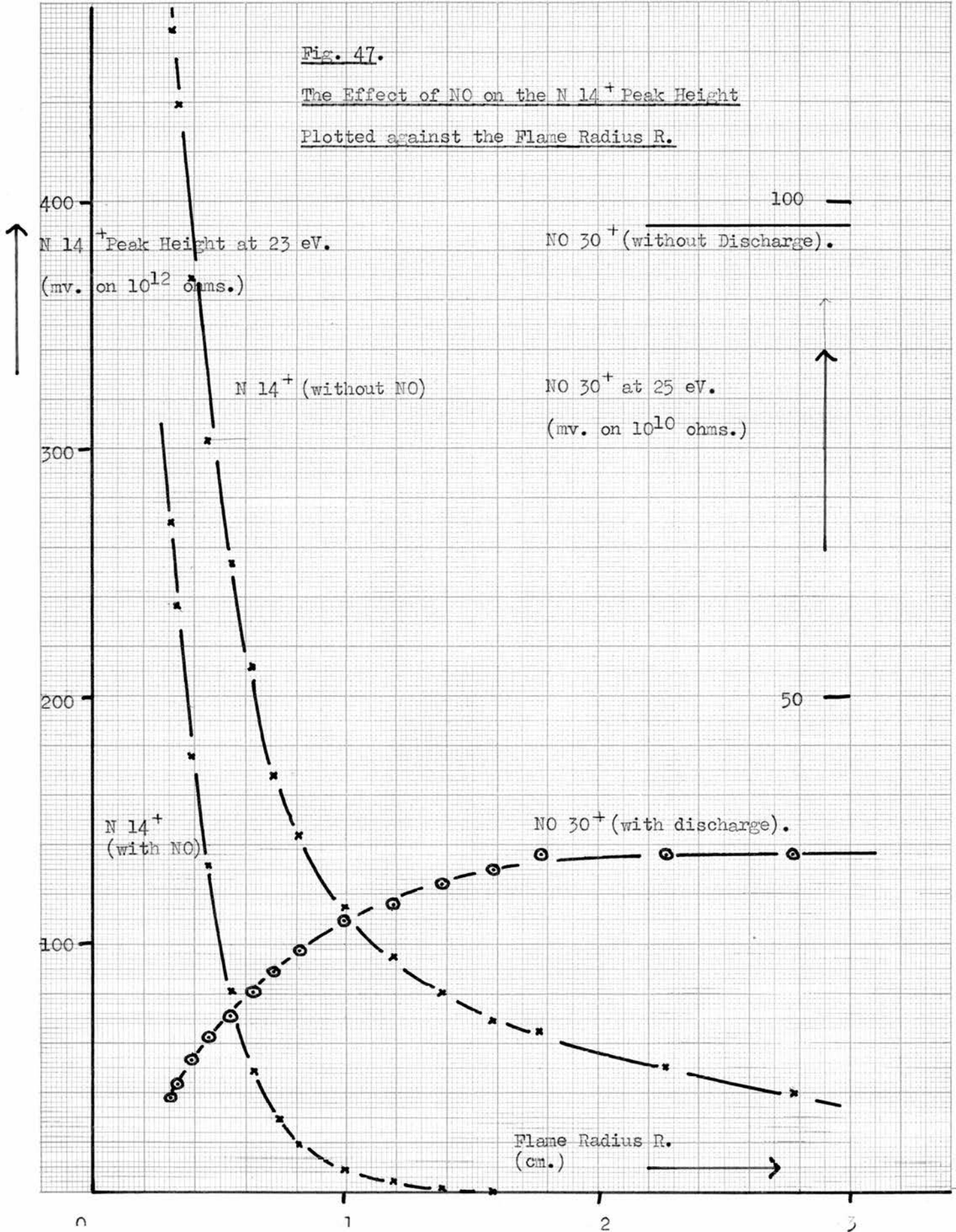

faded slowly and just before extinction passed through a sharp but distinct blue glow which again filled the whole reaction vessel. The blue occurred between 10^{-2} and 10^{-3} mm.Hg. of NO but so sharply that attempts to produce it by steady injection were never successful.

The experimental 14^{+} horizontal scans over the reaction zone with and without NO are shown in Fig. 46. Also shown is the depletion curve of NO during the reaction. The equivalent data plotted against the flame radius R are shown in Fig. 47. As can be seen the rate of decrease of 14^{+} is much more pronounced with NO present, as would be expected when nitrogen atoms are being consumed by reaction. The nitrogen atom concentration is reduced to zero about 1.5 cm. from the nozzle.

With the discharge extinguished the NO pressure in the reaction vessel increased considerably to the value shown in Fig. 47. This gives a method of estimating the absolute atom flow rate since the difference between the two NO pressures (Δ NO) gives the amount of NO consumed by the reaction. It is necessary to assume that the stoichiometry of the N + NO reaction involves one nitrogen atom to one molecule of NO but this is quite reasonable and has been the basis of the well established method of nitrogen atom titration.

FIGURE 48.

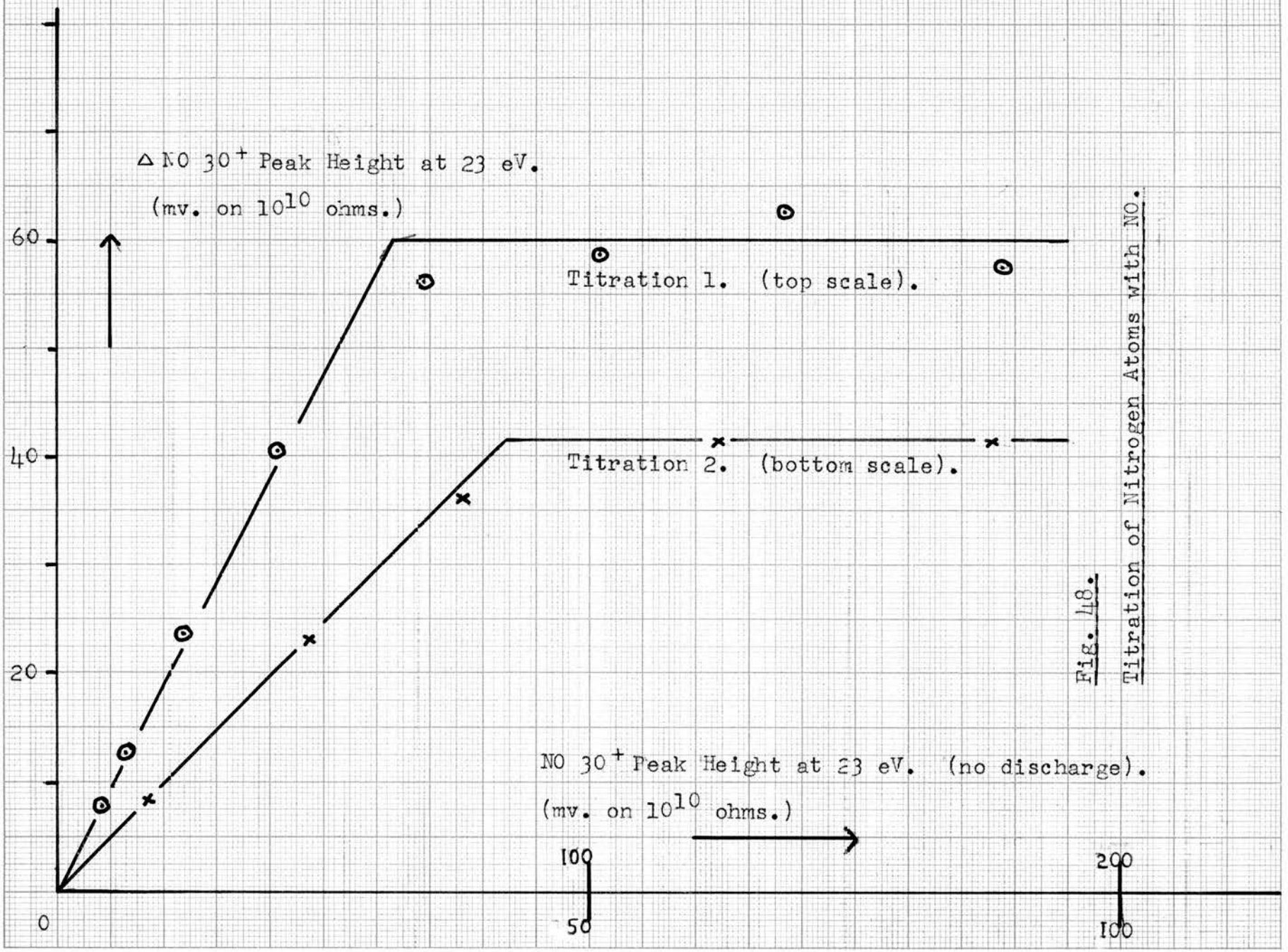

Fig. 48. Titration of Nitrogen Atoms with NO.

16. TITRATION OF NITROGEN ATOMS WITH NITRIC OXIDE.

a) Percentage Dissociation of Nitrogen.

Fig. 48. shows the relationship between the NO consumed by N (Δ NO) and the NO (no discharge) pressure, the values being recorded at the zone periphery in each case. If the input rate of NO is less than the input rate of N , all the NO is consumed leaving an excess of N , such that Δ NO increases linearly with NO pressure. When the input rate of NO is greater than the input rate of N , Δ NO remains constant with increasing NO pressure. The intersection of the two linear portions of the titration graph then indicates the end point when N flow rate NO flow rate.

Two titration plots are shown and were recorded on separate days for comparison purposes.

In general terms at the titration end point,

$$\text{Flow rate}_{NO} = \text{Total flow rate}_{N_2} \times \frac{(P'_{NO})}{(P_{N_2})}$$

where P'_{NO} is the partial pressure of NO at the titration end point without the discharge and P_{N_2} the nitrogen pressure in the reaction vessel. Further,

$$\text{Flow rate}_{NO} = \text{Flow rate}_{N} = \text{Nozzle flow rate}_{N_2} \times \frac{(P_N(\text{Nozzle}))}{(P_{N_2}(\text{Nozzle}))}$$

such that

$$P_N\,(\text{Nozzle}) = \frac{\text{Total flow rate}_{N_2} \times (P'_{NO})}{\text{Nozzle flow rate}_{N_2}}$$

assuming that P_{N_2} (Nozzle) = P_{N_2}. This was justified by comparing the 28^+ peak in the reaction vessel with the 28^+ peak at the nozzle. Only a small percentage difference could be detected. A similar test showed that the NO 30^+ peak height decreased to zero at the nozzle such that there was no back diffusion of NO into the nozzle, as in fact is shown in Fig. 47. page 145. The data obtained from the two titration plots are shown below together with the calculated percentage dissociation of nitrogen at the nozzle.

	Titration 1.	Titration 2.
P'_{NO} 30^+ peak height. (mv. on the 10^{12} ohm resistor)	62.5	42.1
P'_{NO} (mm. Hg.)	3.71×10^{-3}	2.5×10^{-3}
Total flow rate N_2 (ccs. at N.T.P. per sec.)	0.456	0.44
Nozzle flow rate N_2 (ccs. at N.T.P. per sec.)	0.268	0.280
P_N (Nozzle) (mm. Hg.)	6.31×10^{-3}	3.93×10^{-3}
Percentage Dissociation of Nitrogen.	0.525	0.327

b) Some Relevant Diffusion Theory for the Mass-Spectrometer Sensitivity to Nitrogen Atoms.

The calculations above give the partial pressures of nitrogen atoms in absolute terms at the nozzle tip and it now seemed of interest to obtain an idea of the mass-spectrometer sensitivity to atomic

nitrogen.

It was found difficult to measure the 14^+ peak height at the tip of the nozzle as was required for a sensitivity determination, due to the large sampling probe and the danger of breaking the leak by touching the nozzle. Attempts to obtain this value by back-extrapolation of a vertical scan also proved difficult because of the very sharp 14^+ gradient near the nozzle as is shown in Fig. 40 page 131, and so other methods of determining this value were investigated.

Diffusion theory (134) for ideal steady state spherical diffusion predicts the theoretical mass flow through a zone to be given by:-

Nozzle reagent input per second

$$= \frac{4\pi D\,(R_1.R_2)\,(N_1 - N_2)}{(R_2 - R_1)} \qquad \text{(i)}$$

where D is the diffusion coefficient of the nozzle reagent under the temperature and pressure conditions of the experiment and N_1 and N_2 are the nozzle reagent concentrations at distances R_1 and R_2 from the point source.

The application of equation (i) to the nitrogen atom diffusion zone yields:-

Input of nitrogen atoms per second

$$= \text{Nozzle flow rate}_{N_2} \times 14^+_{(\text{Nozzle})}$$

$$= \frac{4\pi D\,(R_1.R_2)\,(14^+_{R_1} - 14^+_{R_2})}{(R_2 - R_1)}$$

where $14^+_{(\text{Nozzle})}$, $14^+_{R_1}$ and $14^+_{R_2}$ represent the 14^+ peak height in mv. on the 10^{12} ohm resistor at the nozzle, and at positions R_1 and R_2

respectively. This expression enables the 14^+ peak height at the nozzle to be calculated from the 14^+ peak heights at any two points in the diffusion zone. Unfortunately, the diffusion coefficient of N into N_2 is not readily available and a calculated value is derived in the next section.

c) The Calculated Diffusion Coefficient of N into Molecular N_2.

There is apparently only one experimental determination of the diffusion coefficient of N into N_2 available in the literature. This was calculated by Young (135) by monitoring the decay of atomic nitrogen towards a catalytic surface by spectral observations giving $D = 280/p$ $cm^2.\ sec^{-1}.$, where p is the pressure in mm. Hg.

A more accurate value may be calculated from collision theory by the general equation (137)

$$D = \frac{2\left(T^3\,(M_1 + M_2)/2\,M_1.M_2\right)^{\frac{1}{2}}}{p\,\sigma^2} \qquad \text{(ii)}$$

where D is the diffusion coefficient,

T is the temperature in degrees absolute,

M_1 and M_2 are the molecular weights of the collision partners,

p is the pressure in mm. Hg.

σ is the average diameter of the collision partners in Å.

for N into N_2, based upon rigid sphere interactions, has been calculated by Hirschfelder and Eliason (138) as 3.26 Å and by Vanderslice et al (139) as 3.32 Å and for the following work an average value of $\sigma = 3.29$ A has been used.

For the diffusion of nitrogen atoms into molecular nitrogen

equation (ii) becomes

$$D = \frac{2\,(0.0535\ T^3)^{\frac{1}{2}}}{3.29\ p}$$

$$= 595 \text{ cm}^2.\ \text{sec}^{-1}.\ \text{at } 22^\circ\text{C and } 1.2 \text{ mm. Hg.}$$

this value of $D = 595\ \text{cm}^2.\ \text{sec}^{-1}.$ has been used in all of the future work described in this thesis.

d) The Mass-Spectrometer Sensitivity to Atomic Nitrogen.

The 14^+ peak height was carefully recorded at certain points ($R_1 = 0.5$ and $R_2 = 1.0$ cm.) in the diffusion zone during the titration experiments shown in Fig. 48. page 147. These were recorded in the absence of NO and are shown below together with the calculated mass-spectrometer sensitivity to nitrogen atoms.

	Titration 1.	Titration 2.
$14^+_{R_1} - 14^+_{R_2}$ (mv. on the 10^{12} ohm resistor)	128	72.1
$4\pi D \dfrac{(R_1.R_2)}{(R_2 - R_1)} (14^+_{R_1} - 14^+_{R_2})$ ($\text{cm}^3.\ \text{sec}^{-1}$)(mv. on 10^{12} ohms)	9.6×10^5	5.4×10^5
Nozzle flow rate N_2 (ccs. at 1.2 mm. Hg. 22°C)	158	165
Calculated $14^+_{(\text{Nozzle})}$ (mv. on the 10^{12} ohm resistor)	5060	3280
P_N (Nozzle) (mm. Hg.)	6.3×10^{-3}	3.93×10^{-3}
Mass-Spectrometer sensitivity to N (volts on 10^{10} ohms per mm. Hg.)	8.41	8.35

The agreement between the two sensitivities recorded on separate days is extremely good. In fact the sensitivity remained relatively constant during the runs given later in this thesis. This was checked by Δ NO for each experiment but since the sensitivity did not enter into the rate constant calculations it is not recorded here. It should be mentioned that all the following data were recorded with the same filament. A filament change or any other modifications to the mass-spectrometer ion-gun assembly could result in sensitivity changes by altering the ion-box wall conditions.

For comparison purposes the nitrogen atom sensitivity is compared with other experimental molecular sensitivities and these are shown below:-

Process.	Electron Volts.	Sensitivity volts on 10^{10} ohms/mm. Hg.
$N \xrightarrow{e} N^+ + e$	23	8.38
$N_2 \xrightarrow{e} N_2^+ + e$	50	20.00
$NO \xrightarrow{e} NO^+ + e$	25	16.85
$N_2O \xrightarrow{e} N_2O^+ + e$	50	24.6
$O_2 \xrightarrow{e} O_2^+ + e$	50	16.8

17. ANALYSIS OF THE N + NO REACTION.

a) Reaction Zone Diffusion Theory.

For a steady state spherical diffusion zone, diffusion theory (25) predicts that when reaction is taking place the rate of loss of nozzle reagent is given in the general case by:-

Rate of loss of nozzle reagent

$$D\left(\frac{d^2C}{dR^2} + \frac{2}{R}\cdot\frac{dC}{dR}\right) \qquad \text{(iii)}$$

where D is the diffusion coefficient of the nozzle reagent and C the concentration of the nozzle reagent at a distance R from the point source.

Assuming that the N + NO reaction is a second order reaction, equation (iii) becomes:-

$$D\left(\frac{d^2[N]}{dR^2} + \frac{2}{R}\cdot\frac{d[N]}{dR}\right) = K[N][NO] \qquad \text{(iv)}$$

where $[N]$ and $[NO]$ represent the concentration of nitrogen atoms and nitric oxide respectively and K is the rate constant of the reaction.

Although the variation of $[NO]$ with R is known, equation (iv) is much easier to handle if $[NO]$ is assumed to be constant over the reaction zone and the equation may now be integrated to give:-

$$[N]\,R = \frac{b}{4\,D}\,e^{-cR}. \qquad \text{(v)}$$

where b is the nozzle flow rate of nitrogen atoms and $c^2 = \frac{K[NO]}{D}$

or expressing equation (v) logarithmically:-

$$\log_{10}[N]\,R = \log_{10}\frac{b}{4\,D} - \frac{cR}{2.303}$$

Thus a plot of $\log_{10}[N]\,R$ against R should give a straight line of

FIGURE 49.

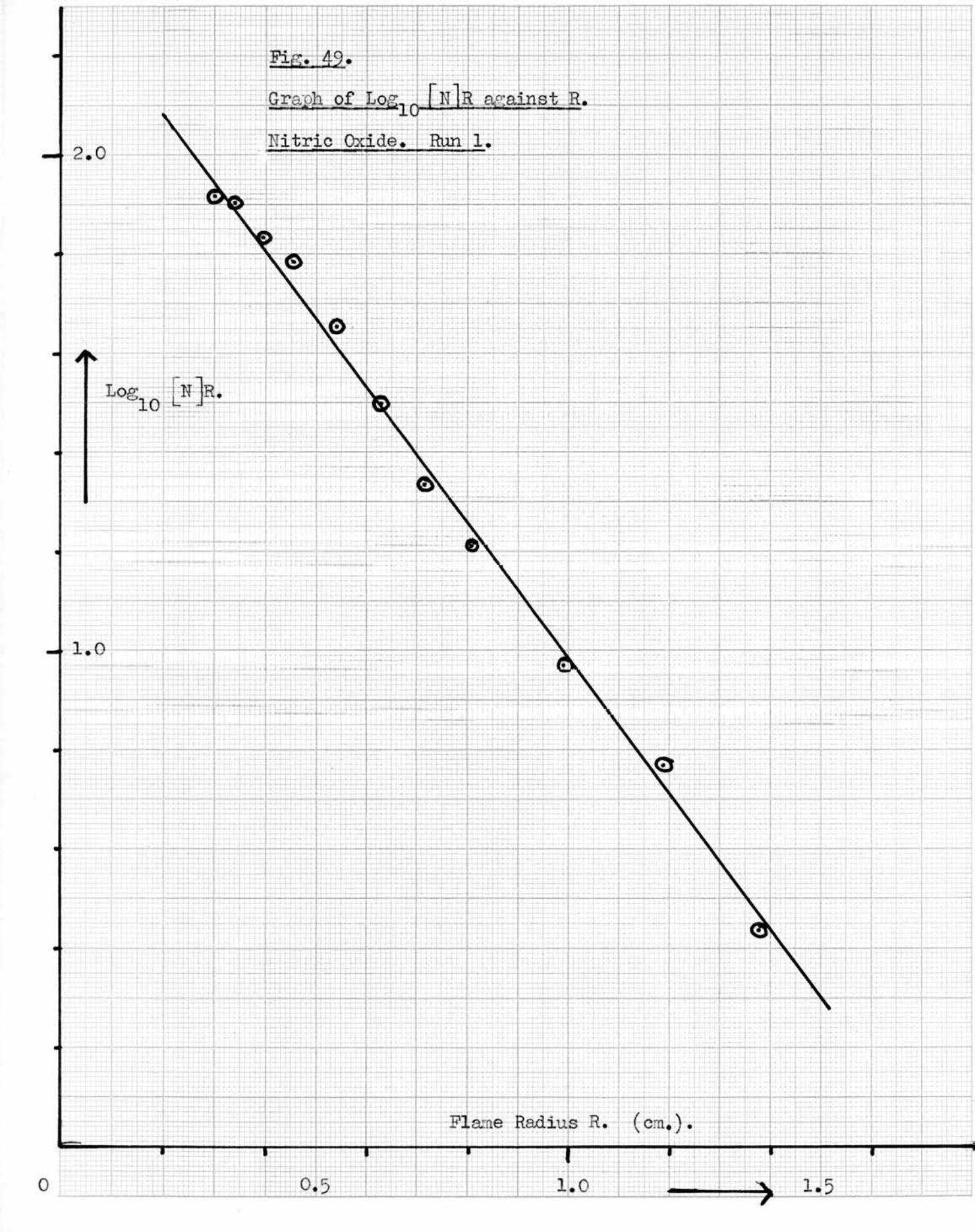
Fig. 49.
Graph of Log_{10} [N]R against R.
Nitric Oxide. Run 1.
2.0
1.0
Log_{10} [N]R.
Flame Radius R. (cm.).
0
0.5
1.0
1.5

FIGURE 50.

Fig. 50.

Graphs of $Log_{10}[N]R$ against R.

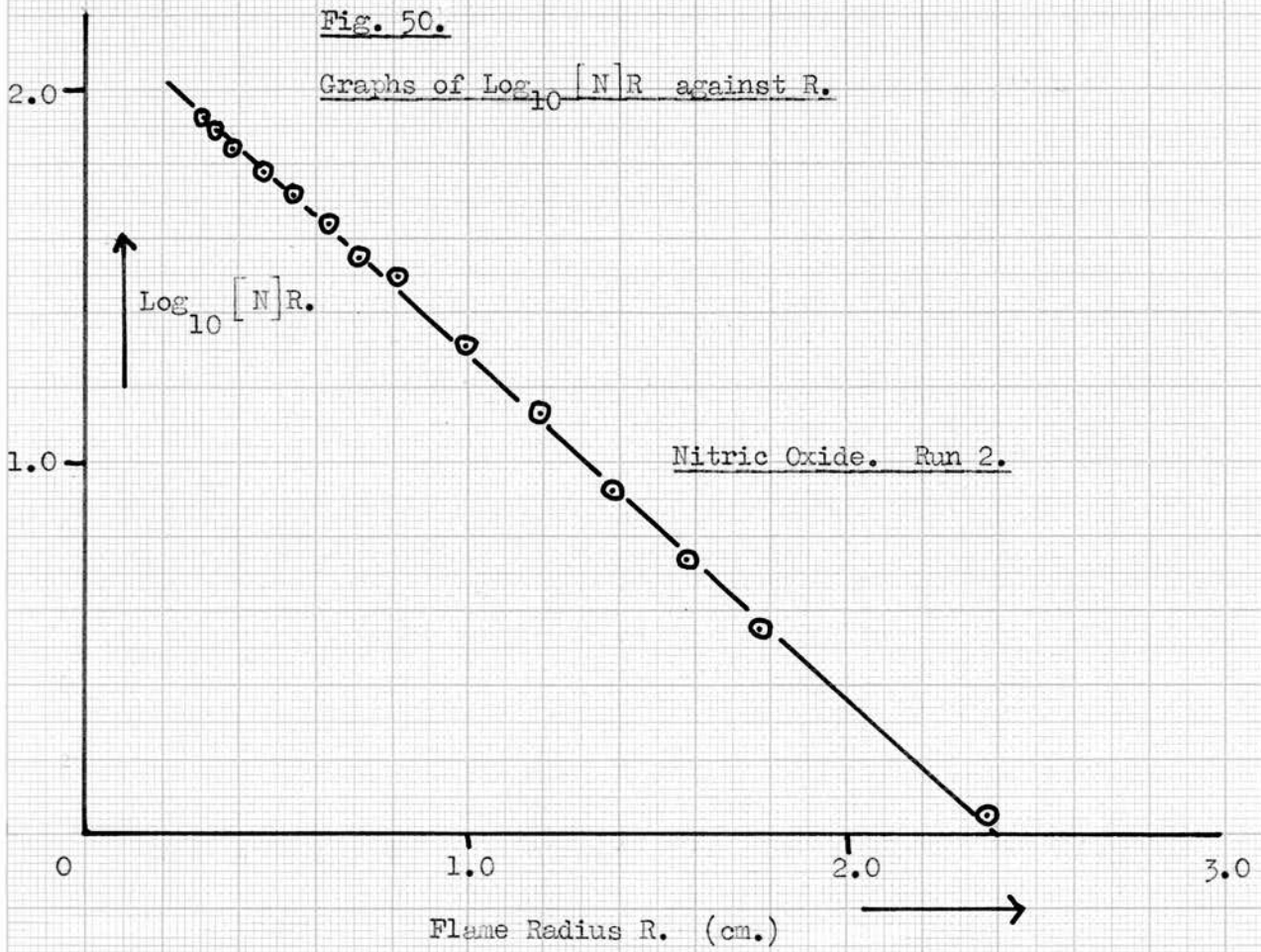

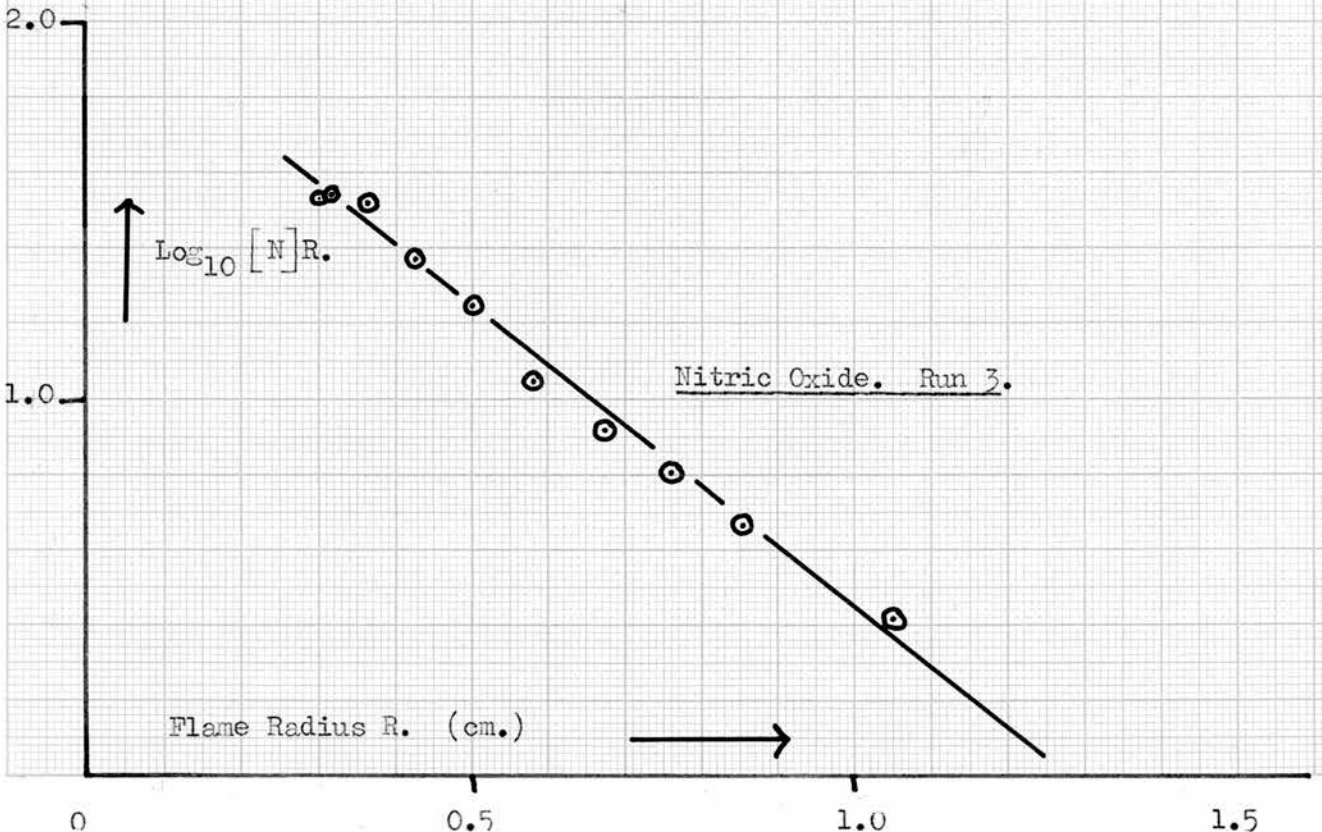

FIGURE 51.

Fig. 51.

Graphs of $\text{Log}_{10}[N]R$ against R.

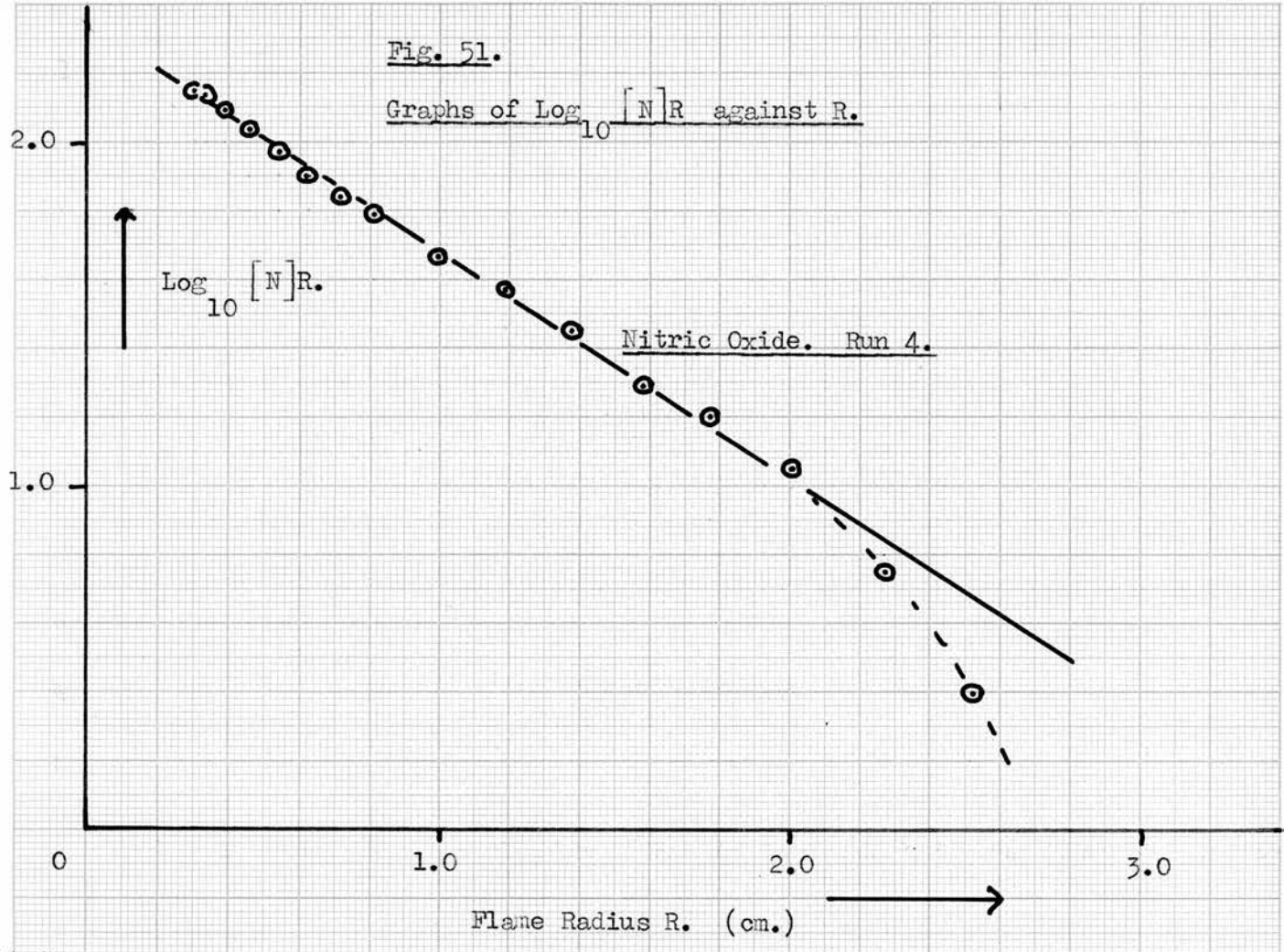

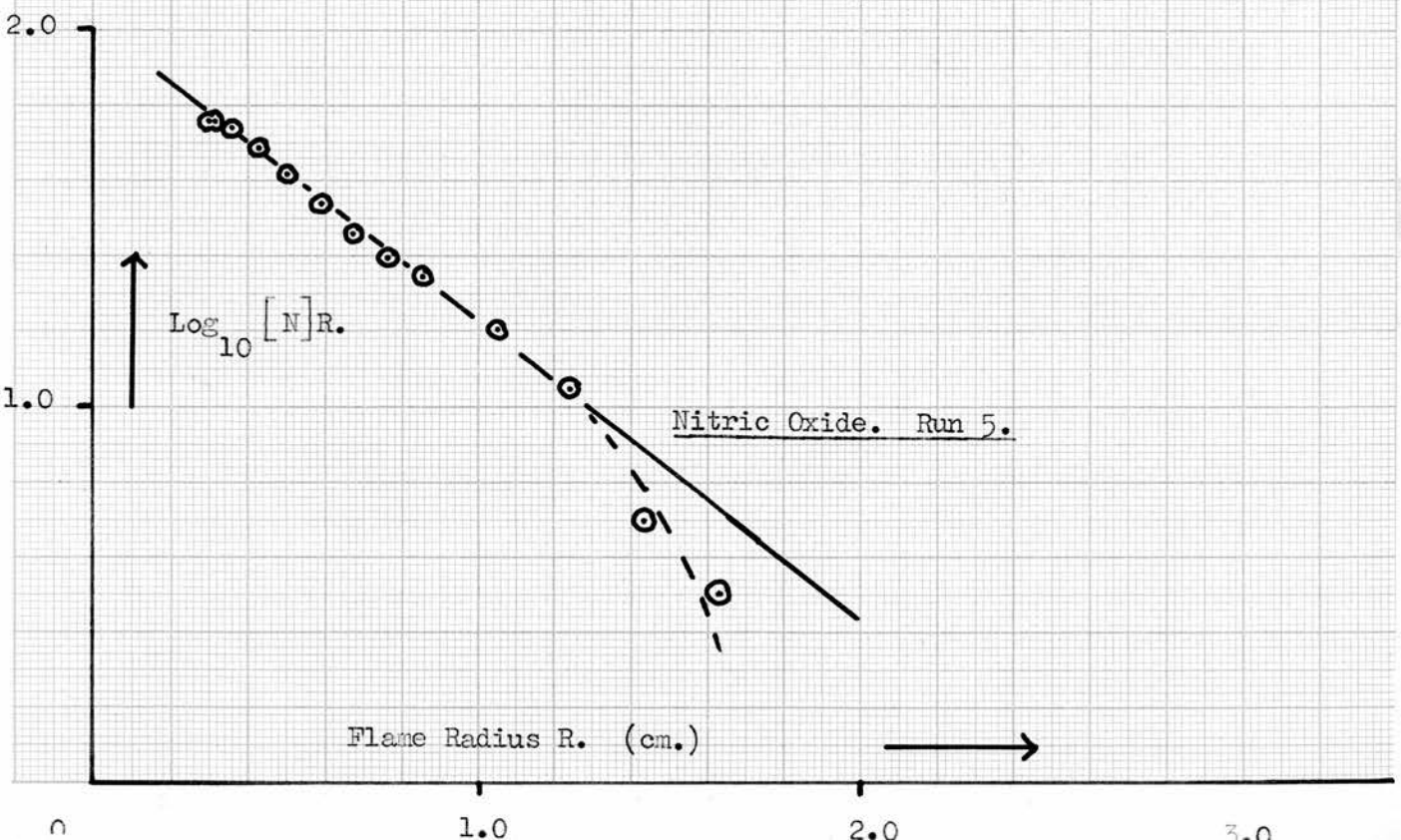

slope equal to $\frac{-1}{2.303}\left(\frac{K[NO]}{D}\right)^{\frac{1}{2}}$ yielding the required rate constant.

The assumption that the $[NO]$ is constant over the reaction zone simplifies the mathematical analysis of the diffusion zone. Polanyi [1] and later workers [23] were unable to monitor the concentration of the atmospheric reagent throughout the zone and therefore tried to maintain this concentration as constant as possible. Heller [14] has calculated accurate nozzle conditions for this such that $5 < v/D < 12$, but as mentioned previously these limits are not directly applicable to the wide bore nozzle used in this work.

As can be seen from Fig. 47 page 145 the $[NO]$ over the reaction zone is not constant. However, as shown later only a part of the reaction zone was used in the determination of the rate constant and the $[NO]$ over this limited region was assumed to be relatively constant.

b) Experimental Results.

Fig. 49. shows a graph of $\log_{10}[N]R$ against R for the data of the run shown in Fig. 47 page 145. The units of $[N]$ were plotted as millivolts on the 10^{12} ohm resistor for convenience since the units do not enter into the determination of the rate constant. Units of R are centimetres. The graph was expected to show a gradual curve due to the $[NO]$ not being entirely constant over the reaction zone, but the graph is remarkably linear.

Fig. 50 and Fig. 51 show a series of $\log_{10}[N]R$ against R for various nitric oxide concentrations. As in Fig. 49 the graphs are linear but show some deviation from linearity at large values of R. This is caused by errors in the measurement of low values of $[N]$. Meter

fluctuations made it impossible to read the $[N]$ to better than $\pm$ 0.25 mv. on the 10^{12} ohm resistor. As can be seen from Fig. 47 page 145 the $[N]$ at reaction distances greater than about 1.2 cm. is only a few millivolts and it is not surprising that the plots of $\log_{10}[N]R$ against R show deviations from linearity at large R distances.

The position of the scan (3 mm. below the nozzle) determined the minimum reaction distance of R = 0.3 cm. It was considered that the reaction zone between R = 0.3 and R = 1.3 cm. would be suitable for rate constant measurements. Over this range the graphs are all relatively linear indicating a second order reaction. Each run is plotted separately for convenience and the calculated rate constants are shown in the table below, the second order rate constant being calculated in ccs. $mole^{-1}$. sec^{-1}. units. The average $[NO]$ is the mean nitric oxide concentration over the reaction zone between R = 0.3 and R = 1.3 cm.

c) Experimental Rate Constants of the N NO Reaction.

Run Number	Average $[NO]$ (mm. Hg.)	Slope of $\log_{10}[N]R$ vs R ($cm.^{-1}$.)	Rate Constant. (ccs. $mole^{-1}.sec^{-1}$)
1.	1.17×10^{-3}	-1.365	9.14×10^{13}
2.	6.11×10^{-4}	-0.925	8.12×10^{13}
3.	1.38×10^{-3}	-1.60	1.06×10^{14}
4.	2.61×10^{-4}	-0.670	9.6×10^{13}
5.	3.45×10^{-4}	-0.792	1.05×10^{14}

The agreement between the rate constants over the almost tenfold range of nitric oxide concentration is extremely good. The average

value for the five runs all at 22°C and 1.2 mm. Hg. of nitrogen is 9.60×10^{13} ccs. $mole^{-1}$. sec^{-1}. The experimental error in this value is rather difficult to estimate. The experimental rate constants for the five runs show a deviation of about $\pm$ 1.3 ccs. $mole^{-1}$. sec^{-1}. This error will be reduced considerably by taking a mean value but there must also be an error introduced by the assumption of a constant concentration of nitric oxide over the reaction zone. Probably a total error of $\pm$ 1.0 ccs. $mole^{-1}$. sec^{-1}. is reasonable.

For comparison purposes the rate constants of the reaction derived by other workers are tabulated below:-

Worker.	Method.	Rate Constant.
Kistiakowsky. (99)(100)(101).	Stirred Reactor. Nitrogen Atom Mass-Spectrometer.	5×10^{13}.
Herron. (113)	Mass-Spectrometric Analysis of NO Consumption.	$1 \pm 0.5 \times 10^{13}$.
Clyne and Thrush. (112)	Nitric Oxide Titration.	$3 \pm 0.6 \times 10^{13}$ $e^{-200 \pm 700/RT}$.
This Work.	Diffusion Flame. Nitrogen Atom Mass-Spectrometer.	$9.60 \pm 1.0 \times 10^{13}$.

d) The Rate Constant by the Total Integral Method.

If the kinetic order of the N + NO reaction is assumed it is possible to determine the rate constant K by a total integral method.

The concentrations of nitrogen atoms and nitric oxide are known at all points in the reaction zone and the integration of the reaction rate at these points gives the total rate of reaction which may be equated to the consumption of nitric oxide. No assumptions as to the approximate linearity of the concentration of nitric oxide over the reaction zone are necessary and the essentials of the method are outlined below.

Consider a volume element dV at a distance R from the zone centre. The rate of consumption of nitric oxide in this element is given by:-

Element rate of NO consumption = $K\left[N\right]\left[NO\right] dV$. Where $\left[N\right]$ and $\left[NO\right]$ represent the concentration of nitrogen atoms and nitric oxide respectively.

Thus

$$\text{Total rate of NO consumption} = \int_{R=0}^{R=R_1} K\left[N\right]\left[NO\right]\, dV.$$

$$= 4\pi K \int_{R=0}^{R=R_1} \left[N\right]\left[NO\right] R^2\, dR. \quad \text{Since } dV = 4\pi R^2\, dR. \qquad \text{equation (vi)}$$

where $R = R_1$ represents the radius of the diffusion zone.

The expression given above is not easy to integrate directly but the value of $\int_{R=0}^{R=R_1} \left[N\right]\left[NO\right] R^2\, dR$ may be determined from the area

FIGURE 52.

Fig. 52.

Graph of $R^2 [N][NO]$ against R.

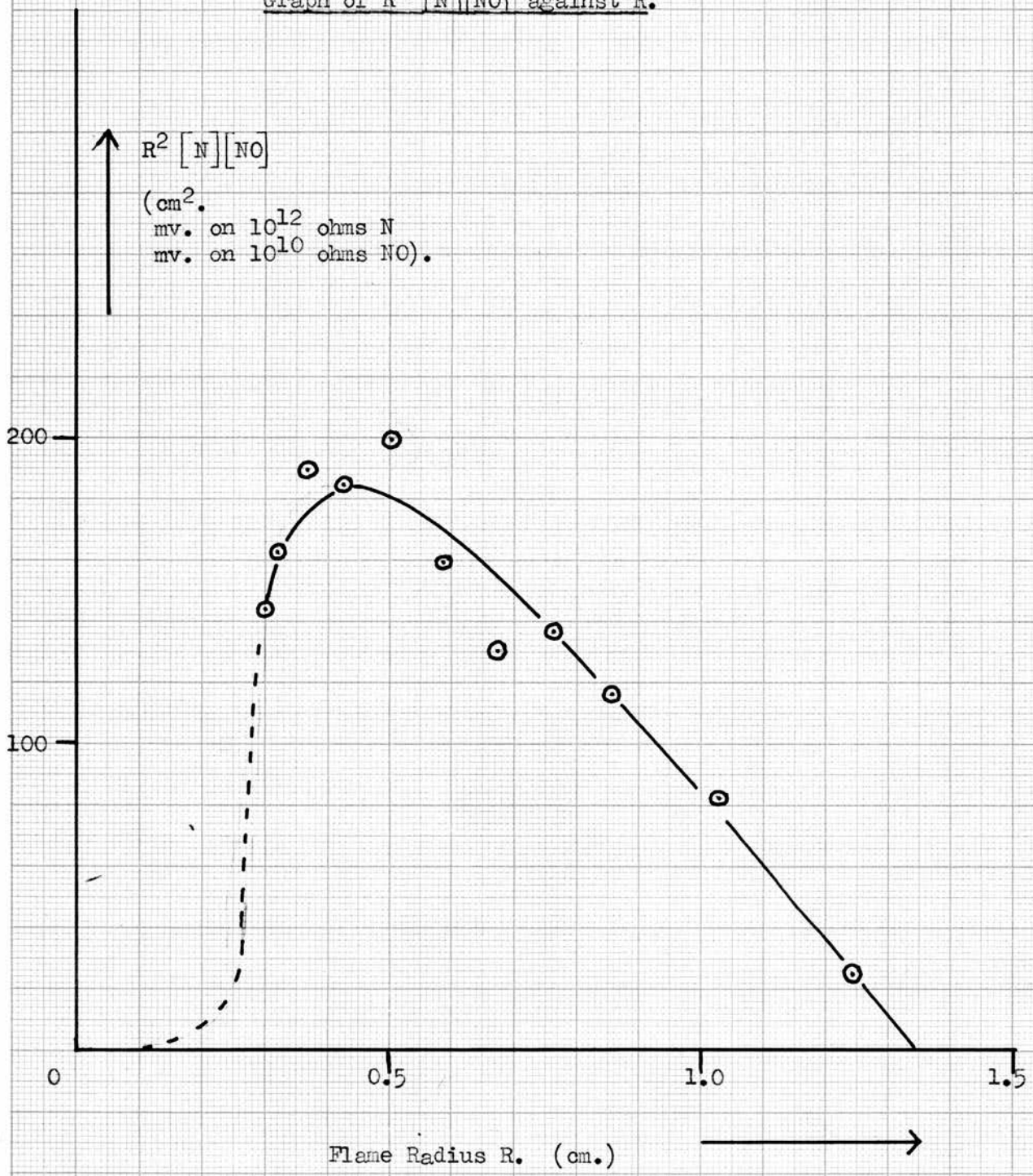

scanned out by the graph of $[N][NO]R^2$ against R, between R = 0 and $R = R_1$.

The potential of the method is outlined by a calculation of the rate constant for run (3) described earlier. Fig. 52 shows a plot of $[N][NO]R^2$ against R with the concentrations of NO and N in millivolts on the 10^{10} and 10^{12} ohm resistors respectively for convenience. Units of R are centimetres.

For this run the rate of loss of NO by N $(\Delta NO) = 4.5 \times 10^{-8}$ mole./sec., computed from the nitrogen flow rate and the partial pressures of nitric oxide.

From Fig. 52:-

Area under curve = 128 cm^3. (mv. on 10^{10} ohms NO) (mv. on 10^{12} ohms N)

$$= \frac{128}{16850 \times 838000}$$

$= 0.906 \times 10^{-8}$ cm^3. $(mm. Hg.)^2$ using the mass-spectrometer sensitivities to NO and N .

$= 2.70 \times 10^{-23}$ $mole^2$. ccs^{-1}.

Equation (vi) then yields:-

4.5×10^{-8} mole. sec^{-1}. $= 4\pi K (2.70 \times 10^{-23})$ $mole^2$. ccs^{-1}.

or $K = 1.32 \times 10^{14}$ ccs. $mole^{-1}$. sec^{-1}.

This value of the rate constant is of the right order of magnitude but slightly larger than the rate constant calculated previously as 9.60×10^{13} ccs. $mole^{-1}$. sec^{-1}. The method was not used generally to calculate the rate constants since the accuracy seems doubtful. Considerable errors can arise both in the computation of $[N][NO]R^2$ especially at small $[N]$ and in the assessment of the area scanned out by

the curve. It is also necessary to know the absolute sensitivity of the mass-spectrometer to nitrogen atoms.

e) Products, Stoichiometry and Some Relevant Comments on the N + NO Reaction.

A complete mass-spectrometer scan of the reaction zone indicated that the detectable products of the reaction were clearly nitrous oxide and oxygen. Several product analysis runs were performed recording the NO consumption (Δ NO) and the corresponding reaction vessel pressures of O_2 and N_2O produced by the reaction.

The NO, N_2O and O_2 in the reaction vessel were extracted to waste by the exit nitrogen stream and the flow rate of each entity would therefore be directly related to the pressure recorded in the reaction vessel by the mass-spectrometer. Thus, the actual measured pressures of NO, N_2O and O_2 in the reaction vessel gave the stoichiometry of the reaction.

In each run it was quite clear that the products were insufficient to comply with the reaction scheme:-

$$N + NO \longrightarrow N_2 + O$$

$$O + O \xrightarrow{M} O_2$$ where M can be the wall of the reaction vessel, and possible formation of nitrous oxide by:-

$$N + NO \longrightarrow N_2O^{*} \longrightarrow N_2O.$$

The typical data obtained from a specific run are shown below:-

Δ NO = 2.10×10^{-3} mm. Hg.

N_2O = 1.67×10^{-4} mm. Hg. $N_2O/\Delta NO$ = 7.95%.

O_2 = 4.23×10^{-4} mm. Hg. $O_2/\Delta NO$ = 20.5%.

Since two oxygen atoms are lost in the formation of a molecule of oxygen the ratio of the loss of nitrogen atoms ($\triangle N$), estimated by the formation of N_2O and O_2, to the loss of nitric oxide ($\triangle NO$) is given by the expression:-

$$\triangle N/\triangle NO = (N_2O + 2O_2)/\triangle NO = 48.95\%.$$

and clearly there appears to be another process taking place.

As explained in the literature section the reaction between nitrogen atoms and nitric oxide is now generally accepted to consist of the following reactions:-(52)

(1) $N + NO \longrightarrow N_2 + O$

(2) $N + O + M \longrightarrow NO^* + M \longrightarrow NO + h\nu$. (Blue)

(3) $O + NO \longrightarrow NO_2^* \longrightarrow NO_2 + h\nu$ (Green)

(4) $O + O + M \longrightarrow O_2 + M$

(5) $N + N + M \longrightarrow N_2 + M$

Reaction (5) is a three body process and as mentioned before is negligible compared with (1). Reaction (2) also requires the presence of a third body and is slow and can only take place in the vicinity of the nozzle where there is an appreciable concentration of nitrogen atoms. Reaction (3) is negligible since NO_2 is not formed as a product. This postulates that the main reactions are:-

$$N + NO \longrightarrow N_2 + O$$

and $$O + O + M \longrightarrow O_2 + M$$

However, the percentage of oxygen formed experimentally is very much less than the theoretical amount and it seems that oxygen atoms are sufficiently long-lived in the gaseous phase to diffuse to the

walls of the reaction vessel and are lost on the copper mesh by:-

$$Cu + O \longrightarrow CuO.$$

It was hoped to prove this theory by performing a product run in the absence of the copper mesh but unfortunately time did not permit this experiment. Attempts to detect atomic oxygen in the diffusion zone, even at high concentrations of nitric oxide were unsuccessful but the atoms could be destroyed in the ion box and gas entry tubes of the mass-spectrometer by surface recombination. Kistiakowsky (100), on the other hand, was able to show enhanced 16^+ peaks in the N + NO reaction.

The accepted reaction scheme outlined above does not include any nitrous oxide production but this was certainly present in all of the product analysis runs on this apparatus. Nitrous oxide is mentioned as a product of the reaction in an early paper by Kistiakowsky (99), who suggested at that time that the reaction proceeded mainly by:- $N + NO \longrightarrow N_2O$. In later work (100)(101) he did not detect N_2O and conveniently forgot about this early comment.

The origin of the N_2O formation seems rather vague. Possibly $N + NO \longrightarrow N_2O^* \longrightarrow N_2O$ can be a competitive reaction to $N + NO \longrightarrow N_2 + O$ but must have a rate constant of a similar magnitude. Nitrous oxide may also originate from a reaction species other than nitrogen atoms present in the discharge. The presence of a second reaction species in active nitrogen has been postulated for some time (73) to account for the differences between the results from NO and C_2H_4 titrations, but recent work with isotopically labelled materials has

been unable to give any support to this idea [124].

It ought to be mentioned at this point that a scan over the discharge area in pure nitrogen showed a species of mass 42, possibly N_3 [97][98]. This was very unstable since it decayed to zero concentration beneath the nozzle and could not be detected in the reaction vessel. An experiment however showed that it did not react with nitric oxide.

As mentioned earlier no visible radiations were evident in the reaction zone during normal running conditions. However, if the nitric oxide concentration was increased markedly to about 10^{-1} mm. Hg., nitrogen atoms could not be detected under the nozzle and the green glow of $O + NO \longrightarrow NO_2^* \longrightarrow NO_2$ filled the whole reaction vessel. With the nitric oxide injection cut off the green glow faded and the blue from $N + O \longrightarrow NO^* \longrightarrow NO$ became visible momentarily then faded. In each case the glows were not confined to, but were more intense near the nozzle. It seems likely that under normal operating conditions the flame is too dilute to give visible glows but at much higher nitric oxide concentrations where there is certainly some back diffusion of NO into the nozzle into regions of high concentrations of nitrogen atoms, the amount of the $N + NO$ reaction taking place is sufficient to give visible radiations.

FIGURE 53.

Fig. 53.

Calibration Data for Ethylene.

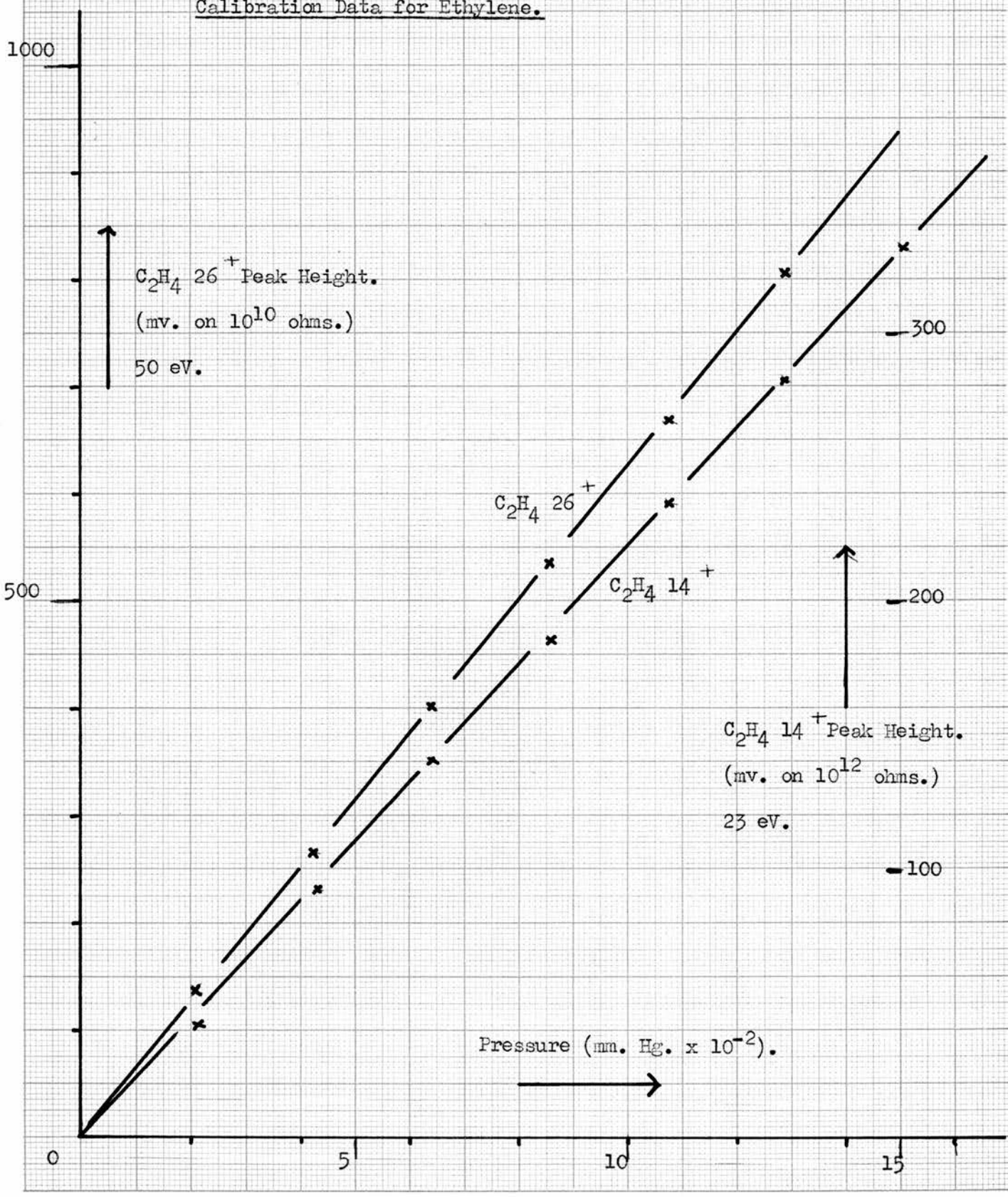

18. PRELIMINARY REACTIONS WITH ETHYLENE.

a) Initial Investigations and Mass-Spectrum of Ethylene.

The nitric oxide storage vessel on the injection line was removed and replaced by a similar bulb containing ethylene (mass-spec. grade). A preliminary injection into the reaction vessel showed that the ethylene produced a CH_2^+ (14^+) peak even at 23 eV. and at first it was thought that this would interfere with the nitrogen atom 14^+ peak height determinations. The reaction $N + C_2H_4$ is known to be fast but some 100 times slower than the $N + NO$ reaction so that it was anticipated that relatively large concentrations of C_2H_4 would be required in the reaction zone to give adequate consumption of nitrogen atoms.

The parent C_2H_4 peak at 28^+ could not be monitored in the presence of nitrogen and the ethylene concentration was followed by the 26^+ ($C_2H_2^+$) at 50 eV. and the calibration graph is shown in Fig. 53. Each point was calibrated at low C_2H_4 pressure in the presence of nitrogen at 1.2 mm. Hg., by the same method as described earlier for the calibration of nitric oxide. Also shown is the 14^+ calibration graph at 23 eV. to give the relative $28^+/14^+$ ratio. This allowed the contribution to the 14^+ peak from ethylene to be determined so that by difference the N 14^+ peak height could be calculated. The calibration plots shown in Fig. 53 are both corrected for a standard nitrogen sensitivity of 200 mv. on the 10^8 ohm resistor per mm. Hg.

FIGURE 54.

Fig. 54.

The Effect of Ethylene on the $N\ 14^+$ Peak Height in the Reaction Zone.

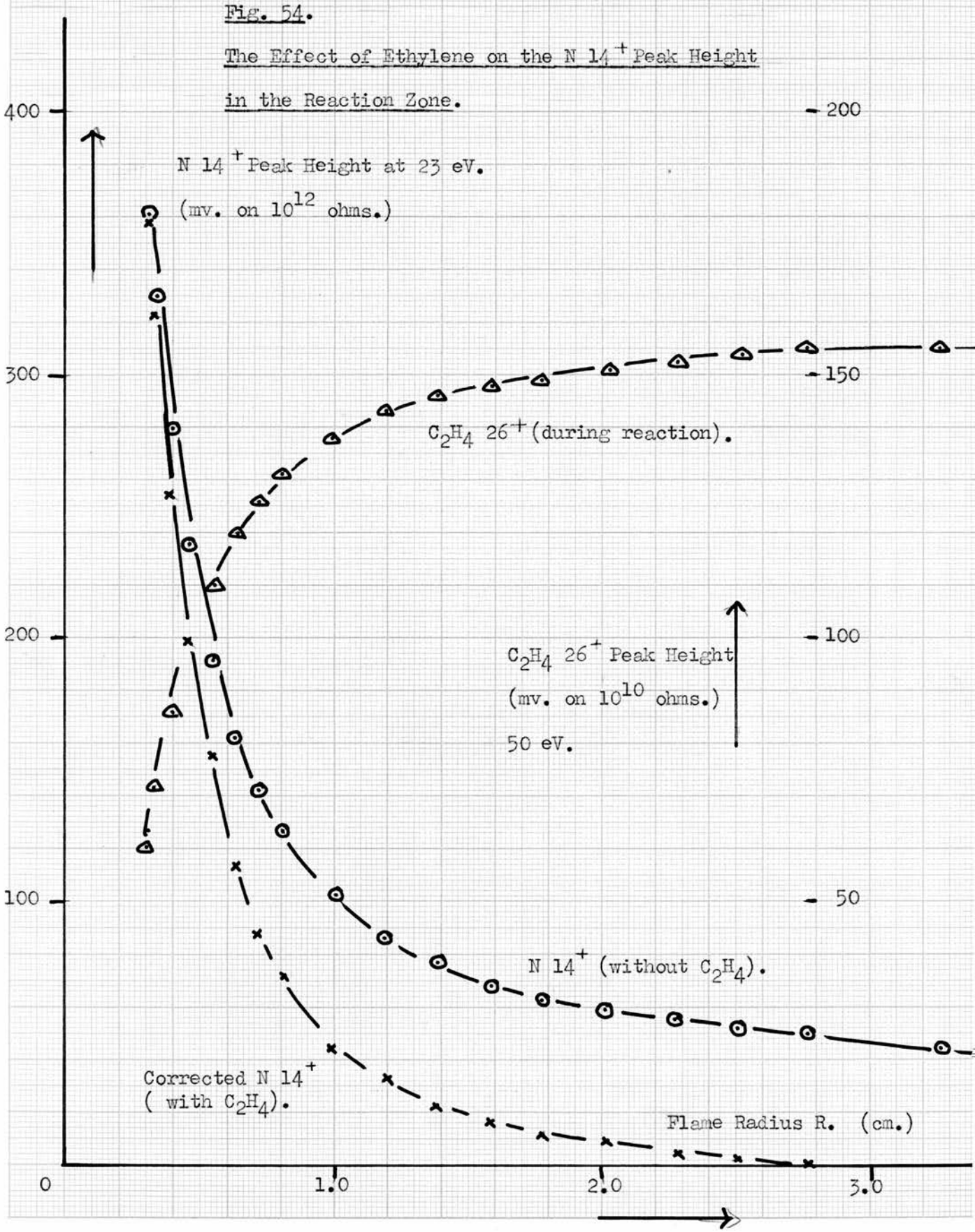

b) Experimental Results.

The general horizontal scans for the N + C_2H_4 reaction zone plotted against the flame radius R are shown in Fig. 54. The run was performed under identical conditions to those used in the nitric oxide study, except that a relatively large pressure of ethylene was necessary to give suitable reaction conditions. This immediately demonstrated that the reaction was much slower than the N + NO reaction. The graph shows the 14^+ peak height across the zone without ethylene and the corrected N 14^+ peak height with ethylene present. Also shown is the ethylene 26^+ depletion curve during the reaction.

A plot of $\log_{10}[N]$ R. against R is shown in Fig. 55. Also shown is a similar log. plot of another complete run under slightly different conditions. Unfortunately, time did not permit any further runs but as can be seen the two plots are remarkably linear over the reaction zone indicating a second order reaction N + $C_2H_4 \longrightarrow$ products. The data obtained from the two plots are tabulated below with the second order rate constant K expressed in ccs. $mole^{-1}$. sec^{-1}. The average C_2H_4 concentration is calculated over the same reaction zone limits as chosen for the N + NO case (R = 0.3 to R = 1.3 cm.).

c) Experimental Rate Constants of the N + C_2H_4 Reaction.

Run Number.	Average $[C_2H_4]$ (mm. Hg.)	Slope of Log. Plot. (cm^{-1}.)	Rate Constant. (ccs. $mole^{-1}$. sec^{-1}.)
1.	1.64×10^{-2}	-0.50	8.8×10^{11}.
2.	1.29×10^{-2}	-0.57	14.8×10^{11}.

The agreement between these two rate constants is not good.

FIGURE 55.

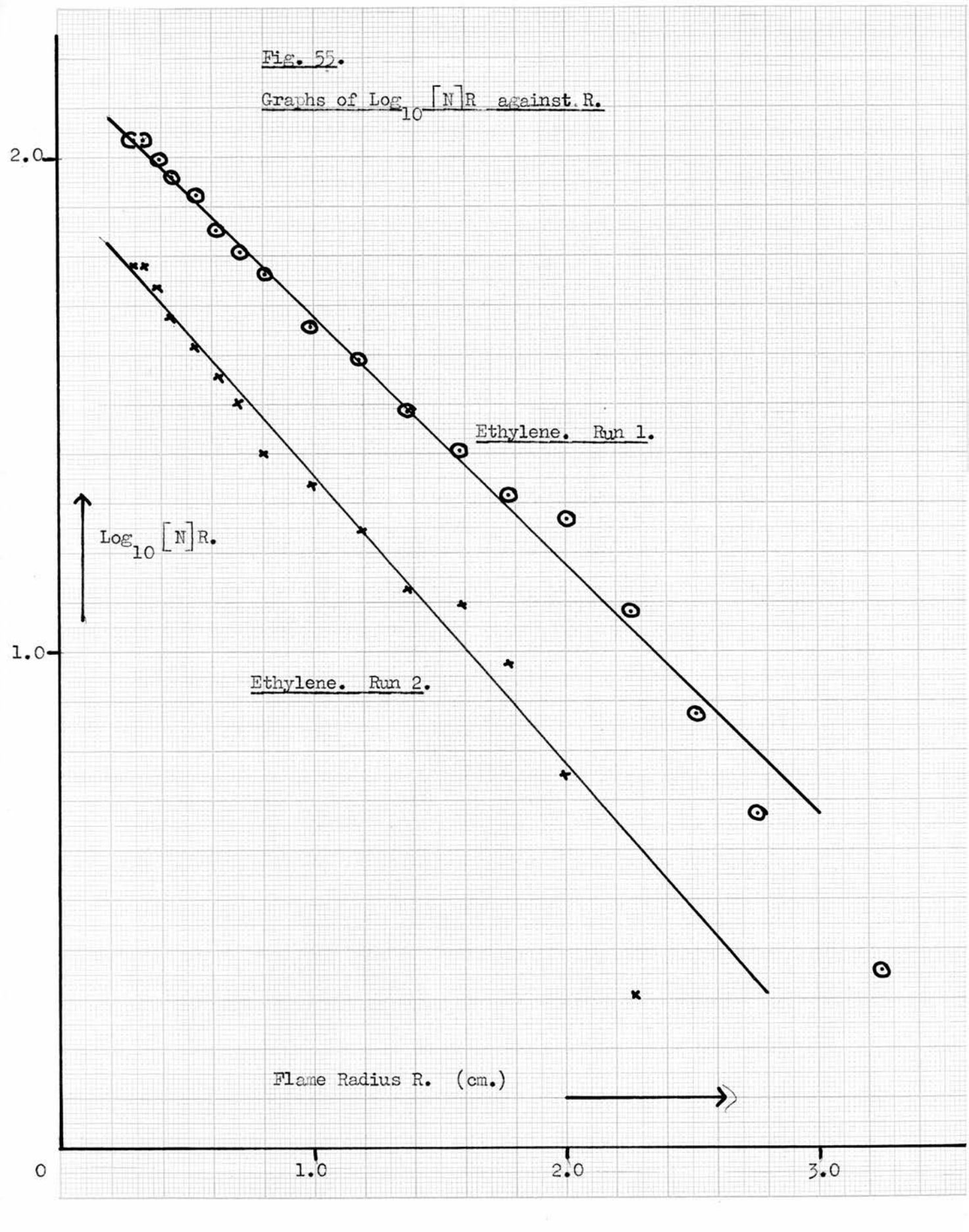
Fig. 55.
Graphs of Log10 [N]R against R.
2.0
1.0
0
Log10 [N]R.
Ethylene. Run 1.
Ethylene. Run 2.
Flame Radius R. (cm.)
1.0
2.0
3.0

Unfortunately, time did not permit further runs but the average value of $K = 1.18 \times 10^{12}$ ccs. $mole^{-1}$. sec^{-1}. shows the general order of magnitude of the reaction velocity which is about 80 times slower than the N + NO reaction.

The average value appears to be somewhat larger than the rate constants computed by Herron [122] as $K = 5.8 \times 10^{10}$ ccs. $mole^{-1}$. sec^{-1}. and by Dunford [123] using a crude diffusion flame method as $K = 9.6 \times 10^{10}$ ccs. $mole^{-1}$. sec^{-1}.

d) Products, Stoichiometry and Some Relevant Comments on the $N + C_2H_4$ Reaction

A complete mass-spectrometer scan over the reaction zone showed virtually no products at all although considerable nitrogen atoms were being removed.

As explained in the literature section the reaction of nitrogen atoms with ethylene has generally been accepted as:-

$$N + C_2H_4 \longrightarrow (C_2H_4N) \qquad (i)$$

followed mainly by:-

$$(C_2H_4N) \longrightarrow HCN + CH_3 \qquad (ii)$$

together with a variety of secondary reactions such as:-

$$2(C_2H_4N) \longrightarrow 2C_2H_4 + N_2 \qquad (iii)$$

$$N + (C_2H_4N) \longrightarrow C_2H_4 + N_2 \qquad (iv)$$

with some HCN formation by:-

$$CH_3 + N \longrightarrow HCN + 2H \qquad (v)$$

Generally, these secondary reactions have been considered negligible and the HCN formation assumed to be quantitative to the loss of nitrogen atoms.

A check for HCN in the reaction zone at mass 27 proved difficult due to the interference from the large 28^+ peak from nitrogen and also from the 27^+ ethylene peak, but small increments should have been detected if any HCN was present.

Because of the difficulty in locating the products the discharge was operated for thirty minutes and the exit gases passed through a liquid air trap. Various fractions of the collected materials were then allowed to flow back into the reaction vessel for mass-spectrometric analysis. The mass-spectrum was then compared with a blank spectrum from the condensed materials obtained by running the apparatus for thirty minutes without the discharge. The two mass-spectra showed almost identical patterns but a peak at mass 43 was enhanced when the discharge was activated. Increments on all other peaks were negligible.

Another run, again for thirty minutes, and a blank run gave similar results with only the 43^+ peak showing any increase when the discharge was activated. There was no HCN and this was proved further by collecting the products of two further runs in a few ccs. of caustic soda frozen in a liquid air trap. Titration with silver nitrate did not show any HCN although a titration sensitivity check showed that even if the reaction had yielded only 1/20th of the stoichiometric yield of HCN this could have been readily detected.

Unfortunately, time did not permit a thorough investigation of this problem but it seemed clear that the 43^+ peak was a product of the reaction but only a very small product.

The actual reaction scheme is difficult to postulate on this

evidence alone. It is reasonable to assume that the reaction proceeds via a (C_2H_4N) intermediate which could be followed by reactions (iii) and (iv) namely:-

$$2(C_2H_4N) \longrightarrow 2C_2H_4 + N_2 \qquad \text{(iii)}$$

$$N + (C_2H_4N) \longrightarrow C_2H_4 + N_2 \qquad \text{(iv)}$$

which would remove nitrogen atoms without forming any products.

An analysis for (C_2H_4N) in the reaction zone proved negative but the radical might be lost on the ion-box walls and this is not evidence for its non-existence in the reaction zone.

The nature of the peak at 43 is more difficult to postulate but could be caused by:-

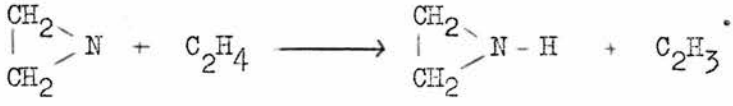

ethylene-imine.

The fate of the C_2H_3 radical is not clear but it could attack C_2H_4 to give a variety of minor products.

It is rather perplexing that HCN could not be detected in any of this work, since the reaction has been widely used, allegedly quantitatively, for nitrogen atom titration. The present accepted mechanism for HCN formation by (C_2H_4N) rearrangement should be favoured at the low nitrogen atom concentrations used in this work, since (C_2H_4N) can survive for an appreciable time without a collision with another (C_2H_4N) or a nitrogen atom. The results described in this thesis seem to suggest that the HCN formation does not occur by this route.

It seems relevant to consider the differences between the technique

of this work and that of other workers. In much of the work by Winkler a system has been used with more vigorous discharges producing high percentage dissociation of nitrogen [42][43]. The dimensions of the glass reactors or reaction tubes have also been much smaller than in this work. If C_2H_4 is fed into a nitrogen atom stream under such conditions the radicals (C_2H_4N) which are formed can easily reach the wall of the vessel. In the conditions of the work described in this thesis this is much more difficult. Any radical of this type has to diffuse through a considerable distance in the presence of excess C_2H_4 in order to reach the wall, and since the vessel is so large the collision frequency for (C_2H_4N and C_2H_4N) or (C_2H_4N and N) may prove adequate to cause the formation of nitrogen, despite the low initial concentration (about 10^{-3}mm. Hg.) of nitrogen atoms. If the (C_2H_4N) radical decomposes to HCN at the wall then it becomes easier to understand the fact that it could not be detected in this work. One of the great advantages of the diffusion flame technique may prove to be this opportunity to study processes of this nature without the intervention of wall reactions.

Both the nitrogen forming reactions (iii) and (iv) will be very exothermic due to the high bond strength of nitrogen and since this exothermicity must be shared between the products of reaction the latter will be in excited vibrational states. By suitable modification of our technique this might be detectable as infra-red emission spectra.

19. SUGGESTIONS FOR FUTURE WORK.

a) The Reaction N + NO.

(i) Attempts should be made to measure the relative concentrations of free oxygen atoms produced in the reaction. This might be possible if electron multiplier detection is applied to the small ion currents involved.

(ii) An exhaustive stoichiometric balance seems desirable on the reactants and products.

(iii) The method provides data on the concentration variations of both nitrogen atoms and nitric oxide molecules in the reaction zone. Further attempts should be made to utilise, in suitable mathematical frameworks, the complete picture of the reaction zone for the deduction of velocity constants. If a suitable method is achieved one of the limitations in the Polanyi diffusion flame treatment is removed, namely, the impoverishment of the atmospheric reagent near the jet, since accurate data can be supplied by this technique.

(iv) If the conditions of reaction are arranged to achieve $N + NO \longrightarrow N_2 + O$ within a small region near the jet then the subsequent reactions of oxygen atoms could be followed.

b) The Reaction N + C_2H_4.

(i) A detailed investigation for products and a stoichiometric balance are very desirable.

(ii) An attempt should be made to see if even a small amount of abstraction type reactions (producing for example NH radicals) occurs. The use of C_2D_4 might be helpful here since the masses of interest in

both stable and unstable products are shifted in the spectrum and some overlaps avoided.

c) Other Reactions of Nitrogen Atoms.

This is a very wide field and the only important issue is the order in which investigations are made. In view of the striking absence of HCN formation in the case of N + C_2H_4 it must be anticipated that the conditions of this technique may cause reaction routes to be favoured which would not be anticipated from existing data. As a result it is suggested that very simple reactants be chosen initially, such as HCl, DCl, HBr and DBr.

20. SUMMARY.

(i) The thesis reports in the previous pages the development of a method of studying the reactions of free nitrogen atoms by studying their concentration in a diffusion 'flame' reaction zone by mass-spectrometric analysis.

(ii) A survey of the relevant literature is given in pages 1 to 70.

(iii) The development of the technique is described in all its stages, begining with the production and detection by conventional methods of jets of nitrogen and hydrogen atoms.

(iv) The production of free atoms by radio-frequency discharges and the coupling of this to a mass-spectrometer without interference to the latter is detailed. The problems here were quite severe since a high sensitivity of detection was essential.

(v) Modifications to the mass-spectrometer are detailed which raised the signal derived from sampling the nitrogen atom stream from a few millivolts to a few volts. These modifications involved alterations to the ion-box and ion collecting system.

(vi) A reactor system containing a fixed sampling orifice and moveable reaction zone are detailed.

(vii) It has been shown that spherical diffusion conditions can be achieved for nitrogen atoms emerging from a nozzle into a low pressure of nitrogen gas and that the diffusion zone can be reproducibly analysed for the free atoms to provide graphs of concentration changes.

(viii) The reaction between nitrogen atoms and nitric oxide has been studied in the equipment described and a rate constant of

$9.60 \pm 1.0 \times 10^{13}$ ccs. $mole^{-1}$. sec^{-1}. has been derived.

(ix) A brief investigation of the reaction of nitrogen atoms with ethylene permitted a rate constant of about 1.18×10^{12} ccs. $mole^{-1}$. sec^{-1}. to be deduced.

(x) Both rate constants deduced are in good general agreement with estimates from other workers.

(xi) Some observations on the $N + C_2H_4$ reaction show that the normally quoted product (HCN) is not formed. This is discussed.

(xii) Suggestions for the further development of the work are briefly listed.

21. APPENDIX.

a) Experimental Data for the N + NO Reaction Zone.

RUN 1.

Total nitrogen pressure 1.2 mm. Hg. Temperature 22°C.

r (cm.)	R (cm.)	$N\ 14^+$ without NO ($mv.10^{12}$)	$N\ 14^+$ with NO ($mv.10^{12}$)	$[NO]$ ($mv.10^{10}$)	$\log_{10}[N]R.$
.05	.30	469	270	9.6	1.91.
.15	.34	439	237	11.0	1.90.
.25	.39	369	176	13.4	1.83.
.35	.46	304	132	15.4	1.78.
.45	.54	254	82	17.7	1.65.
.55	.63	212	49	20.3	1.49.
.65	.72	169	30	22.4	1.33.
.75	.81	144	20	24.3	1.21.
.95	.99	116	9	27.3	0.97.
1.15	1.19	95	5	29.0	0.77.
1.35	1.38	81	2	31.0	0.44.
1.55	1.58	70	0	32.5	-
1.75	1.77	66	0	34.0	-
2.25	2.27	51	0	34.0	-
2.75	2.77	40	0	34.0	-

Average NO over reaction zone between R = 0.3 and R = 1.3 cm.

= 19.8 mv. on the 10^{10} ohm resistor

= 1.175×10^{-3} mm. Hg.

= 6.42×10^{-11} mole. cos^{-1}. at 22°C.

RUN 2.

Total nitrogen pressure 1.2 mm. Hg. Temperature 22°C.

r (cm.)	R (cm.)	$N\ 14^+$ without NO ($mv.10^{12}$)	$N\ 14^+$ with NO ($mv.10^{12}$)	$[NO]$ ($mv.10^{10}$)	$\log_{10}[N]R$.
.05	.30	333	278	6.1	1.92.
.15	.34	299	235	6.5	1.89.
.25	.39	253	179	7.4	1.84.
.35	.46	203	132	8.4	1.78.
.45	.54	163	96	8.9	1.72.
.55	.63	133	70	10.3	1.64.
.65	.72	116	50	11.1	1.55.
.75	.81	101	35	11.9	1.45.
.95	.99	81	20	12.9	1.31.
1.15	1.19	66	11	14.0	1.13.
1.35	1.38	57	6	15.0	0.92.
1.55	1.58	49	3.5	15.7	0.74.
1.75	1.77	45	2	16.5	0.55.
2.25	2.27	36	0.5	17.9	0.05.
2.75	2.77	31	0	18.8	-

Average NO over reaction zone between R = 0.3 and R = 1.3 cm.

= 10.3 mv. on the 10^{10} ohm resistor

= 6.11×10^{-4} mm. Hg.

= 3.34×10^{-11} mole. ccs^{-1}. at 22°C.

RUN 3.

Total nitrogen pressure 1.2 mm. Hg. Temperature 22°C.

r	R	$N\,14^+$ without NO	$N\,14^+$ with NO	$[NO]$	$\log_{10}[N]R$.
(cm.)	(cm.)	(mv.10^{12})	(mv.10^{12})	(mv.10^{10})	
0	.30	246	113	14.2	1.53.
.1	.32	239	110	14.8	1.54.
.2	.36	213	88	16.5	1.52.
.3	.42	168	56	18.3	1.37.
.4	.50	137	35	22.4	1.25.
.5	.58	111	19	24.5	1.05.
.6	.67	96	11	26.2	0.92.
.7	.76	81	8.5	27.8	0.81.
.8	.85	72	5.5	29.0	0.67.
1.0	1.05	57	2.5	31.5	0.42.
1.2	1.24	46	0.5	31.8	- 0.22.
1.4	1.43	41	0	32.5	-
1.6	1.63	36	0	33.0	-
1.8	1.82	31	0	33.5	-

Average NO over reaction zone between R = 0.3 and R = 1.3 cm.

= 23.2 mv. on the 10^{10} ohm resistor

= 1.38×10^{-3} mm. Hg.

= 7.52×10^{-11} mole. ccs^{-1}. at 22°C.

RUN 3 (Continued).

Additional data for the velocity constant by the total integral method.

R	R^2	$N\ 14^+$ with NO	$[NO]$	$R^2[N][NO]$
(cm.)	(cm^2.)	($mv.10^{12}$)	($mv.10^{10}$)	(cm^2.)($mv.10^{12}$ of N)($mv.10^{10}$ of NO)
.30	.09	113	14.2	144.
.32	.10	110	14.8	163.
.36	.13	88	16.5	189.
.42	.18	56	18.3	184.
.50	.25	35	22.4	199.
.58	.34	19	24.5	159.
.67	.45	11	26.2	130.
.76	.58	8.5	27.8	137.
.85	.73	5.5	29.0	116.
1.05	1.08	2.5	31.5	82.5.
1.24	1.54	0.5	31.8	24.4.
1.43	2.05	0	32.5	0
1.63	2.65	0	33.0	0
1.82	3.32	0	33.5	0

NO consumed by N ($\triangle$ NO)

i.e. NO (without discharge) - NO (with discharge)

$= 44$ mv. on the 10^{10} ohm resistor

$= 2.62 \times 10^{-3}$ mm. Hg.

Total nitrogen flow rate through the reaction vessel

$= 0.50$ ccs. at N.T.P. per sec.

$= 2.06 \times 10^{-5}$ mole. sec^{-1}. at 22°C.

Thus, the rate of loss of NO by N .

$$= \frac{(2.62 \times 10^{-3})(2.06 \times 10^{-5})}{1.2}$$

$= 4.5 \times 10^{-8}$ mole. sec^{-1}.

RUN 4.

Total nitrogen pressure 1.2 mm. Hg. Temperature 22°C.

r	R	$N\ 14^+$ without NO	$N\ 14^+$ with NO	$[NO]$	$\log_{10}[N]R$.
(cm.)	(cm.)	(mv.10^{12})	(mv.10^{12})	(mv.10^{12})	
.05	.30	587	474	190	2.15.
.15	.34	539	411	205	2.14.
.25	.39	440	321	235	2.09.
.35	.46	364	237	268	2.04.
.45	.54	289	172	305	1.97.
.55	.63	248	128	340	1.90.
.65	.72	212	96.5	385	1.84.
.75	.81	178	76.5	430	1.79.
.95	.99	142	47.5	515	1.67.
1.15	1.19	115	31.5	600	1.57.
1.35	1.38	103	20.5	660	1.45.
1.55	1.58	91	12.5	725	1.29.
1.75	1.77	79	9.0	800	1.20.
2.00	2.02	71	5.5	-	1.05.
2.25	2.27	63	2.5	860	0.75.
2.50	2.52	57	1.0	-	0.40.
2.75	2.77	52	0	925	-

Average NO over reaction zone between R = 0.3 and R = 1.3 cm.

= 440 mv. on the 10^{12} ohm resistor

= 2.61×10^{-4} mm. Hg.

= 1.43×10^{-11} mole. ccs^{-1}. at 22°C.

RUN 5.

Total nitrogen pressure 1.2 mm. Hg. Temperature 22°C.

r	R	$N\ 14^+$ without NO	$N\ 14^+$ with NO	$[NO]$	$\log_{10}[N]R$.
(cm.)	(cm.)	(mv.10^{12})	(mv.10^{12})	(mv.10^{12})	
0	.30	348	191	315	1.76.
.1	.32	239	183	325	1.76.
.2	.36	211	152	355	1.74.
.3	.42	172	116	425	1.69.
.4	.50	144	84	475	1.62.
.5	.58	119	59	530	1.54.
.6	.67	96	43	580	1.46.
.7	.76	82	33	625	1.40.
.8	.85	71	26	675	1.35.
1.0	1.05	56	15.5	750	1.21.
1.2	1.24	46	9	820	1.05.
1.4	1.43	41	3.5	875	0.70.
1.6	1.63	31	2	925	0.51.
1.8	1.82	32	0	975	-

Average NO over reaction zone between R = 0.3 and R = 1.3 cm.

= 581 mv. on the 10^{12} ohm resistor

= 3.45×10^{-4} mm. Hg.

= 1.89×10^{-11} mole. ccs^{-1}. at 22°C.

b) Experimental Data for the N + C_2H_4 Reaction Zone.

RUN 1.

Total nitrogen pressure 1.2 mm. Hg. Temperature 22°C.

R .	Total 14^+ with C_2H_4	C_2H_4 28^+	Contribution to 14^+ by C_2H_4	Corrected N 14^+	$\log_{10}[N]R.$
(cm.)	(mv.10^{12})	(mv.10^{10})	(mv.10^{12})	(mv.10^{12})	
.30	380	60.5	21.2	358.8	2.03.
.34	350	71.5	25.0	325.0	2.04.
.39	285	86.0	30.1	254.9	1.99.
.46	234	99	34.7	198.3	1.96.
.54	195	111	38.5	155.5	1.93.
.63	157	120	42.0	115.0	1.86.
.72	133	126	44.1	88.9	1.80.
.81	118	131	45.8	72.2	1.76.
.99	94	138	48.4	45.5	1.66.
1.19	83	143	50.0	33.0	1.59.
1.38	73	146	51.0	22.0	1.48.
1.58	68	148	51.8	16.2	1.41.
1.77	64	149	52.2	11.8	1.32.
2.02	62	151	52.8	9.2	1.27.
2.27	58.5	152	53.2	5.3	1.08.
2.52	57	154	54.0	3.0	0.88.
2.76	56	155	54.3	1.7	0.67.
3.26	55	155	54.3	0.7	0.36.

Average C_2H_4 over reaction zone between R = 0.3 and R = 1.3 cm.

= 103 mv. on the 10^{10} ohm resistor

= 1.64×10^{-2} mm. Hg.

= 8.95×10^{-10} mole. ccs^{-1}. at 22°C.

RUN 2

Total nitrogen pressure 1.2 mm. Hg. Temperature 22°C.

R	Total 14^+ with C_2H_4	C_2H_4 28^+	Contribution to 14^+ by C_2H_4	Corrected N 14^+	$\log_{10}[N]R$.
(cm.)	(mv.10^{12})	(mv.10^{10})	(mv.10^{12})	(mv.10^{12})	
.30	217	47.5	16.6	200.4	1.78.
.34	198	55.5	19.4	178.6	1.78.
.39	164	68.0	23.8	140.2	1.74.
.46	133	79.5	27.8	105.2	1.68.
.54	109	89.5	31.3	77.7	1.62.
.63	92	95	33.2	58.8	1.56.
.72	80	101	35.3	44.7	1.51.
.81	68	105	36.8	31.2	1.40.
.99	60.5	110	38.5	22.0	1.34.
1.19	54.5	113	39.5	15.0	1.25.
1.38	50.3	116	40.5	9.7	1.13.
1.58	49.0	117	41.0	8.0	1.10.
1.77	45.0	116	40.6	4.4	0.89.
2.02	43.7	117	41.0	2.75	0.75.
2.27	42.5	119	41.6	0.9	0.31.
2.52	42.0	120	42.0	0	-
3.26	42.0	120	42.0	0	-

Average C_2H_4 over reaction zone between R = 0.3 and R = 1.3 cm.

= 81.3 mv. on the 10^{10} ohm resistor

= 1.29×10^{-2} mm. Hg.

= 7.05×10^{-10} mole. ccs^{-1}. at 22°C.

22. REFERENCES.

1. Polanyi: Atomic Reactions, Williams & Norgate Ltd., 1932.
2. Johnston: Disc. Far. Soc., 17, 14, 1954.
3. Hartridge & Roughton: Proc. Camb. Phil. Soc., 3, 450, 1926.
4. Carrington & Davidson: J. Phys. Chem., 57, 418, 1953.
5. Melville & Gowenlock: Experimental Methods in Gas Reactions, MacMillan & Co. Ltd., 1964, page 289.
6. Norrish, Porter & Thrush: Proc. Roy. Soc., A216, 165, 1952.
7. Norrish & Thrush: Quart. Rev., 10, 149, 1956.
8. Clyne & Thrush: Trans. Far. Soc., 57, 1, 1961.
9. Haber & Zisch: Z. Physik., 9, 302, 1922.
10. Beutler & Polanyi: Naturwiss., 13, 711, 1925.
11. Beutler, Bogdandy & Polanyi: Naturwiss., 14, 164, 1926.
12. Bawn: Chem. Soc. Ann. Rep., 39, 36, 1942.
13. Hartel & Polanyi: Z. Physik. Chem., B11, 97, 1930.
14. Heller: Trans. Far. Soc., 33, 1556, 1937.
15. Hartel, Meer & Polanyi: Z. Physik. Chem., B19, 139, 1932.
16. Warhurst: Quart. Rev., 5, 44, 1951.
17. Frommer & Polanyi: Trans. Far. Soc., 30, 519, 1934.
18. Fairbrother & Tuck: Tran. Far. Soc., 32, 624, 1936.
19. Cvetanovic & Le Roy: Can. J. Chem., 29, 597, 1951.
20. Cvetanovic & Le Roy: Can. J. Chem., 34, 54, 1956.
21. Smith: J. Chem. Phys., 22, 1605, 1954.
22. Reed & Rabinovitch: J. Phys. Chem., 59, 261, 1955.
23. Garvin & Kistiakowsky: J. Chem. Phys., 20, 105, 1952.

24. Garvin, Guinn & Kistiakowsky: Disc. Far. Soc., 17, 32, 1954.

25. Pearson: Ph.D. Thesis., University of St. Andrews. 1960.

26. Wood: Proc. Roy. Soc., A102, 1, 1922.

27. Langmuir: J. Amer. Chem. Soc., 34, 1310, 1912.

28. Storch: J. Amer. Chem. Soc., 54, 4188, 1932.

29. Belchtz & Rideal: J. Amer. Chem. Soc., 57, 1168, 1935.

30. Tollefson & Le Roy: J. Chem. Phys., 16, 1057, 1948.

31. Klein & Scheer: J. Phys. Chem., 62, 1011, 1958.

32. Kroepelin, Vogel & Kremser: Chem. Abstr., 49, 9341, 1955.

33. Steacie: Atomic & Free Radical Reactions, Reinhold Publishing Co. 1954.

34. Noyes & Leighton: The Photochemistry of Gases, Reinhold Publishing Co., 1941.

35. Jennings: Quart. Rev., 15, 237, 1961.

36. Shaw: Chapter 3, The Formation and Trapping of Free Radicals (Bass & Broida), Academic Press, 1960.

37. Jones: Rep. Prog. Phys., 16, 216, 1953.

38. Jones: Ionisation & Breakdown in Gases, Methuen & Co., London, 1957.

39. Taylor & Marshall: Nature, 112, 937, 1923.

40. Bonhoeffer: Z. Physik. Chem., 113, 119 & 492, 1924.

41. Evans, Freeman & Winkler: Can. J. Chem., 34, 1271, 1956.

42. Armstrong & Winkler: J. Phys. Chem., 60, 1100, 1956.

43. Kelly & Winkler: Can. J. Chem., 37, 62, 1959.

44. Prodell & Kusch: Phys. Rev., 106, 87, 1957.

45. Jennings & Linnett: Nature, 182, 597, 1958.

46. Wartenberg & Schulze: Z. Phys. Chem., B6, 261, 1929.

47. Smith: J. Chem. Phys., 11, 110, 1943.

48. Ramsey: Rev. Sci. Instr., 28, 58, 1956.

49. Ramsey: Phys. Rev., 123, 530, 1961.

50. Shaw: J. Chem. Phys., 30, 1366, 1959.

51. Wittke & Dicke: Phys. Rev., 103, 620, 1956.

52. Mannella: Chem.Rev., 63, 1, 1963.

53. Elias, Ogryzlo & Schiff: Can. J. Chem., 37, 1680, 1939.

54. Schwab & Freiss: Z. Electrochem., 39, 586, 1933.

55. Wrede: Z. Physik., 54, 53, 1929.

56. Harteck: Z. Physik. Chem., A139, 98, 1928.

57. Blades & Winkler: Can. J. Chem., 29, 1022, 1951.

58. Greaves & Linnett: Trans. Far. Soc., 55, 1338, 1959.

59. Harris & Steacie: J. Chem. Phys., 13, 554, 1945.

60. Norrish & Thrush: Quart. Rev., 10, 147, 1956.

61. Young: J. Chem. Phys., 34, 1295, 1961.

62. Tanaka, Jursa & Leblanc: The Threshold of Space, Pergamon Press, 1957, page 89.

63. Ingram: Free Radicals - as Studied by E.S.R., Butterworths Scientific Publications, 1958.

64. Cario & Franck: Z. Physik., 11, 161, 1922.

65. Melville & Robb: Proc. Roy. Soc., A196, 445, 1949.

66. Williams: Quart. Rev., 17, 243, 1963.

67. Farkas & Sachsse: Z. Physik. Chem., B27, 111, 1935.

68. Geib & Harteck: Z. Physik. Chem., (Bodenstein Festband), 849, 1931.

69. Farkas: Z. Phys. Chem., B10, 419, 1930.

70. Farkas & Farkas: Proc. Roy. Soc., A152, 124, 1935.

71. Trenner, Morikawa & Taylor: J. Chem. Phys., 5, 203, 1937.

72. Kaufman: Proc. Roy. Soc., A247, 123, 1958.

73. Verbeke & Winkler: J. Phys. Chem., 64, 319, 1960.

74. Lossing: Chapter 2, Mass-Spectrometry (McDowell), McGraw Hill Book Co., 1963.

75. Cuthbert: Quart. Rev., 13, 215, 1959.

76. Lossing: Ann. N.Y. Acad. Sci., 67, 499, 1957.

77. Dunning: Quart. Rev., 9, 23, 1955.

78. Lossing, Ingold & Tickner: Disc. Far. Soc., 14, 34, 1953.

79. Hipple & Stevenson: Phys. Rev., 63, 121, 1943.

80. Robertson: Proc. Roy. Soc., A199, 394, 1949.

81. Eltenton: J. Chem. Phys., 10, 403, 1942.

82. Eltenton: J. Chem. Phys., 15, 455, 1947.

83. Eltenton: J. Phys. Coll. Chem., 52, 463, 1948.

84. Lossing & Tickner: J. Chem. Phys., 20, 907, 1952.

85. Barker, Farren & Linnett: Proc. Roy. Soc., 274A, 306, 1963.

86. Lossing, Marsden & Farmer: Can. J. Chem., 34, 701, 1956.

87. Robertson: Disc. Far. Soc., 14, 115, 1953.

88. Robertson: Applied Mass-Spectrometry, Institute of Petroleum, London, 1954, page 122.

89. Robertson: Mass-Spectrometry, Methuen, London, 1954, page 107.

90. Le Goff: J. Chim. Phys., 53, 359, 1956.

91. Foner & Hudson: J. Chem. Phys., 21, 1374, 1953.

92. Leger: Can. J. Phys., 33, 74, 1955.

93. Leger & Ouellet: J. Chem. Phys., 21, 1310, 1953.

94. Blanchard, Farmer & Ouellet: Can. J. Chem. 35, 115, 1957.

95. Jackson & Schiff: J. Chem. Phys., 21, 2233, 1953.

96. Jackson & Schiff: J. Chem. Phys., 23, 2333, 1955.

97. Strutt: Proc. Roy. Soc. A87, 179, 1912.

98. Uri & Herzberg: Disc. Far. Soc., 14, 127, 1953.

99. Berkowitz, Chupka & Kistiakowsky: J. Chem. Phys., 25, 457, 1956.

100. Kistiakowsky & Volpi: J. Chem. Phys., 27, 1141, 1957.

101. Kistiakowsky & Volpi: J. Chem. Phys., 28, 665, 1958.

102. McKnight: U.K.A.E.A. Report. IGR-R/CA, 243, 1957.

103. Warburg: Arch. de Gen (3), 12, 504, 1884.

104. Lewis: Ann. Phys., 2, 466, 1900.

105. Lewis: Astrophys. J., 12, 8, 1900.

106. Strutt: Proc. Roy. Soc., A85, 219, 1911.

107. Sponer: Z. Physik., 34, 622, 1925.

108. Cario & Kaplan: Z. Physik., 58, 769, 1929.

109. Mitra: Active Nitrogen - A New Theory. Association for the Cultivation of Science, Calcutta, 1945.

110. Jennings & Linnett: Quart. Rev., 12, 116, 1958.

111. Mitra: Phys. Rev., 90, 516, 1953.

112. Clyne & Thrush: Nature, 189, 56, 1961.

113. Herron: J. Chem. Phys., 35, 1138, 1961.

114. Spealman & Rodebush: J. Am. Chem. Soc., 57, 1474, 1935.

115. Gaydon: Dissociation Energies, Chapman & Hall, 1953, page 164.

116. Gaydon: Spectroscopy and Combustion Theory, Chapman & Hall, 1948, page 222.

117. Mavroyannis & Winkler: Can. J. Chem., 39, 1601, 1961.

118. Laidler: The Chemical Kinetics of Excited States, University Press, Oxford, 1955, page 73.

119. See The Threshold of Space, Pergamon Press, 1957 page 53.

120. Clyne & Thrush: Trans. Far. Soc., 57, 69, 1961.

121. Evans, Freeman & Winkler: Can. J. Chem., 34, 1271, 1956.

122. Herron: J. Chem. Phys., 33, 1273, 1960.

123. Milton & Dunford: J. Chem. Phys., 34, 51, 1961.

124. Back & Mui: J. Phys. Chem., 66, 1362, 1962.

125. Lawrence & Edlefson: Rev. Sci. Instr., 1 45, 1930.

126. Thomson: Phil. Mag., 18, 696, 1934.

127. Eastman: Fundamentals of Vacuum Tubes, McGraw Hill, 1937. p. 43.

128. Reich: Theory and Application of Electron Tubes, McGraw Hill, 1939. p 31.

129. Child: Phys. Rev., 32, 498, 1911.

130. Barnard: Modern Mass-Spectrometry, Unwin Bros., Ltd., 1953 p. 123.

131. Craig: Conference on Applied Mass-Spectrometry, Institute of Petroleum Hydrocarbon Research, October 1963.

132. Field & Franklin: Electron Impact Phenomena, Academic Press, 1957. p 245.

133. Gaydon: Dissociation Energies, Chapman & Hall, 1953, page 161.

134. Crank: Mathematical Diffusion Theory, Oxford University Press, 1956.

135. Young: J. Chem. Phys., 34, 1295, 1961.

136. Fernelius: Inorganic Syntheses, 1st, 126, McGraw Hill, 1946.

137. Hirschfelder, Curtiss & Bird: Molecular Theory of Gases and Liquids, Wiley & Sons, 1954, page 539.

138. Hirschfelder & Eliason: Ann. N.Y. Acad. Sci., 67, 451, 1957.

139. Vanderslice, Mason & Lippincott: J. Chem. Phys., 30, 129, 1959.

REALIGNMENT OF MASS-SPECTROMETER ION 'OPTICS'.

Fig. 19.